Fall 12-2006

Regulation of a Dna-Compacting Plastid Nucleoid Protein

Steven William Adamson
University of Southern Mississippi

The University of Southern Mississippi

REGULATION OF A DNA-COMPACTING PLASTID NUCLEOID PROTEIN

by

Steven William Adamson

A Dissertation
Submitted to the Graduate Studies Office
of The University of Southern Mississippi
in Partial Fulfillment of the Requirements
for the Degree of Doctor of Philosophy

Approved:

December 2006

The University of Southern Mississippi

REGULATION OF A DNA-COMPACTING PLASTID NUCLEOID PROTEIN

by Steven William Adamson

Abstract of a Dissertation
Submitted to the Graduate Studies Office
of The University of Southern Mississippi
in Partial Fulfillment of the Requirements
for the Degree of Doctor of Philosophy

December 2006

ABSTRACT

REGULATION OF A DNA-COMPACTING PLASTID NUCLEOID PROTEIN

by Steven William Adamson

December 2006

DCP68, a DNA-compacting nucleoid protein, was further characterized in order to understand how plastid nucleoid proteins affect the structure and function of chloroplast DNA. Previously, DCP68 was identified as ferredoxin:sulfite reductase, an enzyme that participates in reductive sulfur assimilation and inhibits chloroplast DNA replication and transcription *in vitro* [1, 2]. In this study, the portion of SiR that was found to be present in soluble and plastid nucleoid-enriched fractions indicated that most SiR was stromal in *Arabidopsis* and soybean plants. Although SiR was detected in *Arabidopsis* chloroplast nucleoid-enriched fractions, the study of nucleoid dynamics proved to be difficult due to the few nucleoids that could be isolated from this model plant. Furthermore, *Arabidopsis* heterozygous mutants that contained a reduced SiR protein level did not display an obvious mutant phenotype that could be ascribed to the role of SiR in plastid nucleoids. A significantly higher amount of SiR was present in nucleoid-enriched fractions from young soybean leaves than in mature leaves. The variation in the amount of SiR allocated to plastid nucleoids supports the hypothesis that the interaction of SiR with ctDNA is regulated. The factors that may influence the association of SiR with plastid nucleoids remain elusive. *In vitro* evidence suggested that the phosphorylation status of SiR could

potentially regulate its interaction with DNA [2]. The isoelectric point profile of SiR was examined *in vivo,* as a first step towards identifying possible developmental differences in the post-translational modification of SiR. In conjunction with these studies, SiR was found to contain a conserved CK2 phosphorylation site and was capable of being phosphorylated by CK2 *in vitro.*

ACKNOWLEDGEMENTS

I would like to express my sincere gratitude to my advisors Dr. Sabine Heinhorst and Dr. Gordon Cannon for their guidance and support. I also wish to thank Dr. Faqing Huang and Dr. Kenneth Curry for their helpful insight and discussions. Special thanks to Dr. Jeff Evans for his friendship and the opportunity to work in his laboratory during the summer as an undergraduate researcher. I wish to express my thanks to fellow graduate students and the support staff in the Department of Chemistry & Biochemistry, particularly those with a penchant for paintball. The funding for this research project was provided by the National Science Foundation, the United States Department of Agriculture, and the USM T.W. Bennett fund.

TABLE OF CONTENTS

LIST OF ILLUSTRATIONS

Figure

LIST OF TABLES

Table

ABBREVIATIONS

βME	2-mercaptoethanol
AtSiR	*Arabidopsis thaliana* Sulfite Reductase
BASTA	Glufosinate ammonium
bp	Base pair
BSA	Bovine serum albumin
cDNA	complementary DNA
CHAPS	3-[(3-Cholamidopropyl)dimethylammonio]-1-propanesulfonate
CIAP	Calf Intestinal Alkaline Phosphatase
CysG	uroporphyrinogen III methyltransferase (siroheme synthase)
δ–ALA	δ-Aminolevulinic acid
DAPI	4',6-diamidina-2-phenylindole dihydrochloride
dATP	Deoxyadenosine Triphosphate
DCP68	DNA-compacting Protein of 68-kDa
dCTP	Deoxycytosine Triphosphate
DEPC	Diethyl pyrocarbonate
dGTP	Deoxyguanine Triphosphate
ds	Double stranded
DTT	Dithiothreitol
dTTP	Deoxythymidine Triphosphate
E. coli	*Escherichia coli*
EDTA	Disodium ethylenediamine tetracetic acid
GM	Germination medium
HEPES	4-(2-hydroxyethyl)-1-piperazine ethane sulfonic acid
IgG	Immunoglobulin G
IgY	Immunoglobulin Y
IPTG	β-isopropylthiogalactoside
LB	Luria-Bertani broth
MES	2-Morpholinoethanesulfonic acid
MMOM	Murashige Minimal Organics medium
OD_{600}	Optical density at 600 nanometers
PAGE	Polyacrylamide Gel Electrophoresis
PBS	Phosphate Buffered Saline
PCR	Polymerase Chain Reaction
PIC	Protease Inhibitor Cocktail
PMSF	Phenylmethylsulfonylfluoride
PTSF	p-Toluenesulfonylfluoride
RT	Reverse Transcriptase
SB-M	*Glycine max* (soybean) grown photomixotrophically
SDS	Sodium dodecyl sulfate
SiR	Sulfite Reductase
TEMED	N,N,N,N'-tetra-methanol ethylenediamine
Tris	Tris-(hydroxymethyl)-aminomethane base
U	Units

CHAPTER I

INTRODUCTION

The information stored in the genome dictates every trait that is expressed by the individual, from genes that aid in embryonic development to enzymes involved in the biosynthesis of amino acids. Maize contains 10^{10} bp of DNA, which is equivalent to a linear contour length of about 10 m [3]. DNA must be condensed by several orders of magnitude in order for it to fit inside the cell nucleus, but this process cannot damage the genome, and must allow for genome activities such as replication and transcription.

Condensation is achieved by wrapping genomic DNA around a set of histone proteins forming a nucleosome array which can further condense into highly ordered chromatin structures with increasing levels of complexity [4]. Not surprisingly, the level of condensation has a profound impact on gene expression. It has been demonstrated that transcriptionally active genes are present in chromatin that is less condensed [5]. The degree of DNA compaction is affected by post-translational modification of histone proteins. For example, DNA is less compact in nucleosomes in which the histone proteins have been acetylated [4].

The DNA present in plastids originated from a cyanobacterial genome. According to the endosymbiotic theory, plastids arose when a photosynthetic cyanobacterium was engulfed by a primitive eukaryote, establishing a symbiotic relationship [6, 7]. Most of the cyanobacterial-derived DNA was transferred to

the nucleus, while about 100 genes remain encoded by the plastid genome. Since several metabolic pathways occur either predominantly or exclusively in the chloroplast, a vast number of nuclear-encoded proteins must be imported into the plastid such as enzymes that participate in the biosynthesis of amino acids, starch, fatty acids and volatile organic compounds. This requires an extraordinary degree of communication between the nucleus and plastids. For example, the large subunit of ribulose bisphosphate carboxylase/oxygenase (RubisCO) is encoded by the plastid genome but the small subunit is encoded by the nuclear genome [4].

Chloroplasts are thought to be ideal for the production of pharmaceutical proteins and vaccines. Plastids are polyploid, implying that transformed chloroplasts may contain numerous copies of a transgene and could potentially achieve higher levels of the recombinant protein expression. Plastids are capable of properly folding eukaryotic proteins and the maternal inheritance of chloroplasts reduces the likelihood that transgenes may be transferred to related species [8]. Ultimately, the production of foreign proteins in plastids will rely on the ability of researchers to transform the plastid genome [8]. Currently, this is routinely successful only with tobacco plants, which are not ideal hosts for pharmaceutical proteins.

Part of the difficulty in developing novel plastid transformation strategies may originate from the lack of information that describes the underlying mechanisms influencing the structure and function of the plastid genome. It is well established that the DNA in plant nuclei is wrapped into supercoiled

chromatin fibers and transcriptional activity may be influenced by mechanisms such as post-transcriptional modification of histone proteins. By contrast, the structure of chloroplast DNA appears to differ significantly from the nucleus and is probably more similar to bacterial or mitochondrial nucleoids.

Chloroplast DNA is organized by proteins that compact the DNA into structures called nucleoids. Studies with bacterial and mitochondrial nucleoids have indicated that nucleoid proteins affect DNA structure and function. There are documented changes in the compaction of nucleoids during plastid development. These changes coincide with differences in the protein composition of plastid nucleoids, making it tempting to speculate that nucleoid proteins share some functional similarities to histone proteins. It is also possible that the changes in chloroplast nucleoid protein composition and abundance could account for the variation in rates of chloroplast DNA replication and transcription throughout plastid development. Furthermore, several studies of bacterial and mitochondrial nucleoid proteins suggest that the interaction of these proteins with DNA is a regulated process.

Therefore, this study was designed with the goal of understanding how a DNA-compacting plastid nucleoid protein might be regulated. Since few plastid nucleoid proteins have been characterized to any significant degree, this study focused on an abundant plastid nucleoid protein (DCP68) previously purified from the SB-M cell line. The analogous protein (SiR) in *Arabidopsis* and soybean plants was characterized to examine the possibility that plant development may modulate the function of DCP68/SiR.

The biochemical characterization of DCP68/SiR focused on three areas that might support the hypothesis that the interaction of DCP68 with ctDNA is regulated. Since nucleoid protein composition varies during plastid development, the abundance of DCP68/SiR was examined in young and mature tissue. In *Arabidopsis*, the amount of SiR did not vary significantly between young and mature leaf tissues. However, an initial study of the abundance of SiR in *Arabidopsis* indicated that, in contrast to the SB-M cell line, very little SiR was nucleoid-associated. This led to an examination of the portion of SiR distributed to plastid nucleoids. These data indicate that approximately one-third of the total SiR is distributed to plastid nucleoids in young soybean plants, but this falls to less than 5% in mature plants. This supports that the hypothesis that the interaction of DCP68/SiR with ctDNA is a regulated process. Surprisingly, less than 5% of the total SiR is distributed to plastid nucleoids in *Arabidopsis*, but *Arabidopsis* may not be a suitable model system to study plastid nucleoids. Finally, this study examined the possibility that the function of SiR may be regulated by post-translational modification. Similarly, a previous study demonstrated that the DNA-binding affinity of DCP68/SiR was affected by dephosphorylation [2].

CHAPTER II

LITERATURE REVIEW

2.1 Structure and Function of Plastids

Chloroplasts are the most familiar members of a diverse group of organelles termed plastids, marked by broad structural and functional diversity. Plastids are thought to have arisen from an endosymbiotic event in which a photosynthetic prokaryote invaded a primitive eukaryotic host [7]. Since then, these organelles have diversified to support important roles in lipid and amino acid metabolism in addition to photosynthesis [9, 10]. Plastids exist in several interconvertible forms and may undergo a variety of differentiation pathways. The cell type and the presence of light appear to play important roles in plastid development [11].

Chloroplasts are the most abundant members of the plastid family and are the photosynthetic organelles. They are characterized by the presence of organized thylakoid membranes and chlorophyll. Chloroplasts are present in photosynthetic tissues of plant leaves, stems, and unripened fruits. There is considerable variation in chloroplast structure and metabolism. In C_4 plants, photosynthesis is split between the chloroplasts of mesophyll and bundle sheath cells, a mode that enhances the efficiency of CO_2 fixation [4, 9]. Light stimulates the development of chloroplasts from etioplasts or proplastids.

Proplastids are the undifferentiated organelles from which all other plastids are derived. Proplastids are 10-20% the size of chloroplasts and do not

contain chlorophyll or an internal membrane structure [12]. These organelles are found in meristematic tissue, ripening seeds, in young, dark-grown cotyledons, and in the senescent leaves of some plant species [9, 12]. Studies have estimated that there are 10-20 proplastids per meristematic cell [10]. Proplastid development is strongly influenced by cellular and environmental stimuli [10, 13].

Etioplasts are pre-photosynthetic organelles that contain prolamellar bodies, a structure formed by the synthesis of lipids that normally compose the internal membranes of chloroplasts [4]. The high lipid content of etioplasts results in a formation of tubes that branch in three-dimensions to form a semi-crystalline structure. Prolammelar bodies contain the chlorophyll precursor, protochlorophyllide and various membrane proteins [9, 12]. Light triggers the development of etioplasts into chloroplasts, resulting in the conversion of prolammelar bodies into thylakoid membranes and protochlorophyllide into chlorophyll [12].

The diversification of plastids is accompanied by structural changes that accommodate their unique role in plants. Amyloplasts store and synthesize starch granules as a food reserve. These organelles are localized to roots, tubers, endosperm, and cotyledons. They signal the geotropic response in root caps. Amyloplasts are formed directly from proplastids or arise through chloroplast de-differentiation [9, 13]. Leucoplasts or elaioplasts are oil-storing plastids that synthesize terpenoid compounds implicated in allelopathy. These plastids are restricted to the oil glands present in cacti stems and epidermal cells

of some lily and orchid species [9]. Chromoplasts are plastids containing pigments other than chlorophyll. These plastids are present in fruit, petals and sepals and accumulate carotenoids, which are localized in the chromoplast membranes [9].

The ability of plastids to interconvert is underscored by the functional diversity of plastids. Each plastid type requires a different set of proteins to accommodate function. In fact, it has been estimated that the *Arabidopsis* plastid contains approximately 5000 different proteins. Some plastid proteins are encoded by the plastid genome (plastome). Due to the relatively small size of the plastid genome, it is apparent that the vast majority of plastid proteins are encoded by the nucleus and subsequently targeted to the plastid, usually via an N-terminal signal sequence. In other instances, the coding capacity of plastid proteins is split between the nuclear and plastid genomes. Although the large subunit of ribulose bisphosphate carboxylase/oxygenase (RubisCO) is encoded by the plastome, the small subunit is nuclear encoded and imported into the plastid. It is clear that plastid interconversion requires organ-specific, cell-specific, and developmental stage-specific signals to regulate changes in gene expression [9].

2.2 Plastome

Plastid DNA ranges in size from 120 kbp to over 200 kbp and is characterized by the presence of an inverted repeat, 20-30 kbp in size, that is

separated by a large and small single-copy region [14, 15]. The structure, composition and gene arrangement of the plastome are conserved among higher plants, encoding over 100 genes involved in photosynthesis, gene expression and biosynthetic processes [15, 16]. The shape of the plastome varies from closed circular molecules to oligomeric forms. Oldenberg *et al.* have suggested that the predominant form is branched concatamers that arise from recombination-dependent DNA replication [17, 18]. Plastids are polyploid, meaning that there are multiple copies of the plastome per organelle. Chloroplast DNA replication rates in young leaves exceed the rate of organelle division. The resulting amplification of the plastome can be quite dramatic, such as in spinach where the plastome copy numbers reach 22,000 per cell during mesophyll leaf cell expansion [19-24]. There are several reports indicating that the DNA content of developing chloroplasts is higher than that of mature chloroplasts of pea, wheat, beet, and spinach [20, 23-26]. In wheat endosperm amyloplasts, the average copy number per plastid rises five-fold as the plastid matures [27]. Light-grown cultured tobacco cells show a much higher plastome copy number than dark-grown cells [28]. It is interesting to note that the plastome copy number in cultured cells of soybean (SB-M) is approximately four-fold higher than within intact plants [29]. Plastome amplification has been proposed to support an increased need for chloroplast ribosomes by raising the effective gene dosage of rRNA genes [30, 31]. A similar phenomena exists

during the development of amphibian oocytes, in which an amplification of rRNA genes precedes a large increase in protein synthesis [31].

2.3 Plastid Nucleoids

2.3.1 Nucleoid Structure and Function in Organellar DNA Metabolism

Electron microscopy studies of pea and daffodil chloroplast nucleoids have revealed an electron dense central core with naked DNA projecting in the form of loops or supercoils [32-34]. In contrast, daffodil chromoplast nucleoids possess an electron dense central core with no visible naked DNA [32]. Protease treatment or buffers of high ionic strength expose the beaded structure of nucleoids. These observations suggest that nucleoid architecture is formed by ionic interactions between nucleoid proteins and DNA [32, 35].

There is strong evidence to suggest that the nucleoid is the site of DNA replication. Electron microscopy studies of thylakoid-associated nucleoids isolated from spinach have indicated a high incidence in replication forks, and confirmed by the incorporation of [^{3}H]-thymidine [36-38]. It was later shown that isolated chloroplast nucleoids from developing barley and proplastid nucleoids from culture tobacco cells synthesize DNA *in vitro* [39, 40]. A subsequent study evaluating bromo-deoxyuridine incorporation revealed that replicating DNA is not associated with chloroplast nucleoids from cultured soybean cells and the unicellular alga *Ochromonas danica* [1, 41]. This may indicate there is an uncoupling of DNA replication from packaging into plastid nucleoids in soybean

chloroplasts, or may be related to differences in nucleoid structure and function [1].

Isolated nucleoids from daffodil and pea plastids contain a significant RNA components, indicating that nucleoids are likely active in transcription [32-34]. Although RNA was not detected in highly-purified tobacco nucleoids, it did exhibit activity in run-on transcription assays [35, 42-44]. Activity was also observed in nucleoids from developing barley [45].

2.3.2 Nucleoid Changes During Plant Development

Initial studies of chloroplast nucleoids described morphological patterns during organelle development. Using the fluorochrome 4', 6-diamidino-2-phenylindole (DAPI), Kuroiwa *et al.* surveyed 69 plant species and found the number of nucleoids per chloroplast varied between 8 and 40 and ranged in size from 0.2-1.2 μm [46]. Approximately 6-25 plastome copies are present in each nucleoid [47]. Researchers have described morphological differences during plastid differentiation including changes in plastid nucleoid size, number and distribution [32, 43, 46, 48].

There are typically between one and ten small ovoid proplastid nucleoids [22, 49]. The nucleoids observed in leaf proplastids are similar in size and shape to those found in meristematic root tips and stem cells [46]. Proplastid nucleoids found in the center of dry wheat seed increase in size after imbibition and are

then re-localized to the peripheral region of the organelle [22]. Changes in nucleoid distribution can be correlated with thylakoid membrane biogenesis [46].

In the absence of light, proplastids develop into etioplasts accompanied by a two- to four-fold increase in the size of the nucleoid. Etioplast nucleoids are occasionally found in association with the peripheral region of the prolamellar body [22, 46, 47]. In wheat etioplasts, nucleoids change from a cup-shaped to a ring-shaped structure, but this appears not to be the case in wild oat [47, 49].

Light triggers the development of proplastids and etioplasts into chloroplasts. During this transition, the size of wheat nucleoids decreases and their number increases three-fold [22]. Chloroplast nucleoids are localized to the plastid periphery in immature organelles, which is significant based on reports showing the that ctDNA binds to the envelope membrane fraction in developing pea plastids, a developmental time point that has shown to have higher ctDNA replication and transcription activities [50-52]. Mature chloroplasts contain more nucleoids than young chloroplasts and the nucleoids are re-localized to stacked grana. Senescent organelles contain few nucleoids and a reduced plastome copy number per nucleoid [53, 54].

In addition to differences in nucleoid number, compaction and organellar distribution noted in organelle development, it is apparent that the protein complement of nucleoids is unique to plastid type. The protein/DNA ratio in chromoplast nucleoid is 6-fold higher than in chloroplast nucleoids [32]. These differences in nucleoid protein composition in each plastid type coincide with

differences in organellar replication and transcription. Photosynthetically active chloroplasts contain more ctDNA than do the undeveloped plastids of non-green tissue [20, 22, 24, 28, 29, 52, 55-57]. Plastome amplification and organelle division in young leaf cells results in an accumulation of ctDNA copy numbers, as leaf cells age, the organelle division rate surpasses the plastome replication rate, resulting in the distribution of plastome molecules to daughter organelles [19, 24, 26, 40, 52, 54, 56, 58, 59]. Although no ctDNA replication occurs in mature leaves, it is evident that amyloplast DNA synthesis within the wheat endosperm continues after the organelle has ceased dividing [27].

A phytochrome-mediated response controls plastid transcription, accounting for the higher transcription rates in light-grown leaves than in leaves of etiolated plants [51]. The transcription rates of chloroplasts are higher than those observed in amyloplasts and chromoplasts [60-62]. Young plastids possess higher transcription rates than mature chloroplasts [45, 51]. In the basal meristem of barley seedlings, plastid transcription activity varied more than 10-fold, declining with increasing cell age. The observed changes in nucleoid morphology and organellar DNA metabolism are influenced by nucleoid protein composition [51, 63, 64].

Much of the early research on nucleoid proteins documented the nucleoid composition in different plastids as defined by apparent electrophoretic mobility of these proteins [32]. However, few of these proteins have been characterized to any significant degree.

2.3.3 Plastid Nucleoid Proteins

2.3.3.1 PEND. The plastid envelope DNA-binding protein was first identified in developing pea chloroplasts [53, 65]. Protein orthologs of PEND have been found in *Arabidopsis, Brassica, Medicago,* cucumber, and cherry [66, 67]. PEND is a 130 kDa integral membrane protein localized to the chloroplast inner envelope membrane and is only expressed in the very young plants [65]. The DNA-binding activity of PEND derives from the presence of a bZIP domain [53, 66]. The bZIP domain forms a dimer *in vitro* and preferentially binds to the canonical sequence TAAGAAGT. Since it has been demonstrated that nucleoids are localized to the inner envelope of young chloroplasts (the proposed site of plastome amplification), it is possible that PEND may anchor the nucleoid to the envelope membrane during plastome amplification.

In order to further understand the function of PEND, Wycliff *et al.* produced transgenic tobacco plants that overexpress the *Brassica napus* PEND homolog. Approximately 35% of the 60 transgenic plant lines contain chlorotic areas in which there is evidence of aberrant development of palisade cells. Palisade cells of overexpression mutants display a spongy appearance similar to the underlying mesophyll cells, loss of parallel arrangement and a dramatic decrease in the number of chloroplasts [68]. The authors of this report suggest the PEND overexpression phenotype is caused by retention of plastid DNA at the envelope membrane, yet they provide no experimental evidence to support this claim.

2.3.3.2 MFP1. The 80 kDa MFP1 protein was first identified as a nuclear matrix attachment region binding protein [69-71]. It has since been recognized that MFP1 is present in thylakoid membranes of cultured tobacco cells and in Arabidopsis, but is also present in the nuclear matrix [72, 73]. It has been suggested that MFP1 could anchor the nucleoid to the thylakoid membranes in mature chloroplasts. The C-terminal DNA-binding domain is oriented towards the stroma and has no sequence specificity [72]. MFP1 accumulates in light-grown seedlings and its expression positively correlates with the development of thylakoid membranes in young, green tomato fruit [72].

2.3.3.3 CND41. A 41 kDa protein present in tobacco chloroplasts and etioplasts (CND41) binds DNA non-sequence specifically via a helix-turn-helix motif in the lysine-rich N-terminus [35, 74]. Very low amounts of CND41 were detected in roots, leaves, or photoautotrophic cultured cells, relative to the protein abundance found in stems and heterotrophic cultured cells. CND41 transcript abundance is higher in senescing leaves than in young, growing leaves of tobacco, although this study lacks evidence showing that protein levels mirror transcript abundance [75].

Only two transgenic tobacco plant lines carrying an antisense CND41 gene construct contained more than a 50% reduction in CND41 protein. These mutants contain slightly elevated chloroplast gene transcripts and lower levels of gibberellins resulting in a dwarf phenotype. Wild-type leaf morphology is

restored by the exogenous application of gibberellins to the mutants [76]. Antisense plants also show a delayed onset of senescence [75].

There is ~25% amino acid identity of CND41 to some aspartyl proteases and possesses the active site residues of aspartyl proteases [74]. However, aspartyl proteases are acidic proteases and the highest protease activity was demonstrated at pH 2.5 with only 10% of maximum activity remaining at pH 7.0. It seems doubtful that this activity is physiologically relevant, given that the chloroplast pH is ~8.0. In the presence of an aspartyl protease inhibitor, the proteolytic activity of CND41 is only weakly inhibited [77]. It seems more plausible that the proteolytic activity observed in CND41 preparations may be the result of contaminants.

2.3.3.4 CpPTP. The resurrection plant *Craterostigma plantagineum* expresses a 21 kDa abscisic acid- and dehydration-responsive DNA-binding protein. CpPTP has four nearly identical genes in *Craterostigma*, significant homology to a tomato gene, but no other obvious gene homologs [78]. Chimeric green fluorescent protein (GFP) reporter constructs localize to proplastid nucleoids in a transformed tobacco cell line [78]. CpPTP protects DNA from digestion by DNase I *in vitro,* therefore a role in dehydration mediated nucleoid remodeling seems reasonable [78]. DNA is protected from dehydration by the C-terminal DNA-binding coiled-coil motif [78].

2.3.3.5 DCP68/SiR. DCP68 is a unique DNA-binding protein present in plastid nucleoids of cultured cell lines of soybean (SB-M) and tobacco (BY-2) and

garden pea [1, 79-82]. N-terminal amino acid analysis of purified DCP68 revealed strong homology to ferridoxin:sulfite reductase (SiR) from higher plants [81]. Sulfite reductase is a member of the sulfur assimilation pathway. It catalyzes the reduction of sulfite using six electrons donated from reduced ferredoxin [83]. Strong evidence suggested this identification was not an artifact. Purified DCP68 exhibits the same siroheme absorbance peaks expected for SiR [79, 81]. The cDNA of DCP68 contains the conserved active site residues, ferredoxin binding sites, and an overall homology that is 79% identical to SiR from *Arabidopsis* [81]. Immunolocalization of SiR in pea and SB-M chloroplasts suggested that SiR is localized to the nucleoids [81]. This indicates that SiR is a moonlighting protein, participating in sulfur assimilation and present in plastid nucleoids. Moonlighting proteins have a second function often unrelated to their primary or catalytic role, such as in DNA/RNA-binding to regulate transcription and translation or to serve as structural proteins as in the lens of the eye [84].

A series of *in vitro* studies suggest DCP68/SiR may regulate nucleoid function by modulating DNA-compaction. Compact structures reminiscent of plastid nucleoids are observed when purified DCP68/SiR is incubated with DNA. A DNA-synthesis assay demonstrates DCP68/SiR inhibits nucleotide-incorporation in a concentration-dependent manner [1]. Sekine *et al.* has shown that DCP68/SiR inhibits DNA transcription [82]. Interestingly, the compact structures formed by recombinant maize SiR were disrupted by increasing concentrations of heparin [82]. This is thought to be significant since the

transcriptional inhibition by SiR could be partially restored by the addition of heparin [82]. These combined observations suggest that nucleoid compaction by SiR may determine the overall ability of the ctDNA to serve as a template.

2.3.3.6 Other Putative Nucleoid Proteins. A 28 kDa protein isolated from young pea chloroplast nucleoids has considerable homology to the ribosomal protein L19 [85]. A protein resembling the abundant bacterial nucleoid protein HU seems to be present in the nucleoids of algal species [86-89]. HlpA from *G. theta* or its ortholog HC from *C. merolae* are non-sequence specific DNA-binding proteins but display a preference for structural features such as four-way junctions [89]. Mutant *B. subtilis* lacking the functional HU protein can be rescued by complementation with HlpA, suggesting that HlpA is functionally equivalent to HU [89]. Two reports have shown that antisera raised against *E. coli* HU crossreacts with protein(s) in spinach chloroplasts [90, 91]. However, the electrophoretic mobility of the immunoreactive proteins was not similar in these two experiments, suggesting that the identification may have arisen from protein contaminants. More recent attempts to identify HU-like proteins in higher plants have failed. Proteins corresponding to the molecular weight of HU are present in soybean chloroplast nucleoids but do not crossreact with HU antisera [1]. In addition, nuclear and plastid genomes of *Arabidopsis* and rice do not possess an obvious HU homolog [92].

Finally, a recent proteomics survey of proteins in a pea thylakoid-membrane enriched fraction identified several new candidates for nucleoid

protein classification. Mass spectrometry identified RecA isoforms, histone orthologs, ribosomal proteins, RNA binding proteins, RNA helicases, and a ribonuclease S5 ortholog [80]. However, a more quantitative biochemical assay has not yet been performed to substantiate these claims.

2.4 Bacterial Nucleoids

2.4.1 Prokaryotic Nucleoid Structural Dynamics

2.4.1.1 Nucleoid Morphology. The prokaryotic nucleoid has been studied more extensively than plastid or mitochondrial nucleoids. Prokaryotic nucleoids are the site of DNA replication, recombination and transcription [93, 94]. *E. coli* nucleoids range in size from 0.3 to 2 μm and contain one to three genome copies per nucleoid, although this is reduced to one copy in stationary-phase *E. coli* [95-98]. Typically, there are one or two nucleoids per cell that are centrally located [99]. In growing *E. coli*, nucleoids exhibit a bilobed shape that is influenced by growth conditions [94, 99, 100].

2.4.1.2 Proposed Genome Structure. The *E. coli* 4.7 Mbp chromosome has a linear contour length of 1.5 mm but is compacted four orders of magnitude, occupying a total volume of 0.2 μm^3 [94, 101]. Electron microscopy has shown *E. coli* nucleoids form a rosette-like structure with interwoven loops that protrude outwards radially from a central core [102, 103]. The number of loops is comparable to the number of topological domains predicted by biochemical analyses [102, 103]. *E. coli* contains about 40 independent supercoiling domains

but the number of domains is dynamic and depends on the cellular growth rate [102-104].

2.4.2 *E. coli* Nucleoid-Associated Proteins

2.4.2.1 Fis. Factor for Inversion Stimulation (Fis) was originally identified as a cofactor for site-specific recombination [105, 106]. It also has been shown to function in transcriptional activation of rRNA and tRNA operons, oriC-dependent DNA replication, and autoregulation of its own transcription [107]. Fis binds DNA by inserting its helix-turn-helix motif into DNA major grooves [108]. It binds DNA with some specificity upon recognizing a poorly conserved 15 bp binding site. Fis binding sites are present in the genome about every 230 bp, most of which are probably occupied during exponential growth [108]. Fis modulates transcriptional activity through two mechanisms. Transcriptional repression of DNA gyrase in *E. coli* results in nucleoid de-compaction. As discussed later (Section 2.4.4), supercoiling is one of the most important forces promoting nucleoid condensation [106]. Also, it has been documented that Fis competes for H-NS binding sites. Electron microscopy has documented distinct DNA architecture formed by H-NS and Fis [109]. This effect could explain the observed changes in nucleoid conformation observed during growth phase changes.

2.4.2.2 H-NS. The 15.6 kDa H-NS protein is a highly abundant nucleoid protein, consisting of an N-terminal dimerization domain and a C-terminal DNA-binding domain [106]. H-NS mediates transcriptional silencing, site-specific

recombination and the cold-shock response [101, 110, 111]. There are few examples where H-NS positively affects gene expression [106, 112]. In fact, microarray and proteomics data suggest H-NS may act as a global repressor. Up to 5% of *E. coli* genes display changes in expression in the presence or absence of H-NS [113]. When overexpressed, H-NS induces an artificial stationary phase by silencing global transcription [114]. H-NS expression is strongly regulated by temperature and osmolarity. During cold shock, the H-NS to DNA ratio increased three- to four-fold [115].

The mechanism by which H-NS represses transcription has been examined in detail in for the *rrnB* P1 ribosomal gene. H-NS bound preferentially to intrinsically curved A/T-rich stretches of DNA [116, 117]. Due to the presence of multiple binding sites, H-NS dimers at distinct sites may undergo olligomerization, thereby forming a looped structure. Repression occurred when RNA polymerase was trapped inside this loop [118, 119].

2.4.2.3 HU. HU is a non-sequence specific DNA-binding protein but prefers DNA structures that are recognized DNA repair intermediates such as DNA kinks, gaps, and cruciform structures [101, 106, 120-122]. The affinity with which HU binds DNA structures was 1000-fold higher that linear DNA. In fact, binding of HU to repair intermediates protected them from exonuclease degradation [121].

HU is widely distributed among different eubacteria, archaebacteria, and blue-green alga [123]. There is strong evidence to suggest that HU wraps DNA

by a mechanism analogous to the histone-DNA interaction in eukaryotic chromatin. Rouviere-Yaniv *et al.* demonstrated that purified HU decreased the linking number of bound DNA sequences [124].

2.4.2.4 IHF. The Integration Host Factor (IHF) was first discovered as an accessory protein involved in phage recombination [125]. IHF is structurally similar to HU and likely uses a similar mechanism to induce bending. IHF binds to a 35 bp site comprised of a 3' conserved domain and a 5' A/T-rich segment [101]. Variations in the 5' sequence can result in 100-fold changes in DNA-binding affinity [101, 126]. More recently, it has been proposed that IHF may be a very important factor in nucleoid condensation. The concentration of IHF is 30-fold higher than available binding sites [108, 127]. It has been suggested that non-specific-binding by IHF may be the basis for strong global transcriptional repression. Microarray analyses have demonstrated that IHF directly affects the expression of at least 46 genes, and indirectly affects more than 50 others [128].

2.4.2.5 Dps. The 19 kDa Dps is the most abundant nucleoid protein from starvation-phase *E. coli* [129, 130]. Dps binds DNA non-sequence specifically. Dps expression is inducible by nutritional or oxidative factors [131, 132]. The crystal structure of Dps reveals its structural similarity to the iron-storage protein ferritin. Both form a dodecamer with a negatively-charged hollow core that protects DNA from oxidative damage [133]. Mutants lacking Dps have a higher frequency of single-strand lesions generated by hydrogen peroxide and G/C → T/A spontaneous mutations [131]. Frenkiel-Krispin *et al.* have commented on the

effectiveness of the Dps-DNA crystalline assemblies in starved *E. coli*. As starvation proceeds, the nucleoid forms a toroidal structure that grows by a pattern-matching process termed epitaxial growth. This phase transition in nucleoid structure does not require energy but maintains chromosomal organization [134, 135]. Co-crystallization of DNA and Dps results in a greatly enhanced stability to both components, indicating that the structure can withstand prolonged starvation [135].

2.4.2.6 Other E. coli Nucleoid Proteins. A number of other nucleoid-associated proteins have been identified though their biochemical characterization is limited. CbpA is a non-sequence specific DNA-binding protein with a preference for curved-DNA. There is high amino acid sequence homology between CbpA and DnaJ, a chaperone involved in DNA replication [130, 136]. The highest level of expression of CbpA is in the late stationary phase [130, 137]. The related protein CbpB (Rob) is a sequence specific DNA-binding protein involved in the transcriptional regulation of genes coding for resistance to antibiotics and the free-radical superoxide [138, 139].

The 52 kDa DnaA protein initiates chromosomal replication upon binding to the replication origin [140-142]. It was later shown to modulate transcription of *uvrB, pros, dnaA,* and *mioC* [143]. A related protein, the 33 kDa IciA binds a 13 nt consensus sequence in the *E.* coli replication origin [144, 145]. However, some have suggested that IciA contributes to nucleoid condensation by binding non-sequence specifically to A/T-rich regions [129, 144, 146].

StpA exhibits significant amino acid sequence homology to H-NS, binds DNA non-sequence specifically, and is able to complement *hns* mutants [129, 147, 148]. In fact, both H-NS and StpA constrain DNA supercoils and inhibit transcription from promoters containing curved DNA [149]. However, there are differences between these analogues. H-NS regulates a much broader class of genes that are unaffected by StpA. In addition, the RNA chaperone activity is much stronger in StpA [149-151]. The expression of both StpA and H-NS decreases after reaching stationary phase. However, the impact of StpA on nucleoid compaction is not as strong as H-NS given that H-NS expression is 90-fold higher than that of StpA [130, 150].

The leucine-responsive regulatory protein (Lrp) regulates expression of a large number of operons (more than 75 genes) controlling amino acid and one-carbon metabolism, metabolite transport, and pili formation [130, 152-155]. The abundance of Lrp decreases rapidly upon reaching stationary phase [130]. Six different modes of transcriptional regulation have been described for Lrp. The 20 kDa monomer forms higher order oligomers that binds DNA in a cooperative manner leading to the formation of a large nucleoprotein complex [156, 157]. The N-terminal domain is responsible for DNA-binding, a middle domain is required for transcriptional activation, and the C-terminal domain is needed for leucine-responsiveness [158, 159]. The distribution of Lrp between the nucleoid and cytoplasm is modulated by leucine, leading to a 2.5-fold decrease in 'free' Lrp [157, 160].

2.4.3 Nucleoid Architecture Results from a Balance of Forces

The structure and function of nucleoids is determined by a balance of forces [102, 103, 161]. Nucleoid proteins clearly play important roles in DNA-binding and nucleoid compaction. The abundance and composition of nucleoid proteins strongly influences replication, recombination, transcription, and segregation [93, 106, 129, 130]. Electron microscopy has demonstrated that nucleoids from stationary phase *E. coli* are more compact than those in log phase growth, and this is accompanied by global changes in gene expression [93, 162]. Two recent reports have documented changes in nucleoid protein composition and abundance during *E. coli* growth phase transitions. The expression of CbpB, DnaA, H-NS, HU, IciA, Lrp, and StpA are highest during the exponential growth phase. In contrast, the expression of CbpA, Dps, and IHF is highest during stationary phase [93, 129, 130]. Fis and HU are the most abundant nucleoid proteins in the exponential growing phase, but are replaced by Dps in stationary phase [93, 129, 130]. These data suggest that nucleoid function is affected by genome compaction, which is a direct reflection of the nucleoid protein composition and abundance.

There is strong evidence that nucleoid proteins exert a significant condensing force on the bacterial nucleoid structure. Although binding modes may differ, most nucleoid proteins constrain the DNA topology through bending. A bend can occur as a direct result of binding by nucleoid proteins, like the 50-90° bend induced by the *E. coli* nucleoid protein Fis. Compaction of DNA can

occur indirectly, such as when H-NS dimers undergo oligomerization and form a DNA-bridge [108]. Bending by nucleoid proteins can lead to the formation of higher-ordered looped DNA structures that aid in gene repression. For example, a repressor loop is formed by HU that contains both GalR promoters, which prevents RNA polymerase from beginning transcription [101].

Nucleoid proteins are not the only factors that contribute to nucleoid structure. Early estimates of the DNA-binding constants of HU and H-NS were five to ten-fold higher than the predicted intracellular concentration [163]. When macromolecular crowding was simulated by the addition of polyethylene glycol, a seven to ten-fold enhancement in binding was observed, reconciling the apparent paradox between nucleoid protein abundance and *in vitro* estimates of binding constants [163-165].

Negative supercoiling is also an important factor contributing to nucleoid condensation. Negative supercoiling is the driving force in cellular processes requiring DNA strand separation such as transcription, replication and recombination [102]. DNA supercoiling also promotes the formation of non-canonical DNA structures such as cruciforms, Z-DNA, or triple helices that are recognized by some non-sequence specific nucleoid proteins [120]. Some have speculated that nucleoid proteins exert a compaction force by modulating superhelicity [102, 103]. Although some nucleoid proteins are able to wrap DNA and decrease the linking number of bound DNA, experiments in mutants devoid

of HU and H-NS indicate that these two nucleoid proteins are not the source of most of the supercoiling in *E. coli* nucleoids [166].

Several forces exert a de-condensing effect on nucleoid structure. It is apparent that nucleoid proteins themselves can participate in nucleoid de-compaction. Some nucleoid proteins compete for binding sites on specific promoters. IHF and Fis can relieve repression by H-NS at specific promoters [108]. In fact, some have speculated that HU is an antagonist to H-NS, by competing for binding sites. H-NS mediated transcriptional repression is enhanced in mutants that lack HU [106, 167]. In fact, the abundance of nucleoid-associated proteins changes depending on the growth phase, coinciding with changes in gene expression.

DNA replication has a de-condensing effect on the nucleoid because replication is accompanied by positive supercoiling. In addition, the force generated by DNA replication contributes to the movement of nascent DNA strands away from the nucleoid [168, 169].

2.5 Yeast Mitochondrial Nucleoid Proteins

2.5.1 Yeast Mitochondrial Nucleoid Proteins

Eukaryotes contain highly variable number of mitochondria. Yeast cells contain 50-100 copies of the 80 Kbp mitochondrial genome [170, 171]. Mitochondrial nucleoids are the site of replication, transcription, segregation, and recombination [172, 173]. Most research in this field has focused on

characterizing yeast mitochondrial nucleoid proteins. It is of some note that many putative mitochondrial nucleoid proteins appear to have previously characterized roles in primary metabolism.

2.5.1.1 Abf2p. The 20 kDa Abf2p is the primary condensing protein in yeast mitochondrial nucleoids [174]. Two high mobility group motifs in Abf2p suggest its participation in DNA packaging, replication, recombination, and transcription [175]. Abf2p binds DNA without sequence specificity but prefers DNA structures such as Holiday junctions [174, 176]. In the presence of topoisomerases, Abf2p induces negative supercoiling [174, 177]. Double mutants containing null copies of *abf2* and *mgt1* (a cruciform-cutting endonuclease) display a ten-fold decrease in recombination intermediates. This may indicate that, in addition to nucleoid compaction, Abf2p is involved in DNA recombination [176, 178, 179].

2.5.1.2 Mgm101p. Mgm101p encodes a 30 kDa protein with a C-terminal basic region involved in mtDNA maintenance [180]. Mgm101p localizes exclusively to mitochondrial nucleoids [181, 182]. Mgm101p mutants do not show differences in mtDNA replication nor in nucleoid packaging, segregation, or partitioning [181]. Mutant cells lacking a functional copy of Mgm101p are hypersensitive to oxidative damage, suggesting that this protein is involved in the repair of damaged mtDNA [181].

2.5.1.3 Aco1p. Aconitase (Aco1p) is an abundant enzyme of the citric acid cycle that moonlights as a mitochondrial nucleoid protein [183]. It has been shown that Aco1p also has a role in mtDNA maintenance and can rescue mutant

strains lacking Abf2p [159]. Its role in mtDNA maintenance is independent of enzyme activity or the metabolic flux through the citric acid cycle but may be sensitive to redox state [159, 184, 185]. Mammalian aconitase moonlights as an iron-responsive element binding protein (IRP1). Enzyme catalysis and mRNA binding were determined to be mutually exclusive and the functional switch occurs through the loss of an iron-sulfur cluster that is required for aconitase activity [186-188].

2.5.1.5 Hmi1p. The Hmi1p is a helicase required for mtDNA inheritance. Yeast strains without a functional Hmi1p protein possess three-fold more nucleoids that are smaller in size and contained less DNA than wild-type yeast mitochondria [189]. Analysis of intact mtDNA molecules from wild-type and Hmi1p null mutants demonstrated large differences in the size of DNA generated. These data suggest Hmi1p may be a structural factor involved in the synthesis of large concatameric DNA molecules [189].

2.5.1.6 ILV5p. Acetohydroxyacid reductoisomerase (Ilv5p) catalyzes a step in branched-chain amino acid synthesis and moonlights as a mitochondrial nucleoid protein [190]. It has previously been shown that Ilv5p is under control of Gcn4p, a transcriptional activator of amino acid biosynthetic genes. Mutants overexpressing Gcn4p have an increased number of nucleoids and can suppress the mtDNA instability phenotype of abf2pΔ cells[191-193]. This suggests that the number of nucleoids is co-regulated by the general amino acid control pathway [191, 194]. It has also been noted that DNA mutation rates are significantly

higher in cells after the general amino acid control pathway is partially de-repressed [195].

2.5.1.7 Hsp60. The heat shock protein Hsp60 is an essential molecular chaperone expressed during oxidative stress to protect iron-sulfur proteins [196]. It also moonlights as a mitochondrial nucleoid protein. Hsp60 binds to the template strand of active mtDNA *ori* sequences *in vitro* [183]. Mitochondrial DNA is rapidly lost from Hsp60 temperature-sensitive mutants. Yet mtDNA instability in these mutants required transcription from promoter elements within the active ori. Kaufman *et al.* suggested the interactions between Hsp60 and active *ori* elements that may represent a potential regulatory mechanism of mtDNA transmission [182].

2.5.1.8 Moonlighting Mitochondrial Nucleoid Protein Candidates. Many mithochondrial nucleoid proteins have been identified using formaldehyde to covalently crosslink nucleoid proteins to DNA *in vivo*. It has emerged that many of these proteins have important roles in the primary metabolism and are apparently involved in nucleoid maintenance [197, 198]. These proteins are called moonlighting proteins and may facilitate the coupling of metabolism and mtDNA maintenance [159]. Moonlighting mitochondrial nucleoid proteins are shown in Table 1.

Table 1. Moonlighting Mitochondrial Nucleoid Proteins			
Protein	**Primary Function**	**Species**	**References**
Sls1p	Translation	*S. cerevisiae*	[183]
Hsp70p	Mitochondrial chaperone	*S. cerevisiae*	[183]
IDH-E1	NAD-dependent isocitrate dehydroenase	*S. cerevisiae*	[183, 198-200]
IDP1p	NADP-dependent isocitrate dehydrogenase	*S. cerevisiae*	[183]
SCS	Succinyl-CoA ligase, α subunit	*S. cerevisiae*	[183]
PDHC-E1 α	Pyruvate dehydrogenase, E1 α subunit	*S. cerevisiae*	[183, 198]
PDHC-E1 β	Pyruvate dehydrogenase, E1 β subunit	*S. cerevisiae*	[183]
Ilv6p	Acetolactate synthase regulatory subunit	*S. cerevisiae*	[183]
Cha1p	Ser/Thr deaminase	*S. cerevisiae*	[183]
Ant1	Adenine nucleotide translocator	*X. laevis*	[198, 201]
Phb2	Prohibitin2	*X. laevis*	[198, 201]
PDC-E2	Pyruvate dehydrogenase	*X. laevis*	[201, 202]
BCKD-E2	Branched chain keto acid dehydrogenase	*X. laevis*	[201]
Ilv5p	Acetohydroxyacid reductoisomerase	*S. cerevisiae*	[183, 198]
Hsp60	Mitochondrial chaperone	*S. cerevisiae*	[182, 183]
Ald4p	Aldehyde dehydrogenase	*S. cerevisiae*	[183]
Kgd2p	2-Oxoglutarate dehydrogase	*S. cerevisiae*	[183]
Lpd1p	Dihydrolipoamide dehydrogenase	*S. cerevisiae*	[183]
Aco1p	Aconitase	*S. cerevisiae*	[183]
Atp1p	ATPase α subunit	*S. cerevisiae*	[183]
Mdj1p	Mitochondrial chaperone	*S. cerevisiae*	[203]

2.6 Gene Regulation by Phosphorylation

Although there are over 350 distinct post-translational modifications, reversible protein phosphorylation is one of the best characterized [204]. Approximately 5% of the *Arabidopsis* genome encodes protein kinases and phosphatases [205, 206]. These proteins are essential members of signal

transduction cascades that govern plant responses to developmental and environmental changes. Phosphorylation is one of the most common mechanisms for regulating gene expression. It affects chromatin remodeling, transcription factor binding, and plastid nucleoid protein DNA-binding activity.

2.6.1 Nuclear Gene Expression is Modulated by Phosphorylation

2.6.1.1 Chromatin remodeling. In eukaryotes, DNA is wrapped around histone proteins that maintain chromatin in a condensed state. Post-translational modifications may dictate dynamic transitions between the active and repressed chromatin states. The first evidence to be reported was that histone lysine residues are hyperacetylated in actively transcribed genes [207]. Acetylation and phosphorylation alter the overall charge of histones, disrupting electrostatic interactions between histones and DNA, thereby reversibly altering chromatin structure [208]. Furthermore, it is now clear that in some instances phosphorylation promotes acetylation on the same histone [209, 210].

Phosphorylation of histone proteins occurs during cell cycle progression and in response to environmental factors. During the developmental transition from interphase to metaphase, chromatin is condensed in preparation for segregation. Histone H3 phosphorylation coincides with chromatin condensation and is phosphorylated in a cell cycle dependent manner [211-213]. Phosphorylation of the histone variant H2A.X occurs in response to double-strand breaks as well as apoptotic chromatin fragmentation, [214-218]. *In vitro*

studies have suggested that H2A.X phosphorylation may govern nucleosome spacing [219, 220].

2.6.1.2 Transcription factor activity. Perhaps the most common mechanism of modulating transcription factor activity is through reversible phosphorylation [221-223]. Phosphorylation of many transcription factors, such as PTI4 and OsEREBP1, modulates their DNA-binding affinity [224, 225]. In some cases, transcription factor DNA-binding is affected by diurnal changes in phosphorylation [226].

2.6.2 Organelle Gene Expression is Modulated by Phosphorylation

Protein phosphorylation directly affects the translation of the *psbA* gene. The *psbA* 5' untranslated region (UTR) is bound by a complex of four proteins: RB38, RB47, RB55, and RB60. Binding of this complex to the UTR is regulated by a phosphorylation-dependent mechanism that is responsive to light and redox state [227]. RB60 is phosphorylated in chloroplasts through an ADP-dependent mechanism that is principally active in the dark [228]. In the light, RB60 is dephosphorylated which allows the protein to become responsive to redox signals generated during photosynthesis. Reduction of a key vicinal dithiol site on RB60 activates binding of the complex to the UTR, which allows translation to occur [229].

Protein phosphorylation also impacts organellar gene expression indirectly by modulating properties of proteins in the transcription apparatus. Tiller *et al.* discovered that phosphorylation of three sigma-like factors (SLFs) changes the

transcription profile of *Sinapis alba* plastids [230]. SLFs are prokaryotic-type transcription factors that do not bind DNA themselves, but confer promoter specificity and aid in transcription initiation. Chloroplasts and etioplasts contain three SLFs of similar molecular weight, but differ in the preferred binding site in the psbA promoter and the ionic strength need for efficient DNA-binding [231]. The properties of chloroplast SLFs can be mimicked by incubating them with a kinase [231].

Tiller *et al.* later discovered that the kinase responsible for phosphorylation of plastid SLFs is a casein kinase-like enzyme (CK2) that is associated with the plastid-encoded RNA polymerase [232-236]. Plant casein kinases are involved in the regulation of circadian clock genes, cell cycle, seed storage, DNA transcription, and RNA translation [237-241]. *Arabidopsis* contains four genes encoding a CK2. The N-terminal transit peptide of one cpCK2 gene targets this kinase to the chloroplast where it has been demonstrated to phosphorylate plastid-encoded RNA polymerase, SLFs, chlorophyll a/b-binding protein CP29 and the β subunit of ATP synthase [235, 242, 243]. Plastid-targeted CK2 is subject to regulation by changes in phosphorylation and redox state [232, 235, 236, 244]. These observations have led several researchers to suggest that cpCK2 is part of a signal transduction system that coordinates transcription levels and redox state [232, 235].

2.6.3 Nucleoid Protein Phosphorylation

2.6.3.1 Nucleoid protein phosphorylation. The presence of CK2 recognition motifs present within the MFP1 sequence and *in vitro* experiments showing that MFP1 can be phosphorylated by CK2 support the notion that MFP1 is phosphorylated *in vivo* [245]. It was later shown by that the tobacco chloroplast MFP1 is post-translationally modified *in vivo* [245]. A subsequent southwestern DNA-binding experiment demonstrated that the phosphorylated tobacco MFP1 shows a decrease in DNA-binding affinity [245]. It is interesting to note that the *in vitro* dephosphorylation of the 90kDa *Allium cepa* MFP1 disrupts its association with the nuclear matrix [73].

Chi-Ham *et al.* used electrophoretic mobility shift assays to demonstrate the purified DCP68/SiR bound DNA differently than purified DCP68/SiR that had been pretreated with alkaline phosphatase [81]. This could suggest that the DNA-compacting activity of SiR may be regulated by phosphorylation.

CHAPTER III

EXPERIMENTAL PROCEDURES

Materials

Agarose, N,N,N',N'-Tetramethylethylenediamine (TEMED), ammonium persulfate, glycine, nitrocellulose, acrylamide, ampholytes, Triton X-100, Bradford dye reagent, immobilized pH gradient (IPG) strips, XT-MES running buffer, Criterion gels, and silverstaining chemicals were obtained from BioRad, Hercules, CA. 3-[(3-Cholamidopropyl)dimethylammonio]-1-propanesulfonate hydrate (CHAPS), phenylmethylsulfonyl fluoride (PMSF), p-toluenesulfonyl fluoride (PTSF), ficoll, sorbitol, 2-morpholinoethanesulfonic acid (MES), 4-(2-hydroxyethyl)-1-piperazine ethane sulfonic acid (HEPES), sodium azide, thiourea, 2-mercaptoethanol (βME), diethylpyrocarbonate (DEPC), ε-amino-n-caproic acid, formamide, iodoacetic acid, formaldehyde, protease inhibitor cocktail (PIC), and DNAse I were obtained from Sigma, St. Louis, MO. Dithiothreitol (DTT) was obtained from EMD Biosciences, San Diego, CA. RNA was isolated using Plant RNA Purification Reagent from Invitrogen, Carlsbad, CA. Enhanced chemiluminescent substrate (ECL) was purchased from GE Biosciences, Piscataway, NJ. Murashige and Skoog minimal organics medium [246] was purchased from Sigma, St. Louis, MO (no sucrose) and GibcoBRL, Gaithersburg, MD (with sucrose). Gel Code Blue gel stain and CL-Xposure film were purchased from Pierce, Rockford, IL. Cellulysin cellulase and Miracloth were obtained through Calbiochem, San Diego, CA. Small Parts Inc. of Miami Lakes, FL supplied the 53- and 20-μm netting. Restriction enzymes and

recombinant CK2 were obtained from New England Biolabs, Beverly, MA. Integrated DNA Technologies, Coralville, IA, synthesized primers. *Arabidopsis* growing medium, seed, and growing flats were purchased from Lehle Seeds, Roundrock, TX. All other chemicals were obtained from Fisher Chemical Company, Fairlawn, NJ.

Routine Apparatus

Nucleic acid electrophoresis was performed using GibcoBRL Horizon 58 Model 200 and IBI Model MPH multipurpose gel electrophoresis cells. Protein electrophoresis was performed using a BioRad Criterion or Mini-Protean 3 cells. Transfer to nitrocellulose was performed using the BioRad Mini-Transblot or Criterion blotter. Isoelectric focusing was accomplished using a BioRad Protean IEF cell. Long-term storage of samples was achieved using a Puffer Hubbard – 80°C freezer. *E. coli* cells were disrupted using an SLM Aminco French Pressure cell. *E. coli* culture incubation was performed in a Fisher Scientific 650D incubator, a New Brunswick G24 incubator shakers, a New Brunswick Series 25 incubator shakers. *Arabidopsis* plants were grown in a Percival I-60VL growth chamber. The SB-M suspension cell line was maintained upon New Brunswick G10 Gyratory Shakers. Centrifugation was accomplished using a Beckman Coulter Avanti J-30I and Eppendorf 5417 centrifuges. Hybridization was performed using a Techne Hybridizer HB-1D. Solvent evaporation was performed using Savant SpeedVac concentrator. A Techne Genius thermocycler

was used for PCR. Sample masses were determined using Mettler Toledo balances, models AB54-S and PV303-S. Spectrophotometric absorbance was determined using Nanodrop ND-1000 and Beckman DU640 spectrophotometers. Microscopy was performed using an Olympus BX-60 microscope with the Q-Imaging Micropublisher Imaging system. Distilled water was deionized using a Barnstead Nanopure II system. Microliter solution volumes were measured using Pipetman P-1000, P-200, and P-20. Solution pH was determined using a Fisher Accumet pH meter model 915. Labware and solutions were sterilized in Steris Amsco Lab 250 and 3031-S autoclaves.

Media

Antibiotic Stock Solutions
25 mg/ml Ampicillin in water (final concentration: 100 μg/ml)
34 mg/ml Chloramphenicol in ethanol (final concentration: 30 μg/ml)
Antibiotic solutions were sterilized with a 0.2 μm filter and added to the media after cooling to 50°C.

Arabidopsis Growing Medium
33% vermiculite
33% perlite
34% potting soil

Vitamin Mixture (1000x) for KT Medium
200 μg/l Nicotinamide
200 μg/l Pyridoxine HCl
100 μg/l D-Biotin
100 μg/l Choline Cl
100 μg/l Calcium Pantothenate
100 μg/l Thiamine HCl
50 μg/l Folic acid
50 μg/l *p*-Aminobenzoic acid
50 μg/l Riboflavin
0.15 μg/l Cyanocobalamin

Germination Medium (GM)
2.2 g/l Murashige and Skoog basal salts
1% sucrose
0.8% agar
5 mM MES, pH 5.7
(Where noted, 15mg/L BASTA and/or 50μM cysteine were added after the media has cooled.)

KT Medium (KT) [247]
1 mg/l naphthaleneacetic acid
0.2 mg/l kinetin
34.6 g/l Murashige Minimal Organics medium (with sucrose)
1X Complex Vitamin mixture

Luria-Bertani Broth (LB)
10 g/l NaCl
10 g/l tryptone
5 g/l yeast extract

SOC Medium
2% tryptone
0.5% yeast extract
10 mM NaCl
2.5 mM KCl
10 mM $MgCl_2$
10 mM $MgSO_4$
20 mM glucose

Solid Bacterial Media
1.5% (w/v) agar was added to LB or TB before autoclaving.
0.8% (w/v) agar was added to GM before autoclaving.

Terrific Broth (TB)
12 g/l tryptone
24 g/l yeast extract
0.4% (v/v) glycerol
17 mM KH_2PO_4
72 mM K_2HPO_4

Buffers

Agarose Gel Loading Buffer (6X)
0.4% (w/v) Orange G
0.03% (w/v) Bromophenol Blue

0.03% (w/v) Xylene Cyanol
15% Ficoll
10 mM Tris-HCl, pH 7.5
50 mM EDTA, pH 8.0

Buffer A for preparation of *Arabidopsis* soluble protein extracts
20 mM Tris-HCl, pH 8.0
20 mM NaCl
0.4 mM PMSF/PTSF
1% (v/v) Protease Inhibitor Cocktail

Bacterial Cell Lysis Buffer
20 mM Tris-HCl, pH 8.0
500 mM NaCl
1 mM EDTA
0.1 % Triton X-100
0.4 mM PMSF/PTSF

Chitin Column Buffer
20 mM Tris-HCl, pH 8.0
500 mM NaCl
1 mM EDTA
0.4 mM PMSF/PTSF

Chloroplast Isolation Buffer
50 mM HEPES, pH 8.0
400 mM sorbitol
1 mM EDTA
Store at 4°C

Coomassie Blue (aqueous)
0.05% (w/v) Coomassie Blue G250 dye dissolved in water

Denhardt's Reagent (50X)
10 mg/ml Ficoll (MW 400 Kda)
10 mg/ml polyvinylpyrrolidone (MW 30 KDa)
10 mg/ml bovine serum albumin

Dialysis Buffer
20 mM Tris-HCl, pH 8.0
20 mM NaCl
0.4 mM PMSF/PTSF

DNA Compaction Buffer

20 mM Tris-HCl, pH 8.0
20 mM NaCl
0.4 mM PMSF/PTSF
1 mM dithioerythritol (DTT)

Immobilized pH Gradient (IPG) Strip DTT Equilibration Buffer
6 M Urea
50 mM Tris-HCl, pH 8.8
20% (v/v) Glycerol
2% (w/v) SDS
2% (w/v) DTT (Added immediately prior to use)
Store at –20°C

DNA Prehybridization Solution
5X SSC, pH 7.0
5X Denhardt's solution
50% (v/v) formamide
1% sodium dodecyl sulfate
0.1 mg/ml salmon sperm DNA
DEPC-treated water

Immunoblot Transfer Buffer
25 mM Tris-HCl, pH 8.3
192 mM glycine
20% methanol
Chill to 4°C prior to use

IPG Strip Iodoacetic Acid Equilibration Buffer
6 M Urea
50 mM Tris-HCl, pH 8.8
20% (v/v) glycerol
2% (w/v) SDS
2.5% (w/v) Iodoacetic acid (Added immediately prior to use)
Store at –20°C

Laemmli Running Buffer
25 mM Tris-HCl, pH 8.3
192 mM glycine
1% (w/v) SDS

Laemmli Loading Buffer
200 mM Tris-HCl, pH 6.8
40% (v/v) glycerol
2.9 M βME

8% (w/v) SDS
0.01% (w/v) Bromophenol Blue

MES Sorbitol Buffer
50 mM MES, pH 5.8
400 mM sorbitol
2 mM $CaCl_2$

Low-Salt TAN Buffer
20 mM Tris-HCl, pH 7.0
20 mM NaCl
0.5 mM EDTA
1.2 mM spermidine
7 mM 2-mercaptoethanol (βME)
0.4 mM PMSF/PTSF (Added immediately prior to use)
1% Protease Inhibitor Cocktail (PIC) (Added immediately prior to use)

High-Salt TAN Buffer
20 mM Tris-HCl, pH 7.0
2 M NaCl
0.5 mM EDTA
1.2 mM spermidine
7 mM 2-mercaptoethanol (βME)
0.4 mM PMSF/PTSF (Added immediately prior to use)
1% PIC (Added immediately prior to use)

Phenyl-Sepharose Elution Buffer
50 mM Tris-HCl, pH 8.0
50% Methanol
10 mM NaCl
1 mM EDTA
0.4 mM PMSF/PTSF (Added immediately prior to use)
1% PIC (Added immediately prior to use)

Overlay Agarose Buffer
1X XT-MES running buffer (Bio-Rad, Hercules, CA)
0.75% (w/v) agarose
0.002% Bromophenol Blue

PBS blocking Buffer
5% (w/v) non-fat dry milk dissolved in PBS

Phosphate Buffered Saline (PBS)
137 mM NaCl

2.7 mM KCl
4.3 mM Na_2HPO_4
1.4 mM KH_2PO_4
0.1% (v/v) Triton X-100
Adjust pH to 7.4 with 1M HCl

SSC (1X)
150 mM NaCl
15 mM sodium citrate, pH 7.0

TBE Buffer
89 mM Tris, pH 8.3
2 mM EDTA
89 mM boric acid

2D IPG Rehydration Buffer
7 M urea
2 M thiourea
50 mM DTT
4% CHAPS
0.0002% Bromophenol Blue
0.066% 3-10 ampholytes
0.133% 5-8 ampholytes
1% PIC
0.4 mM PMSF/PTSF
Store buffer at –20°C
DTT, PIC, PMSF/PTSF, and ampholytes added immediately prior to use

Cultures

Glycine max Cell Line SB-M

The SB-M suspension cell line was developed by Widholm *et al.* from *Glycine max* (L.) Mer. V. Corsoy [248]. SB-M cells were grown photomixotrophically in KT medium supplemented with sucrose. Cells were grown in 2L Erlenmeyer flasks with approximately 500-600 mL of medium shaking at 160 RPM. The cell line was maintained under constant lighting at an intensity of 45 $\mu E \cdot m^{-2} \cdot s^{-1}$ using eight 34 W fluorescent bulbs. The cell line was diluted 1:2 with KT medium every

seven days. The cell line was used for preparation of various cellular extracts as well as in nucleoid and chloroplast isolations.

Plants

Arabidopsis thaliana ecotype Columbia. *Arabidopsis* seeds were surface sterilized prior to sowing by vigorously mixing them in a solution containing 70% ethanol for 60 sec, followed by 10 min in a 10% bleach solution. The seeds were washed four times in sterile water and suspended in a sterile solution of 0.1% agarose. The seeds were sown on *Arabidopsis* Growing Medium. The flats were wrapped in SaranWrap and several slots were made to allow for gas exchange. To synchronize germination, the flats were incubated at 4°C for 96 hours. After germination, the plants placed on a 12 h light/dark cycle at 22-25°C with a photosynthetic light flux of 150 $\mu E \cdot m^{-2} \cdot s^{-1}$.

Seed viability was assessed by plating *Arabidopsis* seeds onto solid Germination Medium. Plates were grown vertically under a light intensity of ~150 $\mu E \cdot m^{-2} \cdot s^{-1}$ and a 12 h light/dark cycle. Seed from the 1223 SAIL line was grown on GM supplemented with BASTA for selection of T-DNA containing plants.

Glycine max Mer. V. Corsoy. Soybean seed was obtained from the National Plant Germplasm Center in Beltsville, MD. The seeds were washed in a 10% bleach solution for 10 min, rinsed in water and planted in *Arabidopsis* Growing Medium. Soybeans were grown with a 12 h light/dark cycle with a photosynthetic light flux of 150 $\mu E \cdot m^{-2} \cdot s^{-1}$.

Methods

Preparation of Arabidopsis Soluble Protein Extracts. Arabidopsis leaves and roots were routinely harvested five hours into the light cycle. Plant material was ground for approximately 30 s in 800 μl Buffer A per gram of fresh weight. The extract was subjected to a centrifugation step of 10,000*xg* for 10 min at 4°C. The supernatant was dispensed into aliquots and stored at –80°C until further use.

Protein Analysis. Protein concentration was measured according to the dye binding assay of Bradford using BSA as a standard [249]. One-dimensional protein gel electrophoresis was performed using homemade 7.5% reducing denaturing polyacrylamide gels (SDS-PAGE) [250]. Gels were rinsed in distilled water for 15 min prior to staining with Gel Code Blue for 60 min. Gels were destained overnight in distilled water.

Isoelectric Focusing Sodium Dodecyl Sulfate-Polyacrylamide Gel Electrophoresis (IEF)/SDS-PAGE or 2D) Sample Preparation. Nucleic acids were removed from 2D samples by digestion with 20 U of DNase I at room temperature for 30 min. Protein precipitation occurred after the addition of one volume of 10% trichloroacetic acid (TCA) in acetone and incubated at –20°C for 90 min. The resulting precipitate was centrifuged at 10,000xg for 5 minutes. The pellet was washed twice in cold acetone and dried in a SpeedVac concentrator. The pellet was resuspended in 125 μl of 2D IPG Rehydration Buffer, shaken

vigorously for 15 min, and incubated at 30°C for 60 min. This was then centrifuged at 10,000xg for 5 min and the supernatant collected. To the pellet, 55 μl of 2D IPG Rehydration buffer was added, vigorously shaken, and incubated at 37°C for 15 min. The resuspension was centrifuged at 10,000xg for 5 min and the supernatants were pooled and used to rehydrate the IPG strip. Adequate swelling of the IPG gel matrix required at least 16 h for the IPG strip to rehydrate. Eleven cm IPG strips covering a pH range of 3-10 were used for IEF analysis.

IEF/SDS-PAGE. Isoelectric focusing occurred in three stages. Throughout the run a temperature of 20°C and a maximum current of 50 μAmp per strip were maintained. A preconditioning stage (250 V; 20 min) was used to remove contaminating charged compounds. A linear voltage ramping stage of isoelectric focusing was conducted with a maximum voltage of 8,000 V for a total period of 10,000 V·h, which was followed by a rapid voltage ramping stage for 25000 V·h. The strips were removed from the isoelectric focusing tray and excess mineral oil was removed. The strips were then incubated in 5 ml of IEF Strip DTT Equilibration Buffer for 10 min, followed by incubation with IEF Strip Iodoacetic Acid Equilibration Buffer. The strips were immersed briefly in XT-MES Running Buffer, placed onto a 4-12% Bis-Tris gradient gel and covered with overlay agarose. Electrophoresis was conducted at 150 V for 90 min. 2D gels were fixed overnight, washed for 6 hours with distilled water, and visualized by silver staining for approximately 7 min.

Transfer of Protein to Nitrocellulose. Gels were incubated in freshly prepared, chilled Transfer Buffer for 15 min and transferred to nitrocellulose (pore size 0.2 μm). Homemade 7.5% reducing, denaturing gels were transferred at 100 V for 90 min. Bis-Tris gradient gels were transferred at 70 V for 45 min.

Development of the Immunoblot. Nitrocellulose was incubated with PBS Blocking Buffer for 45 min followed by one-hour incubation with the primary antibody (αSiR chicken IgY 1:300, or αSiR rabbit 1:6,000 dilution). The blot was washed successively (15 min each) in PBS, PBS Blocking Buffer, and PBS, then incubated for 60 min with a secondary antibody conjugated to horseradish peroxidase (αchicken goat HRP conjugate 1:250,000, or αrabbit goat HRP conjugate 1:12,000 dilution). The blot was washed successively (15 min) in PBS, PBS Blocking Buffer, and PBS and developed in 0.125 ml/cm^2 of ECL substrate. The blot was wrapped in SaranWrap® and photographed.

Chloroplast Isolation from SB-M Suspension Cells. SB-M cells were routinely harvested two days post transfer into fresh medium as a source for chloroplast preparations, as outlined by Cannon et al. [1]. Approximately 125-250 g of SB-M cells were collected on a fritted glass filter, washed and resuspended in approximately 400 ml of MES-Sorbitol Buffer. Cellulysin cellulase was added to 0.2% (w/v) and incubated at 37°C for 2-3 hours to partially digest the cell walls. The cells were resuspended in the same volume of HEPES-Sorbitol Buffer and further disrupted with three passes using a Dounce homogenizer (shaft A), followed by filtration through 53 μm nylon mesh netting. The homogenate that

remained was again resuspended, disrupted with the Dounce homogenizer, and filtered with the 53μm nylon mesh. This step was repeated twice more, and then the filtrate was passed over a 20μm nylon mesh netting. The filtrate was centrifuged at 150*xg* for 8 min to remove ruptured cell wall debris. The supernatant was then centrifuged at 1,400*xg* for 10 min to pellet chloroplasts. The pellet was carefully resuspended in 30 ml of HEPES-Sorbitol Buffer using a small paintbrush, and centrifuged at 750*xg* for 10 min to pellet chloroplasts. The pellet was stored at –80°C until further use.

Chloroplast Isolation from Arabidopsis thaliana. Arabidopsis leaves (approximately 150 g) were placed in a Braun blending unit and homogenized in 30 ml HEPES-Sorbitol Buffer for approximately 10 sec. This homogenate was filtered through four layers of Miracloth®. The retained leaf matter was homogenized a second time in HEPES-Sorbitol and passed again through the Miracloth®. This procedure was repeated twice more. The filtrate was then passed over a 20 μm nylon mesh netting to remove cell debris, and a clearing spin was performed for 1 min at 300*xg*. Chloroplasts were pelleted by a centrifugation step at 2,500*xg* for 10 min. The chloroplasts were gently resuspended in 30 ml of HEPES-Sorbitol Buffer using a small paintbrush. One final centrifugation step of 2,500*xg* for 10 min was sufficient to isolate chloroplasts. The pellet was stored at –80°C until further use.

Isolation of Chloroplast Nucleoids from SB-M Chloroplasts. SB-M plastid nucleoids were isolated based on the protocol outlined by Chi-Ham et al. [251].

In this method, chloroplasts from 2.5 kg of SB-M cells were resuspended in 100 ml of Nucleoid Isolation buffer and Nonidet P-40 was slowly added to a final concentration of 2%. The chloroplasts were stirred for 30 min at room temperature and subsequently centrifuged at 7,800*xg* for 30 min to pellet nucleoids. The pellet was resuspended in 50 ml of Nucleoid Isolation Buffer and Nonidet P-40 was added to 2%. The suspension was stirred for 30 min and centrifuged at 7,800*xg* for 30 min. This step was repeated twice more, except in the final step no Nonidet P-40 was added.

RNA Isolation from Arabidopsis thaliana. Approximately 100 mg *Arabidopsis* tissue was frozen in liquid nitrogen and ground with a mortar and pestle. The powder was transferred to a cold microfuge tube, to which 500 μl of Plant RNA Purification Reagent was added and mixed vigorously. The tube was incubated for 5 min at room temperature and the suspension was clarified by centrifugation for 2 min at 12,000*xg*. The supernatant was removed, and 100 μl of 5 M NaCl and 300 μl of chloroform were added to the solution. After thorough mixing by inversion, the sample was centrifuged for 10 min at 12,000*xg*. One volume of cold isopropyl alcohol was added to the supernatant and the mixture was allowed to stand at room temperature for 10 min. The RNA was pelleted by centrifugation step at 12,000*xg* for 10 min. Salt was removed by washing the pellet in 1 ml of 75% ethanol. The RNA was again pelleted by centrifugation of 12,000*xg* for 1 min. The remaining solvent was removed by centrifugation in the

SpeedVac® concentrator, and the RNA was stored at –80°C until further use (typically no more than 4 days after isolation).

Northern Blotting. Transcript abundance was analyzed by using 10 μg of total RNA for electrophoresis on a 1.5% agarose gel containing 0.41 M formaldehyde and 1 X MOPS Running Buffer. Gel electrophoresis was conducted at 70 V for 4.5 h and rinsed in 500 ml of DEPC-treated water for 15 min. The gel was transferred to a nylon membrane by gravity-assisted flow. The blot was irradiated on a UV transilluminator for 2 min to fix the RNA to the membrane and incubated in DNA Prehybridization Solution for 100 min at 42°C. Denatured *sir* and *act2* gene probes were added and allowed to hybridize for 24 h. The blot was washed twice in 16 ml of 2 X SSC, 0.1% SDS for 5 min (22°C), and then washed twice in 0.2 X SSC, 0.1% SDS for 15 min at 42°C, and twice more at 68°C. The PhosphoScreen® was exposed to the blot for 24 hours and densitometry was performed using Bio-Rad's QuantityOne software.

Preparing the Northern Blotting Probes. Radioactive probes were generated using the Prime-A-Gene labeling system from Promega according to t to the manufacturer's instructions. Unincorporated label was removed using a homemade G-50 spin column. Typically, probes with a specific activity of 1 X 10^7 cpm/μl were used for hybridization.

DNA Compaction Assay. A 25 μl reaction containing 1 X DNA-Binding Buffer, 500 ng of pUC19 plasmid DNA, 0.1 μg/μl 4,6'-diamidinophenolindole (DAPI), and

3.5 μg rAtSiR were incubated overnight at 4°C. Compaction was assessed using epifluorescence microscopy at 100X magnification [2].

Generation of Polyclonal Antisera. Recombinant AtSiR was gel-purified on a 7.5% SDS-PAGE. The gel was rinsed in distilled water and stained with 0.05% aqueous Coomassie Blue for 10 min. The gel was then washed extensively in distilled water and the 63 kDa band was excised. Rabbit inoculation of 100 μg of rAtSiR was followed by four 50-μg boosts of the same antigen over a period of two months. Cocalico Biologicals, Reamstown, PA handled all aspects of animal inoculation, boosting, and bleeds.

In Silico Data Mining. The SiR gene sequences from *Arabidopsis thaliana* (CAA71239), *Nicotiana tabacum* (BAA33796), *Glycine max* (AAG59996), *and Pisum sativum* (BAD12837) were obtained from NCBI. Promoter analysis was performed using the *Arabidopsis* Gene Regulatory Information Server (AGRIS) [252, 253]. Phosphorylation predictions based on the primary sequence of mature AtSiR (without the N-terminal signal sequence) was performed using NetPhos [254, 255]. Sequence alignment and analysis were performed using ClustalX and MEGA 3.0.

DNA Isolation. DNA extraction for PCR was performed using the REDExtract-N-Amp Plant PCR Kits from Sigma. DNA was extracted from a small disk of tissue from *Arabidopsis* leaves according to the manufacturer's instructions. Plasmid DNA was isolated using a Qiagen Plasmid Extraction Kit according to the manufacturer's instructions.

Polymerase Chain Reaction (PCR) of β-Actin Gene. The AACTF and AACTR primers (Table 2) were used to amplify a 669 bp fragment of exon 3 from the β-actin gene of *Arabidopsis*. This PCR reaction contained 1X *Pfu* polymerase buffer, 1.25 U of *Pfu* DNA polymerase, 0.8 mM dNTPs, and 1.3 μM of each primer. DNA extracted from an *Arabidopsis* leaf disc was used as template in this reaction. This reaction underwent 30 cycles of 95°C for 20 sec, 57.3°C for 30 sec, and 72°C for 2 min.

PCR of Detection of the T-DNA Insertion. A PCR reaction was used to determine the genotype of the 1223 SAIL line mutant plants. To accomplish this task, two PCR reactions were performed using DNA extracted from a leaf disc of the mutant plants. The first PCR reaction determined the presence of a T-DNA insert in the *sir* gene. The AtKoR and TMRI-LB2 primers (Table 2) were used to amplify a 3.7 Kbp fragment containing a portion of the T-DNA border. This PCR reaction contained 1X *Ex Taq* polymerase buffer, 1.25 U of *Ex Taq* polymerase, 0.8 mM dNTPs, and 1.3 μM of each primer. This reaction was thermocycled through 30 cycles of 94°C for 18 sec, 57.3°C for 30 sec, and 69°C for 3 min. If DNA isolated from a 1223 SAIL mutant plant generated a 3.7 Kbp PCR amplimer, then this indicated the test plant was not a wild-type plant.

A second PCR reaction was used to determine if the mutant plant was homozygous or heterozygous, by detecting the presence of a wild-type *sir* gene. The AtSiRF and AtSiRR primers (Table 2) were used to amplify a 2.4 Kbp fragment of the wild-type *sir* gene. This fragment included the T-DNA insertion

Table 2. Primer Sequences.

Primer Name	Sequence	Tm (°C)	Direction
AtKoR	5'-CAGTTCAGACAGAGACATTACATTACATGA-3'	62.9	Reverse
AtSiRF	5'-CGGCACAACCGCCTGAACAGAAGTG-3'	67.5	Forward
AtSiRR	5'-AGGCGAAGAACTCGACGAAGAAGCGG-3'	67.4	Reverse
AACTF	5'-TCTTGACCTTGCTGGACGTGAC-3'	61.5	Forward
AACTR	5'-TGTGAACGATTCCTGGACCTGC-3'	61.5	Reverse
TMRI-LB2	5'-GCTTCCTATTATATCTTCCCAAATTACCAATACA-3'	65.6	Forward

site, which, if present, would prevent amplification of the wild-type allele. This PCR reaction contained 1X *Ex Taq* polymerase buffer, 1.25 U of *Ex Taq* polymerase, 0.8 mM dNTPs, and 1.3 μM of each primer. This reaction was thermocycled through 30 cycles of 94°C for 20 sec, 57°C for 30 sec, and 69°C for 3 min. In a final step, the extension time was lengthened to 10 min. If DNA from a test plant generated both a 3.7 Kbp product from the first PCR and a 2.4 Kbp product from the second PCR, then the plant was considered a heterozygous mutant.

Expression of AtSiR Containing Siroheme. The C-terminus of AtSiR was fused, via a self-cleaving intein, to a chitin-binding domain to facilitate purification (vector construction and transformation performed by C. Chi-Ham) [81]. *E. coli* does not naturally express sufficient amounts of siroheme to support the demand for heme following induction, and therefore the proteins lack this cofactor. To circumvent this difficulty, the construct was co-expressed with *cys*G, which encodes an enzyme involved in porphyrin biosynthesis.

E. coli cotransformed with the AtSiR and *cys*G constructs was grown at 37°C in Terrific Broth with stirring but without aeration until reaching an OD_{600} of 0.5 to 0.8. The cultures were incubated at 16°C for 16 h after the addition of 0.5 mM isopropylthiolgalactoside (IPTG) and 0.2 mM δ-aminolevulinic acid (δ-ALA). The cultures were spun at 5,000*xg* for 10 min and the pellet was resuspended in 50 ml of Chitin Column Buffer. The cells were disrupted using a French press and a clarification step was performed by centrifugation at 20,000*xg* for 30 min to pellet insoluble material. The supernatant was batch-adsorbed to 6 ml of chitin affinity resin for 3 h at 4°C on a rotating drum. The resin/supernatant mix was poured into a column and washed with 5 bed volumes of Column Buffer containing 1 M NaCl, 5 bed volumes of Chitin Column Buffer containing 1.5 M NaCl, 10 bed volumes of Chitin Column Buffer containing 1 M NaCl, and 10 bed volumes of Chitin Column Buffer containing 0.5 M NaCl. Passing 3 bed volumes of Cleavage Buffer over the resin induces self-cleavage of the intein. The column was incubated at 4°C for 40 h and eluted with Chitin Column Buffer in 3 ml fractions. The fractions were dialyzed and analyzed for impurities on a 7.5% SDS-PAGE. The presence of a single band on a silver stained gel at 63 kDa indicated the presence of rAtSiR.

Isolation of Chloroplast Nucleoids from Arabidopsis thaliana. Three *Arabidopsis* chloroplast pellets were resuspended in 11.5 ml of Low-Salt TAN buffer and stirred until the suspension reached room temperature. The chloroplasts were lysed by the slow addition of Nonidet P-40 to a final

concentration of 2% and stirred for an additional 30 min. The suspension was centrifuged at 3,000*xg* for 10 min and the supernatant was carefully removed and spun at 48,000*xg* for 40 min to pellet the nucleoids. The supernatant was decanted and the pellet was frozen at –80°C.

Purifying Chloroplast Nucleoid Proteins from Arabidopsis thaliana. The *Arabidopsis* nucleoid pellet was resuspended in 3 ml of chilled High-Salt TAN Buffer. The suspension was mixed for 15 min and passed twice through a syringe fitted with a 23 g needle, after which it was centrifuged at 7,800*xg* for 10 min. The supernatant was saved and the pellet resuspended in 0.6 ml of High-Salt TAN Buffer. The nucleoid proteins were stored at –80°C until further use.

Analysis of the Portion of SiR Distributed to Plastid Nucleoids. The protocol used to determine the distribution of SiR is outlined in Figure 6. Leaves were ground in liquid nitrogen and resuspended in Low-Salt TAN Buffer containing Nonidet P-40 to solubilize membranes. A centrifugation step was used to separate the soluble proteins from the insoluble material, including nucleoids. The volume of the supernatant was determined and the pellet was resuspended in an equivalent volume of High-Salt TAN Buffer to disrupt the electrostatic interactions between ctDNA and nucleoid proteins. The resuspension was batch-adsorbed to pre-equilibrated phenyl-sepharose resin used in the purification of DCP68/SiR [2].

The phenyl-sepharose resin was washed twice with High-Salt TAN Buffer to remove unbound proteins. Bound proteins were eluted from the column in a

Phenyl-Sepharose Elution Buffer that contained 50% methanol to disrupt the hydrophobic interaction. The fraction enriched for nucleoid-bound SiR was subjected to vacuum centrifugation to remove the methanol and was subsequently resuspended to the initial volume with methanol-free Phenyl-Sepharose Elution Buffer.

The portion of SiR distributed to plastid nucleoids was determined by analyzing an equivalent volume of nucleoid-enriched as well as soluble SiR fractions by quantitative immunoblotting. The signal intensity of SiR in each fraction was calculated as a percentage of the total SiR.

Epifluorescence Microscopy of Arabidopsis Leaves. Leaves were cut into small pieces and fixed in a solution containing 5% glutaraldehyde, 4% formaldehyde, and 25 mM Phosphate Buffer (pH 7.2) for 2 h. The leaf material was rinsed in buffer containing 100 mM glycine to quench the reaction, and placed onto poly-lysine coated slides, stained with 0.5 μg/ml DAPI, covered with a solution of antifade reagent, and allowed to dry overnight.

CHAPTER IV

RESULTS

The plastome is compacted by DNA-binding proteins into the nucleoid, the site of organellar DNA replication and transcription. Plastid nucleoid protein composition changes during plastid development but the mechanism by which these proteins affect nucleoid structure and function has not been examined thoroughly. The current research aims to identify the molecular basis of the interaction between an abundant plastid nucleoid protein and ctDNA. SiR is an enzyme of the sulfur assimilation pathway that moonlights as a chloroplast DNA-binding nucleoid protein. Therefore, a study was undertaken to characterize the distribution, abundance, and potential post-translational modifications of SiR in *Arabidopsis* and soybean plants. These experiments were designed to determine the regulation and biological significance of the interaction between SiR and ctDNA.

4.1 Detection of SiR in *Arabidopsis* Chloroplast Nucleoids

DCP68/SiR is an abundant protein present in purified SB-M chloroplast nucleoids [1, 2]. An effort was therefore made to isolate *Arabidopsis* chloroplast nucleoids and to evaluate its presence in other model plants. After chloroplasts were isolated from mature *Arabidopsis* leaves, they were resuspended in the buffer used to isolate SB-M chloroplast nucleoids. The chloroplast membranes were solubilized by the addition of detergent and the solution was centrifuged at

7,800*xg* in an attempt to pellet the chloroplast nucleoids. However, no SiR was detected on immunoblots of the chloroplast nucleoid-enriched fractions. In addition, there was not a significant amount of DNA present in chloroplast nucleoid-enriched fractions. The DNA within chloroplast nucleoids was stained using the fluorophore 4',6-diamidino-2-phenylindole (DAPI), which fluoresces bluish-white upon binding to DNA. These observations suggested there may be fewer *Arabidopsis* chloroplast nucleoids or they may be structurally different from those observed in SB-M cells. Therefore, a method was adapted from protocols used to isolate plastid transcriptionally active chromosomes (TACs), which may represent partially unwound nucleoids [48]. A centrifugal force of 48,000*xg* was necessary to pellet *Arabidopsis* chloroplast nucleoids, rather than the 7,800*xg* used in SB-M nucleoid isolation. The presence of SiR in chloroplast nucleoid fractions was confirmed by immunoblotting. An *Arabidopsis* chloroplast nucleoid-enriched fraction displayed a 63 kDa band of moderate intensity corresponding to the expected molecular weight of the AtSiR monomer (Figure 1). The relative amount of SiR present in the 48,000*xg* supernatant was, however, higher than in the 48,000*xg* pellet, suggesting that most of the SiR was present as a soluble protein in mature leaf chloroplasts of *Arabidopsis*. The additional bands in the immunoblot of the 48,000*xg* supernatant are proteins that exhibit immunological crossreactivity to the SiR antiserum.

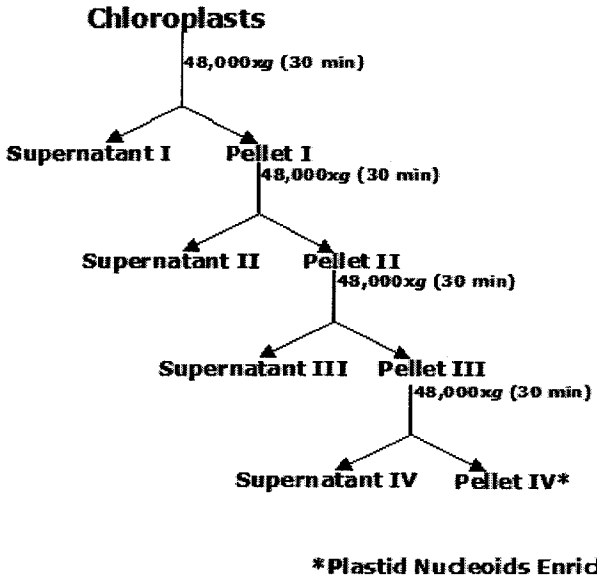

Figure 1. *Arabidopsis* Chloroplast Nucleoid Purification Scheme. Flow chart outlining the protocol used to isolate *Arabidopsis* chloroplast nucleoids.

Fraction	Protein (mg)	ctDNA (mg)	Protein/DNA
Chloroplasts	23.6	61.3	0.4
48000xg pellet I	10.2	42.4	0.2
48000xg super I	75.8	72.7	1.0
48000xg pellet II	6.2	43.0	0.1
48000xg super II	9.8	12.3	0.8
48000xg pellet III	2.4	39.0	0.1
48000xg super III	9.4	8.3	1.1
48000xg pellet IV (Ct Nucleoids)	6.1	34.4	0.2
48000xg super IV	0.1	2.1	0.0
2M super (Nucleoid Proteins)	0.5	1.2	0.4
2M pellet (CtDNA)	5.4	32.8	0.2

Table 3. Protein/DNA Ratio of Fractions During Nucleoid Isolation.

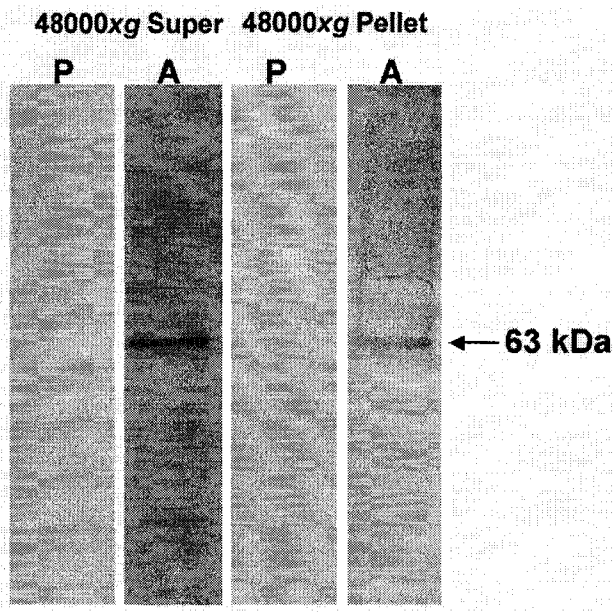

Figure 2. Identification of SiR in *Arabidopsis* Nucleoids. Immunoblots of approximately 24 μg of the 48,000*xg* pellet I and supernatant I fractions probed with (**A**) SiR antiserum raised in chicken or (**P**) preimmune serum.

The relatively low abundance of SiR in the nucleoid-enriched fraction was somewhat surprising. DCP68/SiR is an abundant nucleoid protein in SB-M cells and was detected on an immunoblot of 1 μg of SB-M nucleoid proteins (data not shown). However, the immunological detection of SiR in the *Arabidopsis* nucleoid-enriched fraction required a significantly higher protein load (Figure 1). This may be due to differences in the purity of nucleoid preparations that was attainable. Whereas SB-M nucleoids can be purified, the isolated *Arabidopsis* nucleoids may have contained contaminating membrane proteins, as judged by the green color of the nucleoid pellet. Alternatively, SiR may not be an abundant chloroplast nucleoid protein in *Arabidopsis*.

4.2 Abundance of SiR in *Arabidopsis*

No comprehensive study of the abundance of SiR has been published, but some previous experimental observations suggest that the abundance of this plastid nucleoid protein might affect nucleoid function [1, 2, 82]. There are well-documented differences in nucleoid compaction and organellar distribution in young and mature chloroplasts, which may be related to differences in nucleoid protein composition [32, 53, 72, 256]. Moreover, *in vitro* studies demonstrating that AtSiR inhibits DNA synthesis in a concentration-dependent manner suggest that the abundance of SiR affects the activity of nucleoid-associated processes [1]. Therefore, the transcript and protein abundance of SiR was analyzed in young and mature *Arabidopsis* plants.

4.2.1 Relative SiR Protein Abundance. Due to the limited amount of SiR in isolated *Arabidopsis* nucleoids, the abundance of SiR was analyzed in soluble leaf and root protein extracts by quantitative immunoblotting. Protein extracts were separated by SDS-PAGE, transferred to nitrocellulose and probed with polyclonal antiserum raised against rAtSiR. The signal intensity was quantified by densitometry and normalized to the level of SiR present in mature leaves. Immunoblots had a single band with an estimated molecular weight of 63 kDa, corresponding to the AtSiR monomer (Figure 2A). Mature roots and leaves possessed equivalent soluble-SiR protein levels (Figure 2B); young leaves contained approximately 20% less soluble SiR, while the relative abundance of

soluble SiR in young roots was less than 10% of that in mature leaves.

4.2.2 Relative SiR Transcript Abundance in Arabidopsis. Bork *et al.* found that the transcript abundance of SiR was higher in leaf tissue than in roots [83, 257]. However, this research did not make use of a Northern blotting control gene to normalize the gene expression data and only examined SiR transcripts in mature plants. Therefore, the SiR transcript abundance was determined in young and mature *Arabidopsis* tissues.

4.2.2.1 Generation of a β-actin gene probe. In addition to probing the gene of interest, Northern blots must also probe a control gene in order to account for differences in the quality of RNA preparation and in RNA amounts loaded onto agarose gels. Although there is no gene that is uniformly expressed under all growth conditions and in all tissues, β-actin is used by many investigators to standardize Northern hybridizations [258]. Genomic DNA was prepared from a leaf disc to amplify a portion of exon 3 from the β-actin gene from *Arabidopsis*. A PCR reaction with primers AACTF and AACTR (Table 2) yielded a product close to the expected size of 669 bp (Figure 3A). To confirm the product was correctly inserted into the vector, a restriction digest analysis was performed on plasmid DNA isolated from three colonies, two of which were shown to possess the insertion (Figure 3B).

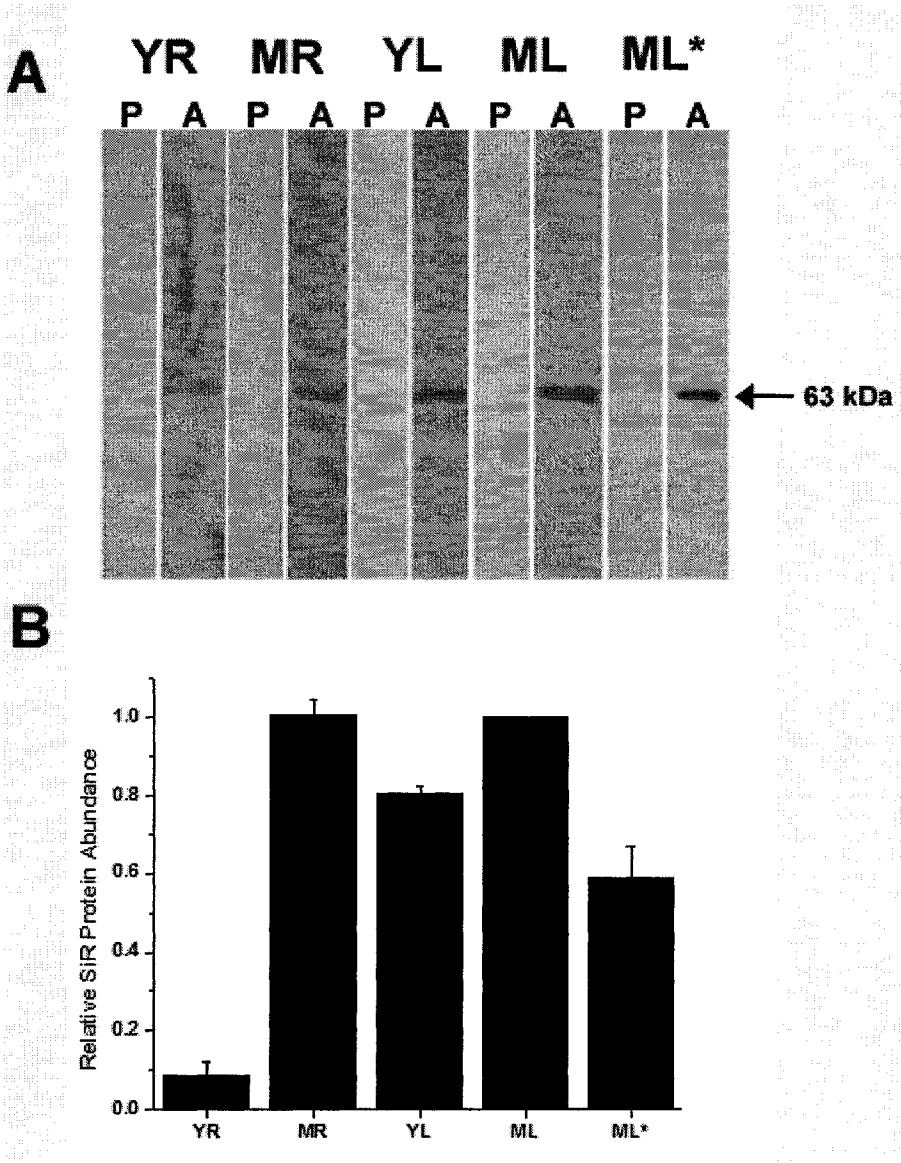

Figure 3. AtSiR Protein Abundance in Roots and Leaves.
Panel A: Representative immunoblot signals from 5 μg of soluble protein isolated from *Arabidopsis* tissues (**YR**=Young Roots; **MR**=Mature Roots; **YL**=Young Leaves; **ML**=Mature Leaves; **ML***=Mature Heterozygous 1223 SAIL Mutant Leaves; **P**=Preimmune serum; **A**=SiR antiserum raised in chicken)
Panel B: Relative SiR protein abundance normalized to the value in mature leaves. The error bars represent that standard error of signal intensity from at least three independent preparations of soluble leaf extracts.

from young and mature plants. Northern blot analyses were performed using three different sets of independently prepared RNA. The signal intensity ratio of β-actin to SiR was calculated for each sample and normalized to the ratio observed in mature leaves. The results of these analyses indicated that the SiR transcript abundance was highest in mature leaf tissue. The SiR transcript abundance in young leaves was approximately two-thirds of that in mature leaves, whereas the SiR transcript abundance in young and mature roots was less than half of that in mature leaves (Figure 5).

Taken together with the results from the SiR protein abundance study, these data suggested that SiR was regulated differently in leaf and root tissues. The SiR transcript abundance in young and mature leaves was similar to level of SiR protein that accumulated in the leaves at these two developmental stages. This could indicate that the abundance of SiR was controlled primarily at the level of gene transcription in leaf tissues. This is in contrast to observations in root tissues. In young and mature roots, the SiR transcript abundance was approximately equal, but SiR protein accumulated to significantly higher levels in mature roots. These data suggested that in roots, the abundance of SiR was controlled at the post-transcriptional level.

4.3 Distribution of SiR to Chloroplast Nucleoids in *Arabidopsis*

The SiR signal present on immunoblots of the nucleoid-enriched 48,000*xg* pellet and 48,000*xg* supernatant, obtained from the *Arabidopsis* chloroplast nucleoid isolation, suggested that most SiR was soluble in mature leaves (Figure 1).

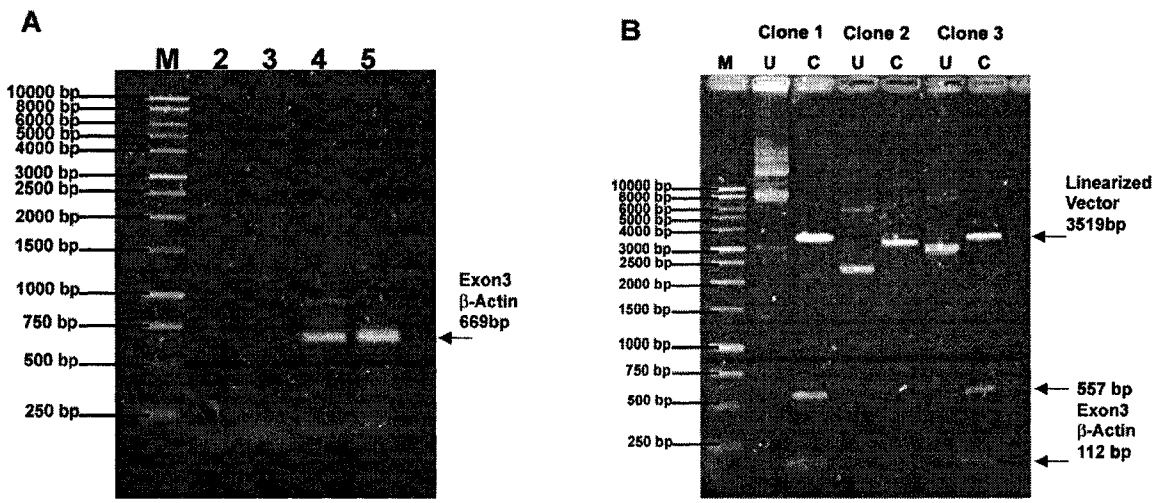

Figure 4. Cloning of β-Actin Exon 3 from *Arabidopsis*.
Panel A: The PCR reaction products of *Arabidopsis* DNA primed with AACTF and AACTR primers were analyzed on a 0.8% agarose gel, stained with ethidium bromide and visualized on a UV transilluminator. M indicates the molecular weight marker, 2 is the no-template negative control, and 3-5 are independent PCR reactions.
Panel B: Three clones were analyzed by restriction digestion. Two EcoRI restriction sites flank the β-actin exon 3 insertion site in the plasmid, and one EcoRI site cleaved the inserted DNA into two fragments. Digestion of clones 1 and 3 revealed fragments of the expected size for the cloned β-actin exon 3 fragment. The letter U or C indicates whether the reactions were performed in the absence or presence of restriction endonuclease, respectively.

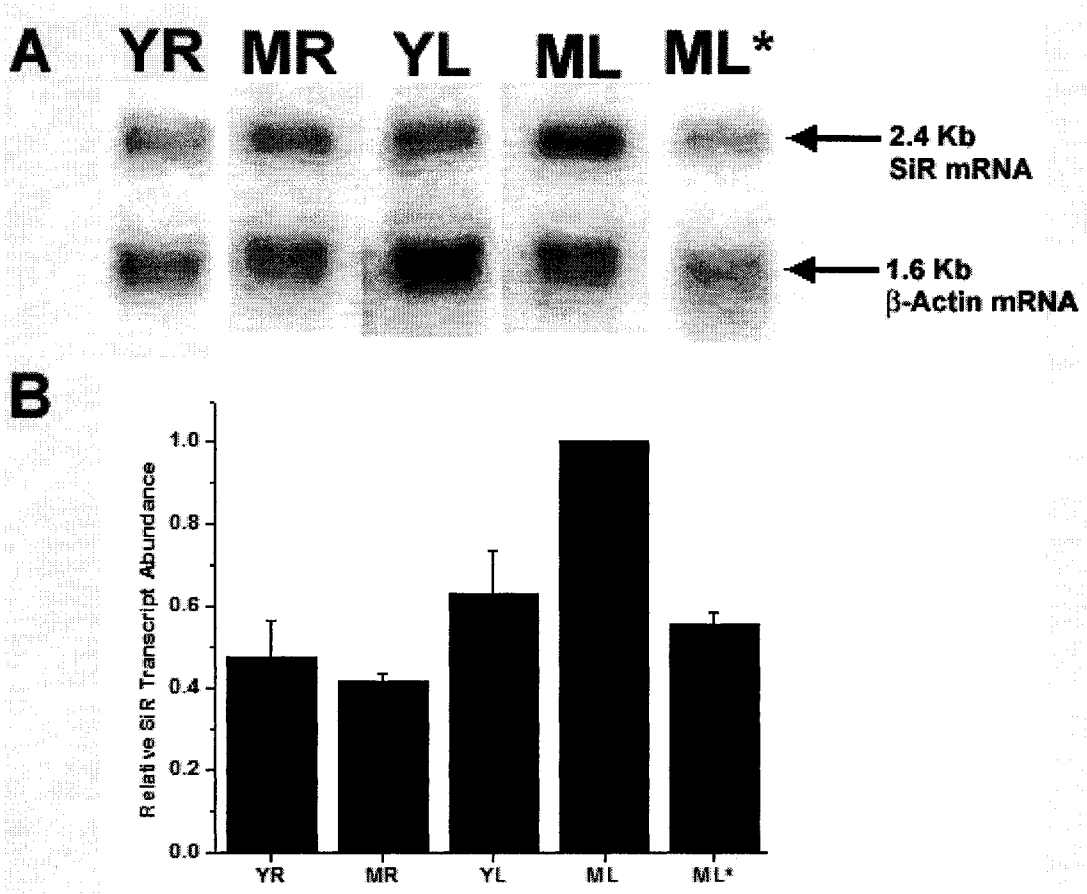

Figure 5. Relative SiR Transcript Abundance in *Arabidopsis*.
Panel A: Total RNA (10 μg) was prepared from different *Arabidopsis* tissues and blotted onto a nylon membrane. The nylon membrane was hybridized with SiR and β-actin DNA probes for 24 h, washed, and exposed to a Phosphorimager screen.
Panel B: The relative transcript abundance in each tissue sample, normalized to the value in mature leaves. The error bars represent the standard error of transcript abundance in at least three independent RNA preparations from *Arabidopsis*.
(**YR**=Young Roots; **MR**=Mature Roots; **YL**=Young Leaves; **ML**=Mature Leaves; **ML***=Mature Heterozygous 1223 SAIL Mutant Leaves)

Since there are documented changes in nucleoid protein composition that accompany plastid development, it seemed possible that SiR may be associated with chloroplast nucleoids only in young *Arabidopsis* leaves [32]. However, it was not feasible to prepare nucleoid extracts from young *Arabidopsis* leaves, given the small size of *Arabidopsis* and the apparent scarcity of chloroplast nucleoids. If most SiR was nucleoid-associated in young *Arabidopsis* leaves, then it is possible that the amount of soluble SiR in mature leaves might be significantly higher than in young leaves. However, the abundance of soluble SiR in mature *Arabidopsis* leaves was only slightly lower in young leaves (Figure 3). Therefore, the portion of SiR distributed to chloroplast nucleoids was examined in young and mature *Arabidopsis*.

Young or mature *Arabidopsis* leaves were ground in liquid nitrogen and resuspended in buffer containing a detergent to solubilize membranes (Figure 6). The mixture was subjected to a centrifugal force of 48,000*xg* to separate soluble proteins from insoluble material (including chloroplast nucleoids). The insoluble pellet was extracted with a high-salt buffer to disrupt any interactions of proteins with DNA. As noted previously, dialysis of high-salt chloroplast nucleoid extracts results in partial nucleoid re-formation [1]. To prevent this from occurring, the high-salt extracts were batch-adsorbed to phenyl-sepharose resin and then washed with high-salt buffer to elute unbound proteins. The phenyl-sepharose resin was washed with a buffer containing methanol to elute the bound protein.

The portion of SiR distributed to the chloroplast nucleoid-enriched fraction was determined by quantitative immunoblotting. The densitometry of SiR immunoblot signal in the nucleoid-enriched and soluble protein fractions was considered to be 100% and the portion of SiR distributed to the nucleoid-enriched fraction was represented as a percent of the total SiR.

Less than 5% of the total SiR was present in the nucleoid-enriched fraction prepared from mature *Arabidopsis* leaves, which was consistent with the earlier attempt to detect SiR in *Arabidopsis* chloroplast nucleoids (Figure 7). The signal corresponding to soluble SiR in the 48,000*xg* supernatant was considerably stronger than the SiR signal in the 48,000*xg* chloroplast nucleoid-enriched fraction (Figure 2). Surprisingly, there was no detectable nucleoid-associated SiR present in young leaves of *Arabidopsis.* Young leaves are active in cellular and plastid division and are likely undergoing significant plastome amplification [4, 259].

The fact that no nucleoid-associated SiR was detectable in young leaves and only a small proportion of SiR was present in the chloroplast nucleoids of mature *Arabidopsis* leaves raises the possibility that AtSiR may not be a chloroplast nucleoid protein. Cannon *et al.* have commented on the 'sticky' nature of chloroplast nucleoids [1]. Perhaps this resulted in the non-physiological association of SiR with chloroplast nucleoids in *Arabidopsis.* Alternatively, if the association of SiR with chloroplast nucleoids in *Arabidopsis* was correct, why would so little SiR be present in *Arabidopsis* nucleoids.

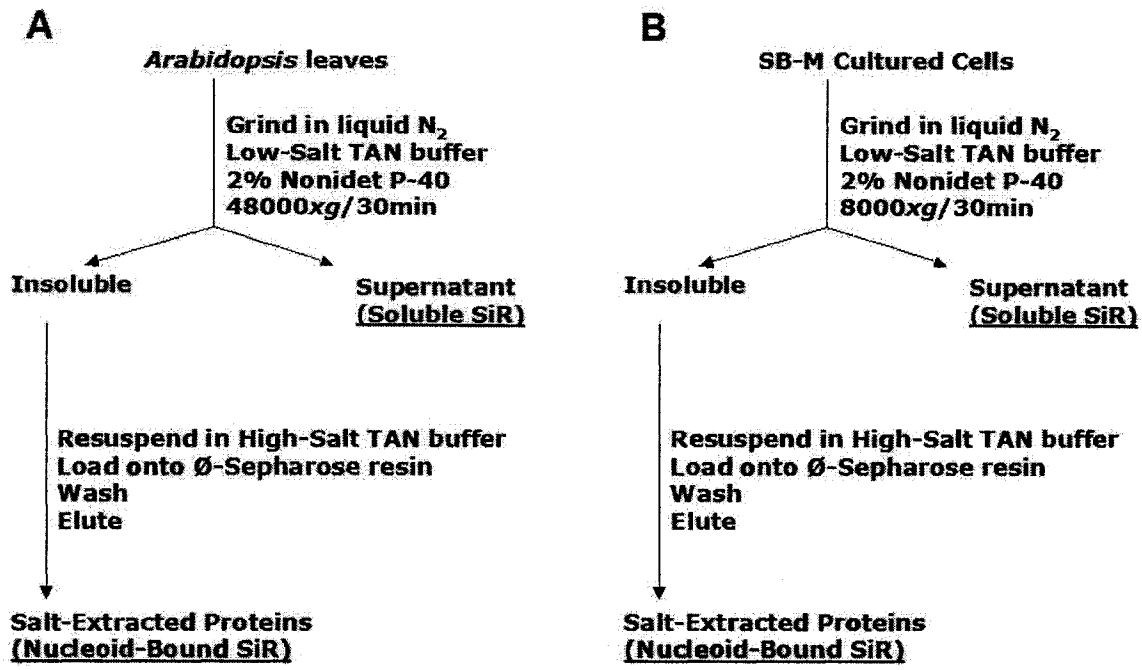

Figure 6. The Portion of SiR Distributed to Chloroplast Nucleoids.
This flow chart outlines the process used to determine the amount of total SiR that was distributed to chloroplast nucleoids from (**A**) Arabidopsis and soybean leaves as well as (**B**) cultured SB-M cells.

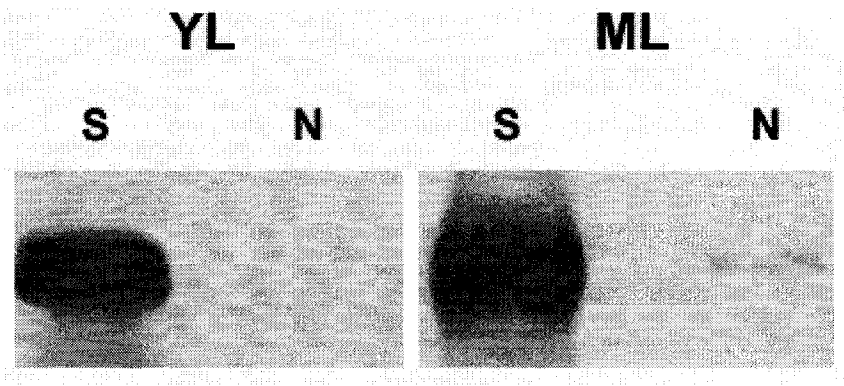

Figure 7. Distribution of SiR in *Arabidopsis*.
Immunoblots of soluble (**S**) and nucleoid-enriched (**N**) fractions isolated from *Arabidopsis* and probed with SiR antiserum (raised in rabbit) demonstrated that less than 5% of the SiR in mature leaves was distributed to the nucleoid. There was no detectable SiR present in the nucleoid-enriched fraction isolated from young leaves of *Arabidopsis.* Young leaf fractions: 83 μg of soluble protein and 0.4 μg nucleoid-enriched protein loaded; mature leaf fractions: 106 μg of soluble protein and 0.9 μg of nucleoid-enriched protein loaded. (YL=Young leaves; ML=Mature leaves)

Immunolocalization data suggested that virtually all SiR is nucleoid-associated in young pea and SB-M chloroplasts [2].

4.4 *Arabidopsis* SiR DNA Compaction Assay

Purifying sufficient amounts of AtSiR to test for DNA binding would be problematic due to the absence of an established protocol to purify *Arabidopsis* nucleoids, the limited amount of SiR present in *Arabidopsis* chloroplast nucleoids, and the small size of the plant. Although it would be possible to adapt

the method used to purify soluble spinach SiR, the soluble *Arabidopsis* SiR may not bind DNA, if enzymatic activity and the DNA-compacting activity of AtSiR are mutually exclusive and regulated accordingly. As a first step towards examining the possibility that AtSiR may not be a chloroplast nucleoid protein, the DNA-compacting activity of recombinant AtSiR was examined *in vitro*.

Chi-Ham *et al.* determined that the recombinantly expressed AtSiR did not bind DNA in a DNA-compaction assay [260]. It was believed that this was related to the lack of siroheme in rAtSiR. Co-expression of *cysG* with AtSiR was necessary to express catalytically active recombinant maize SiR that contained siroheme [261]. The *E. coli cysG* gene product is uroporphyrinogen III methyltransferase, the rate-limiting enzyme in siroheme biosynthesis. However, coexpression of AtSiR and *cysG* did not yield a recombinantly expressed AtSiR that contained siroheme [260]. To express an enzymatically active recombinant spinach nitrite reductase (NiR), it was necessary to culture the transformed *E. coli* in Terrific Broth with stirring but without aeration [262]. In addition, the porphyrin precursor, δ-amino levulinic acid (δ-ALA), was added when the culture was induced. Arabidopsis SiR and nitrite reductase have an amino acid sequence homology of approximately 44% [2].

When AtSiR was co-expressed with *cysG* under these conditions, a 63 kDa protein exhibited the signature siroheme absorbance peaks at 386 and 587 nm (Figure 8) [263, 264]. A subsequent assay demonstrated that rAtSiR compacted pUC19 plasmid DNA into structures that are reminiscent of plastid

A

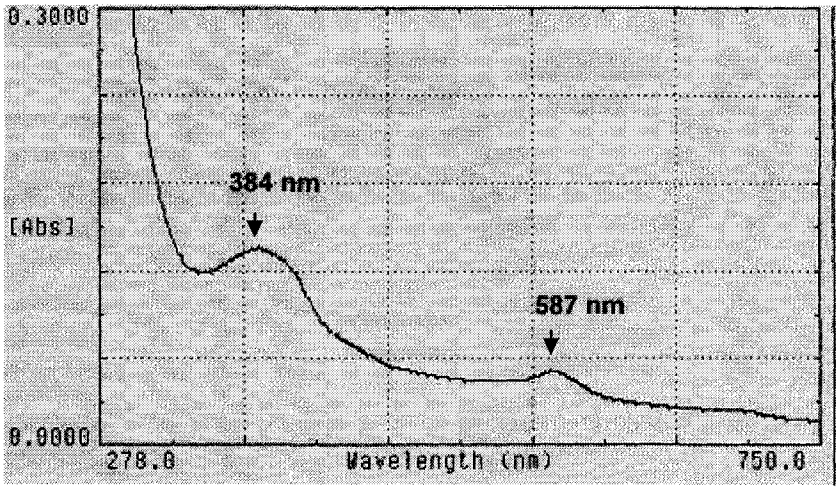

B

Abs (λ) / Abs (384 nm)

λ (nm)	Spinach SiR	DCP68/SiR	rAtSiR
278	2.17	7.60	5.39
384	1.00	1.00	1.00
542	0.21	0.28	0.33
587	0.30	0.38	0.34
712	0.10	0.12	0.16

Figure 8. Siroheme presence in rAtSiR.
Panel A. Siroheme was detected in rAtSiR by spectrophotometric absorbance maxima at 384 and 587 nm.
Panel B. Comparison of relative absorbance of spinach SiR, DCP68/SiR and rAtSiR.

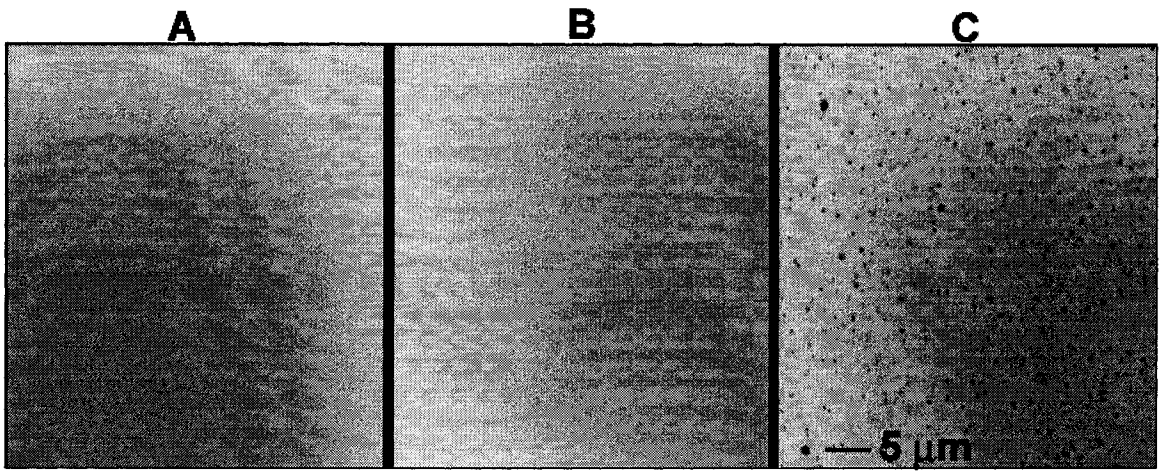

Figure 9. DNA Compaction Assay with rAtSiR.
AtSiR expressed recombinantly under conditions that facilitate siroheme incorporation was capable of forming structures that resembled plastid nucleoids when stained with 0.1 µg/µl DAPI. All three images had the same exposure time. For clarity, the image colors were inverted. (**A**) 500 ng pUC19 DNA; (**B**) 3.5 µg rAtSiR; (**C**) 500 ng pUC19 DNA and 3.5 µg rAtSiR.

nucleoids (Figure 9). Although DCP68/SiR purified from SB-M cells was able to compact DNA almost instantaneously [260], no immediate DNA-compaction by rAtSiR was observed but was noted after a 16 h incubation. A similar incubation time was required to confirm DNA compaction by recombinantly expressed maize SiR [261]. This may be related to differences in siroheme incorporation (Figure 8). It is possible that siroheme incorporation was needed for proper folding of SiR but may inhibit DNA-binding. The absorbance ratio of 278 to 384 nm can be used to estimate the amount of siroheme incorporation. SiR purified from chloroplast nucleoids has the lowest ratio and, therefore, the lowest amount of incorporated siroheme. This may indicate SiR loses its siroheme prior to becoming nucleoid-associated. The amount of incorporated siroheme is higher in soluble spinach SiR and no DNA binding has been reported.

Alternatively, the differences in DNA-compaction between recombinant and purified SiR may be related to differences in post-translational modification. Chi-Ham *et al.* used electrophoretic mobility shift assays to demonstrate that the phosphorylation state of DCP68/SiR modulates DNA-binding affinity [2]. Purified DCP68/SiR treated with calf intestinal alkaline phosphatase resulted in a larger shift in mobility than untreated DCP68/SiR at the same concentration. These data suggest that the DNA-binding affinity of dephosphorylated DCP68/SiR is different from that of untreated SiR. Differences in the extent of phosphorylation of rAtSiR and purified DCP68/SiR could account for the slower rate of DNA compaction by recombinantly expressed SiR from *Arabidopsis* and maize.

4.5 Characterization of *Arabidopsis* T-DNA Mutants

By compacting ctDNA, nucleoid-associated SiR may regulate template accessibility and, therefore, modulate plastid DNA replication and transcription [1, 82]. To investigate how AtSiR affected nucleoid morphology, a reverse genetics approach was employed by characterizing mutant plants with a null copy of the *sir* gene. Previous attempts to generate *Arabidopsis* plants that underexpress SiR due to the presence of an antisense construct were not successful. Hell *et al.* determined that the SiR protein level was not diminished in these plants, and that they did not display a strong phenotype [265]. Therefore, the best probability of determining the phenotype of SiR mutants would be in mutants that express no SiR protein at all.

4.5.1 SiR T-DNA Mutants. The Syngenta Arabidopsis Insertion Library (SAIL) contains more than 100,000 T-DNA insertion mutants generated by *Agrobacterium*-mediated gene transfer. The T-DNA is transferred from the Ti plasmid of *Agrobacterium* and inserted more or less randomly into the plant nuclear genome [4]. An electronic database contains the DNA sequence flanking the T-DNA insertion site of each mutant in the SAIL line. The SiR DNA sequence was submitted to this database, which identified several candidate plants lines with T-DNA insertions at various positions in the SiR gene. There is a single SiR gene in the annotated *Arabidopsis* genome database and since plants have a

requirement for reduced sulfur, the complete disruption of this gene, and therefore the sulfur assimilation pathway, could be lethal to plants.

The 1223 SAIL plant line possessed a T-DNA insertion in the promoter region of AtSiR (Figure 12). The expected phenotype of the 1223 SAIL lines might be similar to the effects of sulfur deficiency in plants: smaller and fewer leaves that are chlorotic [265]. The initial observations of plants from the 1223 SAIL line had noted smaller and fewer siliques, lower seed viability, slower growth, and smaller leaves. To further examine the phenotype in the 1223 SAIL line, the leaf span, root length, plant height, seed set, silique length, and number of siliques were measured and compared with wild-type plants grown under the same conditions. Mutant plant lines were grown on medium containing a selection marker to ensure that only transformants would grow.

The 1223 SAIL phenotypic data was compiled from several different seed pools. Seed from many different 1223 plants was collected to create a large pool of 1223 SAIL mutants (bulk 1223). In addition, the F2 generation of seed from a single 1223 plant was kept as individual pools (i.e. 1223-61). The leaf span and root length was measured with 10-day old plants, while the plant height was determined in mature plants. These data indicated that vegetative plant growth in the 1223 SAIL line was not considerably different from that of wild-type plants. The mean leaf span of plants grown from bulk 1223 seed was not statistically smaller than that of wild-type plants (Figure 10A). Although plants from the 1223-61 individual seed pool had a smaller mean leaf span than wild-

type plants, this was not observed in plants grown from the 1223-64 and 1223-65 seed pools, indicating this was probably natural variation in leaf span rather than a characteristic of the mutant. Similarly, the mean root length of the 1223 SAIL line was not statistically different from that of wild-type plants (Figure 10B). The mean height of plants grown from bulk 1223 seed (27.2±0.9 cm) was slightly shorter than that of wild-type plants (30.1±1.6 cm) (Figure 10C). The plant height was not determined in plants grown from the 1223-61, -64, and –65 seed pools.

The number of siliques per plant and the seed set indicate that reproductive growth of *Arabidopsis* was impaired in the 1223 SAIL line (Figure 11). The number of siliques per plant was more than 2.5-fold higher in wild-type plants than in plants grown from bulk 1223 seed. Similarly, the seed set of wild-type plants was approximately two-fold higher than that of plants grown from bulk 1223 seed. The observed phenotype in 1223 mutants could be related to deficiency in sulfur assimilation. The seeds of *Arabidopsis* are normally filled with sulfur-rich storage proteins such as glycinin that contribute to seed metabolism. Since the 1223 SAIL mutants did not exhibit the symptoms of sulfur deficiency, the abundance of SiR was determined in 1223 SAIL mutants.

4.5.2 SiR Abundance in T-DNA Mutants. Northern blotting and quantitative immunoblotting were used to determine if the SiR transcript and protein abundance in the 1223 mutants was lower than wild-type plants (Figures 2 and 4). The SiR transcript and protein abundance in mature leaves of heterozygous 1223 mutants was reduced by approximately 50%, compared to wild-type plants.

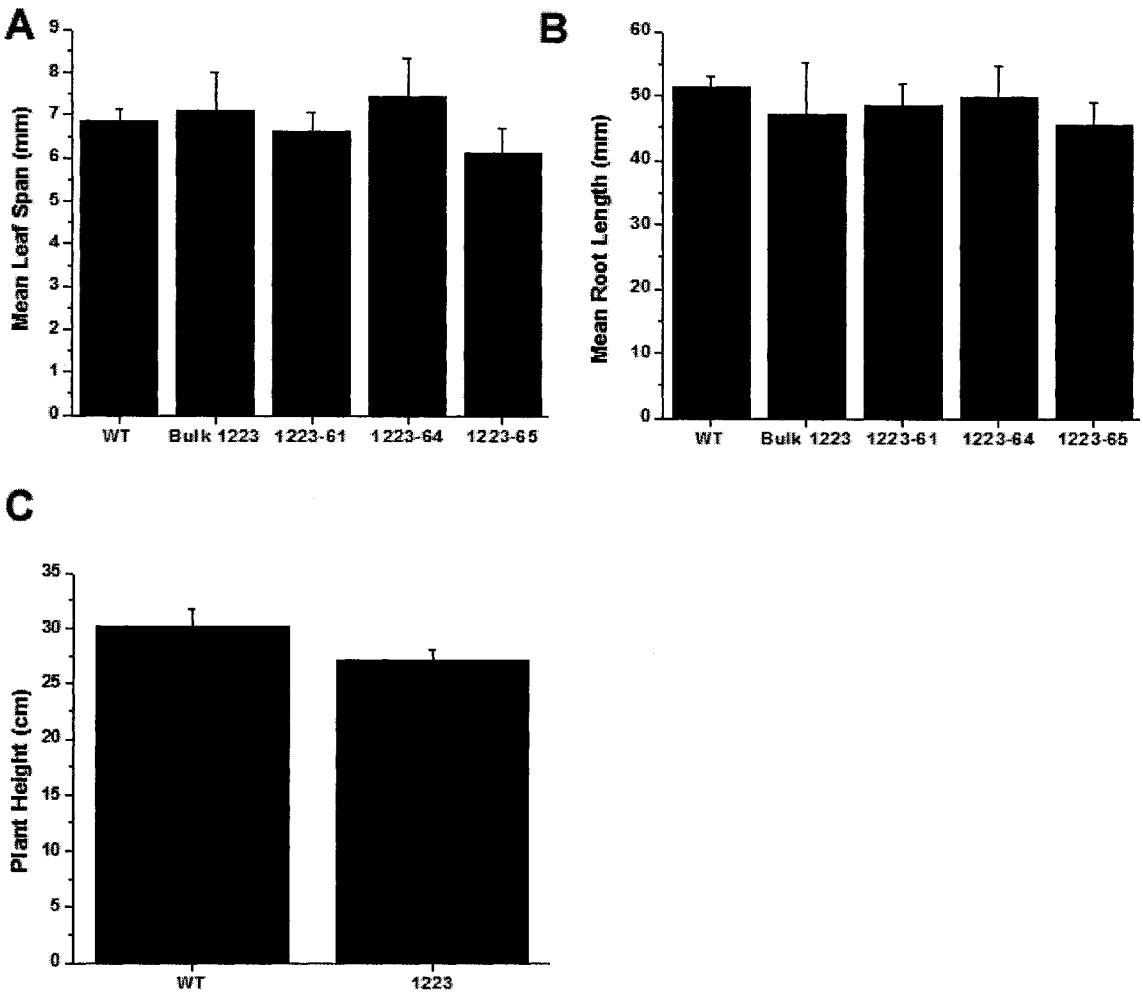

Figure 10. Vegetative Growth Phenotypes of the 1223 T-DNA Insertion Mutant Line of *Arabidopsis thaliana*.
(**A**) Mean leaf span; (**B**) mean root length; (**C**) plant height of wild-type and the 1223 SAIL line. Mean leaf span and root length were determined from 10-day old plants, while the plant height was determined from mature 6-week old plants. The error bars represent the standard error of mean leaf span, mean root length, and plant height from at least three different plants.

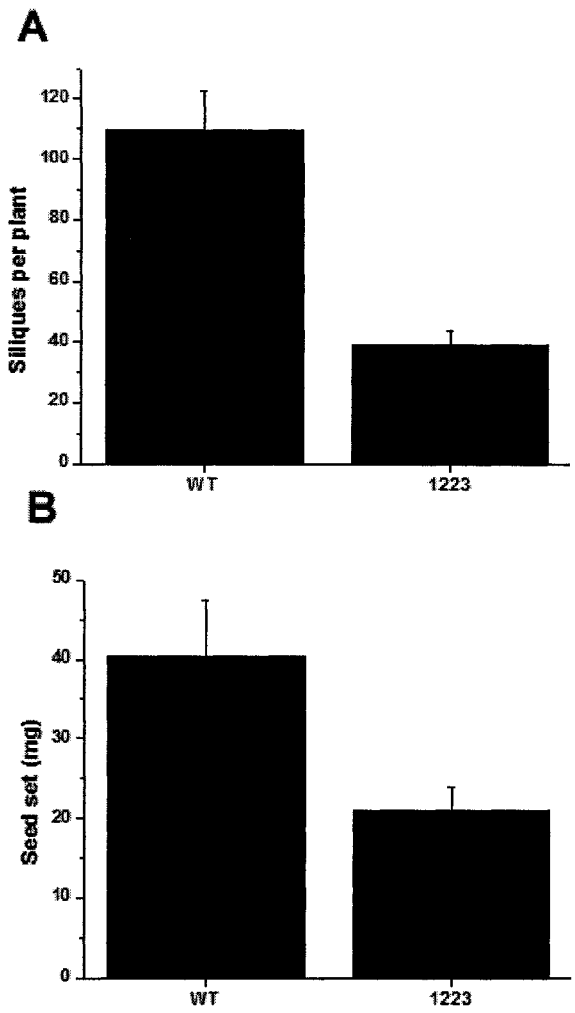

Figure 11. Reproductive Growth Phenotypes of the 1223 T-DNA Insertion Mutant Line of *Arabidopsis thaliana*.
(**A**) The number of siliques per plant; (**B**) seed set of wild-type (WT) and the 1223 SAIL line (1223). The error bars represent the standard error of the siliques per plant and seed set based on measurements of at least three different plants.

These data support regulation of SiR abundance at the transcriptional level, because the observed reduction of SiR transcripts in heterozygous mutants was similar to the reduction in protein abundance. It is probable that the reduction in SiR protein level was not sufficient to observe a phenotype in nucleoid morphology, since less than 5% of the SiR was distributed to chloroplast nucleoids in mature leaves (Figure 7). In this instance, a change in nucleoid morphology would most likely be observed in a homozygous T-DNA mutant that lacks SiR. Homozygous mutants were expected to be present in 25% of the 1223 seed population. PCR and immunoblotting were used to screen for homozygous mutants.

4.5.3 Screening for Homozygous Mutants. Initially, the identification of homozygous mutants was attempted using two PCR reactions to screen individual plants. The relative positions of the T-DNA insertion site and primer binding sites are outlined in Figure 12. The first PCR reaction was used to confirm the presence of a T-DNA insertion in the AtSiR gene. Plants are diploid and a second PCR reaction was needed to determine if the T-DNA insertion was present in both SiR genes. This PCR used primers that flank the T-DNA insertion site. This PCR reaction would amplify a 2.4 Kbp fragment in mutant plants that have a T-DNA insertion in only one of the SiR genes. However, no product would be amplified in plants that contained T-DNA insertions in both SiR genes.

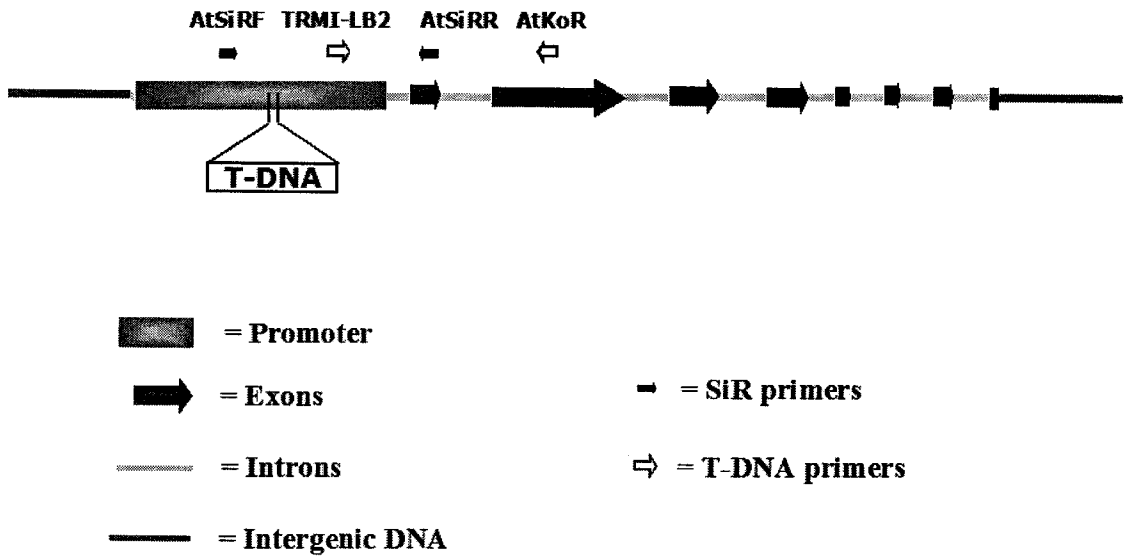

Figure 12. Diagram of the 1223 SAIL Line T-DNA Insertion Site and Primer Binding Sites.
Screening T-DNA mutants by PCR required the use of two separate PCR reactions. The insertion of T-DNA in the SiR gene promoter was detected in the first reaction (TMRI-LB2 and AtKoR primer pair; Table 2). Homozygous mutants would contain a T-DNA insertion in both SiR alleles. The large size of the T-DNA insert (7.5 Kbp) prevents the amplification of a product using primers that flank the T-DNA insertion site (AtSiRF and AtSiRR primer pair; Table 2).

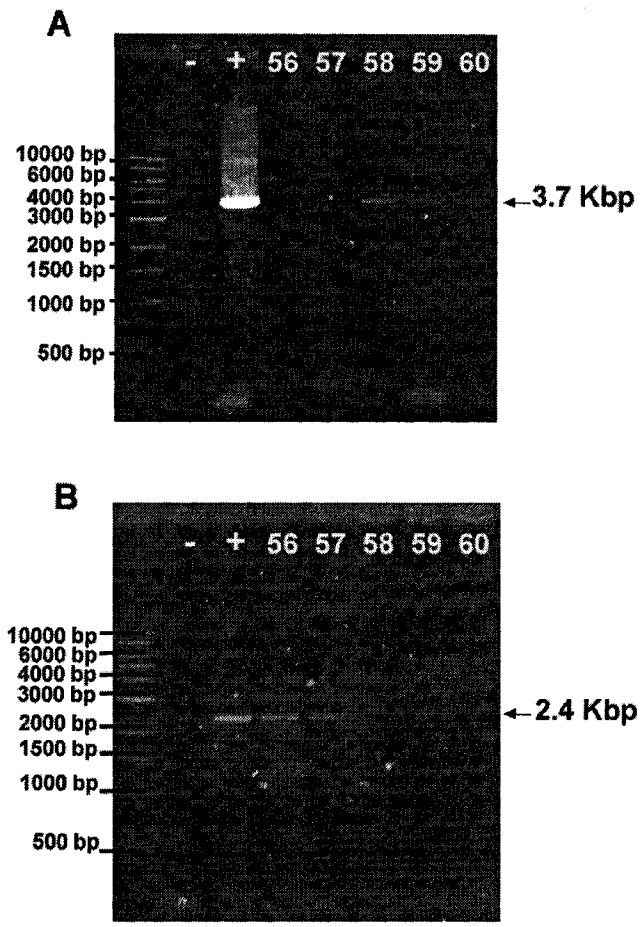

Figure 13. PCR Screen for Homozygous Mutants.
A representative two-stage PCR screen for homozygous mutants. Negative (-) and positive (+) controls are indicated for each reaction. The lanes numbered 56-60 are five mutant plants.
Panel A. The 3.7 Kbp amplification product indicates the presence of a T-DNA insert in plants 58-60.
Panel B. The 2.4 Kbp amplification product indicates that plants 56 and 57 are wild-type, while plants 58-60 are putative homozygotes.

The first round of PCR used the TMRI-LB2 and AtKoR primers (Table 2) to amplify a 3.7 Kbp fragment. This identified those plants that contained T-DNA insertions (Figure 13A, lanes 58-60). In order to identify mutants without a functional SiR gene, the second round of PCR used the AtSiRR and AtSiRF primers (Table 2) to amplify a 2.4 Kbp fragment (Figure 13B, lanes 56-57). This approach identified mutants that may not have a functional SiR gene.

After identification by PCR, the level of SiR protein in these plants was determined by immunoblotting. SiR protein was detected in all of the putative homozygous mutants, which indicates that the PCR method used to screen mutants may have identified false positives and may not be a valid method of screening. Therefore, mutant plants were screened by immunoblotting. However, no mutant plants were identified that were found to lack SiR protein, despite screening more than 75 mutant plants (Figure 14).

4.5.4 Germination Efficiency of the 1223 SAIL Mutant Seeds. It was suspected that the lack of homozygous mutants might be related to the requirement of plants for reduced sulfur to support growth. A germination efficiency assay was performed to assess the viability of mutant seeds. The germination efficiency of the 1223-61 seed pool (172 seeds) was 76% of wild-type germination efficiency (190 seeds) by day 10 (Figure 15A). Seeds from the 1223-61 mutant were also screened on medium containing BASTA. The selection agent BASTA does not affect seed germination but wild-type plants do not progress beyond the cotyledon stage. In the presence of BASTA, the

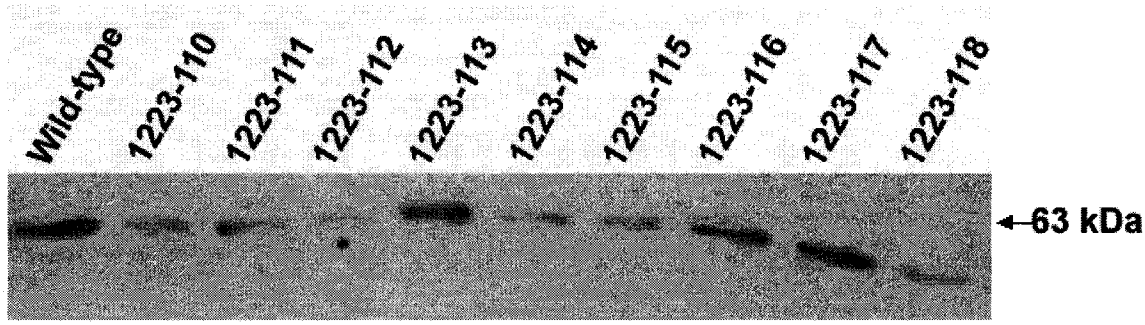

Figure 14. Immunoblot Screen for Homozygous Mutants. Soluble leaf protein extracts were prepared from wild-type and 1223 T-DNA insertion mutants. Ten micrograms of total protein was analyzed by immunoblotting and probed with SiR antiserum (raised in chicken). The presence of an immunocrossreactive band at 63 KDa indicated that all putative homozygous plants were, in fact, heterozygous because they contained SiR protein.

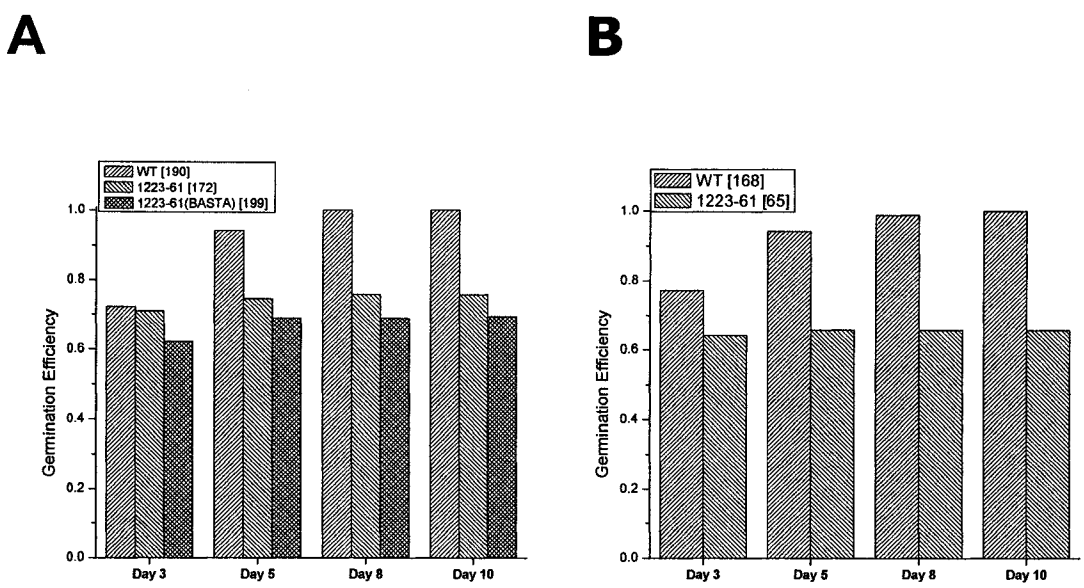

Figure 15. Seed Viability of the 1223 Mutant SAIL Line.
The germination efficiency of wild-type and mutant seed grown in the absence (**A**) and presence (**B**) of 50 μM cysteine. The number in brackets in the figure inserts indicates the number of seeds tested. The germination efficiency of the *Arabidopsis* seed was represented as the ratio of seeds that germinated out of the total seeds planted.

germination efficiency of the 1223-61 SAIL line (199 seeds) was 69% of wild-type by day 10. If all mutant seeds were viable, the 1223-61 seed pool would have had a similar germination rate to the wild-type seed.

It is possible that the absence of a functional SiR gene in homozygotes is lethal to the embryo. Therefore the medium was supplemented with 50 μM cysteine, a form of reduced sulfur that is absorbed by maize plants and is the end product of the sulfur assimilation pathway [266]. Under these conditions, the germination efficiency of the 1223-61 seed pool (65 seeds) was 66% of wild-type (168 seeds) by day 10 (Figure 15B). Medium supplemented with cysteine did not contain the selection agent BASTA. Since the supplementation of cysteine to the growth medium resulted in a slight decrease in germination efficiency, rather than a large increase, this could indicate Arabidopsis did take up sufficient cysteine to support plant growth.

4.5.5 Epifluorescence Microscopy of Nucleoids. Although the best chance of detecting aberrant nucleoid morphology would have been within the homozygous mutants, their apparent lack of viability eliminates this possibility from being tested. The nucleoid morphology in heterozygous plants was evaluated by epifluorescence microscopy. Wild-type and heterozygous plant leaves were fixed and stained with the DNA-binding fluorophore DAPI. A qualitative assessment of nucleoid compaction and shape did not reveal significant differences between wild-type and heterozygotes. The number of nucleoids per chloroplast in young wild-type and heterozygous plants of the 1223 SAIL line was

determined by scoring the DAPI-stained nucleoids visible within chloroplasts. Wild-type plants contained approximately 17 nucleoids per chloroplast, whereas in heterozygous plants the number of nucleoids per chloroplast ranged from 12-24 (Figure 16).

Since the number of nucleoids per chloroplast seemed to vary significantly between mutant plants, an attempt was made to detect shifts in the number of nucleoids in the presence of a cysteine. The yeast mitochondrial nucleoid protein Ilv5p is part of the branched chain amino acid pathway. Upregulation of this pathway results in an increase in the number of nucleoids [191]. Perhaps a similar scenario exists for SiR, whereby plants grown on cysteine may have a different number of nucleoids per chloroplast than plants grown without cysteine. In wild-type plant leaves, the number of nucleoids per chloroplast was slightly higher when grown in the presence of cysteine (Figure 16). Plants grown from bulk 1223 seeds contained a higher number of nucleoids per chloroplast than wild-type plants. Plants grown from the 1223-61 and 1223-65 seed pools had a lower number of nucleoids per chloroplast, whereas plants from the 1223-62 seed pool had a higher number of nucleoids per chloroplast. Collectively, these data may indicate that the number of nucleoids per chloroplast cannot be accurately determined in whole *Arabidopsis* leaves at the resolution offered by light microscopy.

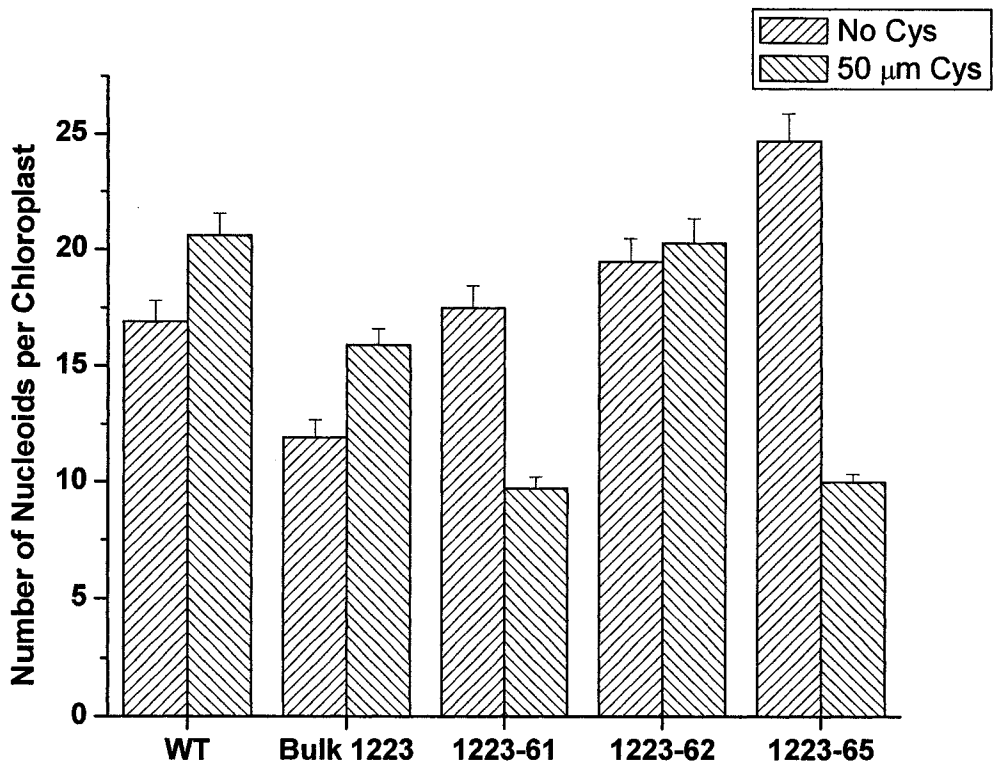

Figure 16. Number of Nucleoids per Chloroplast.
Two-week old plants were fixed briefly and stained with DAPI. All images were captured with the same settings. The number of nucleoids per chloroplast was scored in leaves of *Arabidopsis* wild-type and mutant plants. The number of nucleoids per chloroplast was determined from four wild-type and two of each *Arabidopsis* mutant plants. The error bars represent the standard error of the mean number of nucleoids per chloroplast obtained from screening approximately 20 chloroplasts from each plant.

4.6 Distribution and Abundance of DCP68/SiR in SB-M Cells

Since only a small portion of SiR was found to be nucleoid-associated in mature *Arabidopsis* leaves, it was important to assay the portion of SiR distributed to chloroplast nucleoids in the SB-M cell line. At the resolution offered by light microscopy, Chi-Ham *et al.* found that most SiR colocalized with chloroplast nucleoids in SB-M clls and young pea plants [2].

4.6.1 Intracellular Distribution of DCP68/SiR. The protocol used to determine the distribution of SiR in SB-M cells was similar to the one used to evaluate the distribution of SiR in *Arabidopsis*, except that the SB-M nucleoid-enriched fraction was centrifuged at a lower rate (Figure 6). To determine the effect of cell age on the portion of SiR distributed to chloroplast nucleoids, the distribution of SiR was examined over the course of 16 days. SB-M cells have a cell doubling time of approximately 7 days, therefore, at 16 days post-transfer, ctDNA replication rates would likely be greatly reduced [248].

Approximately 97% of the SiR was found in nucleoid-enriched fractions prepared from SB-M cells two days post-transfer (Figure 17). The amount of SiR fell to approximately 79% in nucleoid-enriched fractions prepared from SB-M cells 16 days post-transfer. The large disparity in the amount of SiR found in *Arabidopsis* leaves and in SB-M chloroplast nucleoid-enriched fractions may be related to a difference in the rate of cell and organelle division. SB-M cells have a short cell doubling time, are very active in ctDNA replication and accumulate

ctDNA to approximately 30% of the total DNA [29, 57]. It is likely that the amount of ctDNA is much lower in *Arabidopsis* leaves. This could indicate that the portion of SiR distributed to chloroplast nucleoids may be related to ctDNA replication rates. It is well known that nucleoid protein composition changes during chloroplast development, and this is thought to influence nucleoid structure and function [32]. Perhaps the amount of SiR allocated to plastid nucleoids is influenced by organelle or cell development. To examine this possibility, the abundance of SiR was quantified in nucleoid-enriched fractions from cultured SB-M cells over the course of 16 days.

4.6.2 DCP68/SiR Nucleoid Abundance. The nucleoid-enriched extracts were subjected to SDS-PAGE and transferred to nitrocellulose for immunoblotting. The intensity of the signals from the immunoblot was determined by densitometry. These values were normalized to the two-day post-transfer level of DCP68/SiR present in this extract. The abundance of SiR was highest in fractions obtained from SB-M cells two-day post-transfer into fresh medium. By four days post-transfer, the abundance of SiR had dropped to approximately 42% of the original level (Figure 18). Eight and 16 days post-transfer SB-M cells contained approximately 33% and 27% of the original SiR level, respectively. Since the amount of SiR present in nucleoid-enriched fractions changed with cell age, it is possible that the amount of SiR that was associated with SB-M chloroplast nucleoids may be influenced by a developmental factor associated with cell or organelle aging.

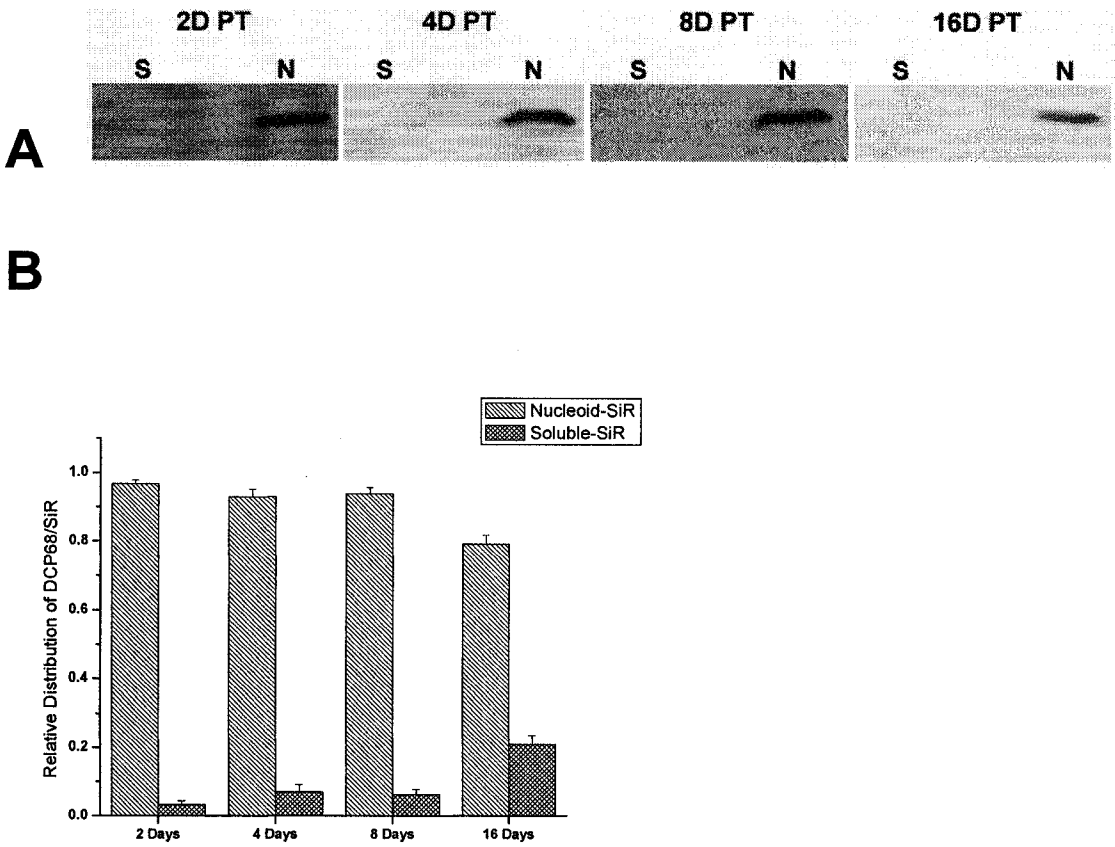

Figure 17. Distribution of DCP68/SiR in SB-M Cells.
Panel A. The signal intensity of the 63 KDa band on immunoblots of (N) nucleoid-enriched and (S) soluble SiR indicated the portion of nucleoid-associated SiR was relatively constant over a time period of 16 days. Total protein analyzed: (2D PT) 68 μg of soluble protein, 2.5 μg of nucleoid-enriched extract, (4D PT) 58 μg of soluble protein, 2.2 μg of nucleoid-enriched extract, (8D PT) 72 μg of soluble protein, 2.0 μg of nucleoid-enriched extract, (16D PT) 53 μg of soluble protein, 1.8 μg of nucleoid-enriched extract.
Panel B. The signal intensity from the immunoblots was quantified using densitometry. The combined intensity of nucleoid and soluble SiR was considered to be 100%. The sample time points are expressed in days post-transfer into fresh medium. The error bars represent the error in the proportion of SiR distributed to nucleoid-enriched and soluble fractions. At least three independently prepared soluble protein fractions, and the corresponding nucleoid-enriched fractions, were used for this analysis.

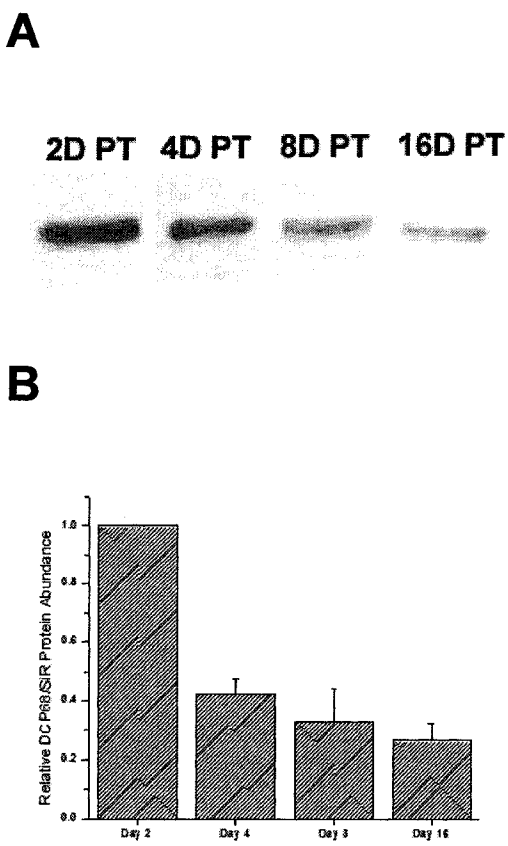

Figure 18. Abundance of DCP68/SiR in Nucleoid-Enriched Fractions from SB-M Cells.
Panel A. Immunoblots of nucleoid-enriched fractions from SB-M cells demonstrated that the relative abundance of DCP68/SiR in the nucleoid-enriched fraction was highest in the youngest SB-M cells. The total protein of each sample was approximately 2 μg.
Panel B. The signal intensity of each sample and a standard of 60 ng rAtSiR were quantified using densitometry. The ratio of signal intensity of each sample to the standard was used to account for differences in signal intensity between blots. These values were then normalized to the abundance of DCP68/SiR in two-day post-transfer cells. Sample time points are expressed in days post-transfer into fresh medium. The error bars represent the error in the abundance of SiR in at least three independently prepared nucleoid-enriched fractions for each timepoint.

It was surprising that the highest amount of SiR was present in chloroplast nucleoid-enriched fractions from the youngest SB-M cells, given that the ctDNA synthesis rate was expected to decrease with cell age, and SiR inhibits ctDNA synthesis *in vitro* [1]. This could indicate that SiR may not have an inhibitory role in ctDNA synthesis *in vivo*.

4.7 Distribution and Abundance of SiR in Soybean Plants

The portion of SiR in SB-M chloroplast nucleoid-enriched fractions far exceeded that found in *Arabidopsis*, but it is difficult to directly compare the accumulation of SiR in SB-M chloroplast nucleoids, a developmentally uniform cell line, to data from *Arabidopsis* plants. Since SiR accumulated in SB-M chloroplast nucleoids to significantly higher levels than in *Arabidopsis*, the allocation of SiR to chloroplast nucleoids was examined in soybean plants. *Glycine max* (L.) Merr. Var. Corsoy was chosen because it is the cultivar that was used to generate the SB-M callus [248].

4.7.1 Distribution of DCP68/SiR in Soybean Plants. The portion of SiR distributed to chloroplast nucleoids in soybean plants was determined as described in Figure 6. Soluble SiR and nucleoid-bound SiR fractions were prepared from cotyledons, young emerging leaves and fully expanded mature leaves. The portion of total SiR in the nucleoid-enriched fraction was less than 1% in cotyledons and approximately 36% in young leaves (Figure 19). Less than 5% of the total SiR was nucleoid-associated in mature leaves. The large amount

of DCP68/SiR distributed to chloroplast nucleoids in young emerging leaves may facilitate DNA-compaction during ctDNA amplification. As cells leave the meristematic state, the plastome copy number per plastid decreases with the distribution of ctDNA to daughter organelles, as shown in pea and spinach [31, 267]. This could indicate why the portion of SiR distributed to chloroplast nucleoids is higher in young soybean leaves than in mature leaves. It is noteworthy that a similar portion of total SiR from mature soybean leaves was present in *Arabidopsis* (Figure 7). It is difficult to reconcile why the portion of SiR distributed to young leaves of *Arabidopsis* and soybean is not comparable, suggesting there were differences in nucleoid composition between the two plants at the developmental stages examined.

4.7.2 Abundance of DCP68/SiR in Soybean Nucleoids. The allocation of a significant portion of SiR to chloroplast nucleoids in young soybean leaves does not necessarily indicate that the nucleoid composition in young leaves is different from mature leaves. Therefore, the abundance of SiR was examined in nucleoid-enriched fractions. An equal mass of each nucleoid-enriched fraction from cotyledons, emerging leaves, and mature leaves was analyzed by quantitative immunoblotting. The DCP68/SiR signal in each sample was normalized to the value observed in mature leaves. The abundance of DCP68/SiR in nucleoid-enriched fractions from cotyledons was approximately 14% of the value found in mature leaves (Figure 20). By contrast, the SiR abundance in plastid nucleoid-enriched fractions prepared from young leaves was 2.5-fold higher than that of

A

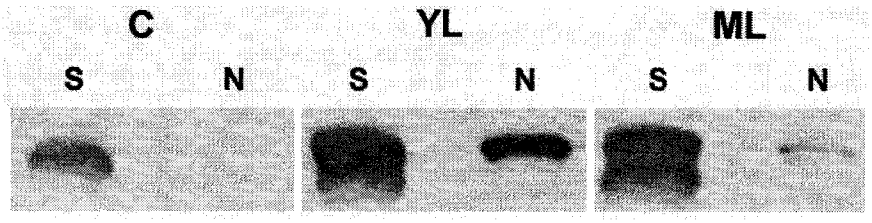

B

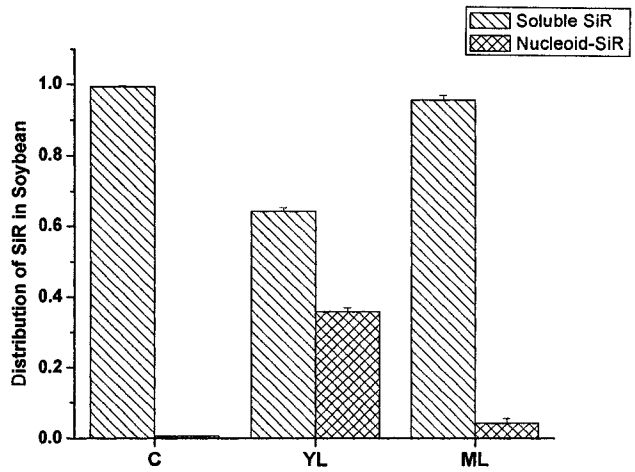

Figure 19. Distribution of SiR in Soybean Plants.
Panel A. The signal intensity of the 68 KDa band on immunoblots of (N) nucleoid-enriched and (S) soluble SiR indicated the proportion of nucleoid-bound SiR was higher in emerging leaves than in other developmental stages. Total protein analyzed: (C) 77 μg of soluble protein, 1.8 μg of nucleoid-enriched extract, (YL) 68 μg of soluble protein, 2.2 μg of nucleoid-enriched extract, (ML) 55 μg of soluble protein, 2.8 μg of nucleoid-enriched extract.
Panel B. The signal intensity was quantified using densitometry as described in Figure 18. The error bars represent the error in the proportion of SiR distributed to nucleoid-enriched and soluble fractions. At least three independently prepared soluble protein fractions, and the corresponding nucleoid-enriched fractions, were used for this analysis. (**C**=Cotyledons; **YL**=Emerging leaves; **ML**=Mature Leaves)

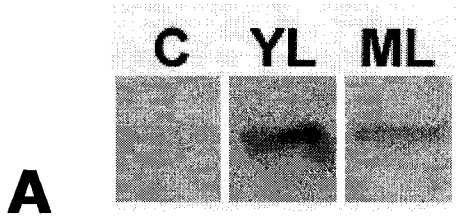

A

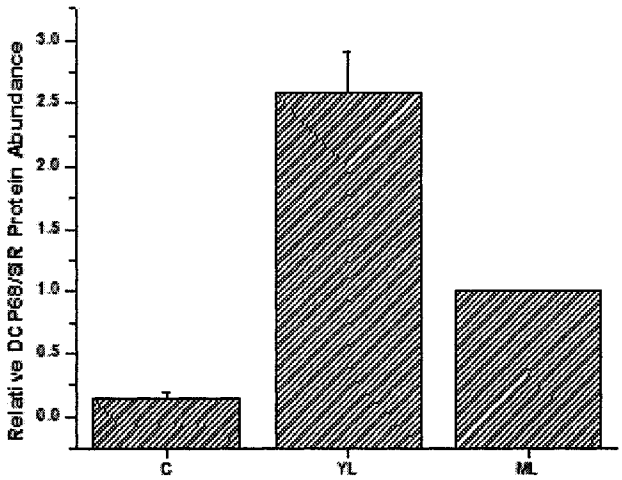

B

Figure 20. Abundance of SiR in Plastid Nucleoid-Enriched Fractions from Soybean Plants.
Panel A. Representative immunoblots of nucleoid-enriched fractions containing SiR (1.5 μg total protein loaded per lane).
Panel B. Densitometric measurements of the signal intensity in each fraction indicated that the relative abundance of SiR in nucleoid-enriched fractions was highest in young leaves of soybean. Analysis was performed as described in Figure 18. The error bars represent the error in the abundance of SiR distributed to nucleoid-enriched fractions in different leaf types. At least three independently prepared nucleoid-enriched protein fractions, at each growth stage, were used for this analysis. (**C**=Cotyledons; **YL**=Emerging leaves; **ML**=Mature Leaves)

mature leaves. These data suggest that the nucleoid composition changes as young chloroplasts develop into mature chloroplasts. The high abundance of SiR in nucleoids of young chloroplasts may be related to the ctDNA amplification occurring during this stage.

4.8 Effect of Light on SiR Abundance

4.8.1 In Silico Description of the AtSiR Promoter. It was first speculated that the expression of SiR was light-regulated by R. Hell when the gene for SiR was identified in *Arabidopsis* [83]. Several light-responsive elements such as G-box and T-box are present in the putative SiR promoter region. A number of genomics tools have become available to plant researchers, including the *Arabidopsis* Gene Regulatory Information Server (AGRIS), which allows the user to identify potential transcription factor binding sites and gene responsive elements in a given promoter [252, 268]. The AtSiR promoter was found to contain putative binding sites for transcription factors regulated by abscisic acid, a plant hormone involved in seed dormancy and water stress-induced closure of the stomata (Figure 21) [4]. Additionally, the AtSiR promoter contained the GATA, T-box, I-Box, and G-box promoter motifs, which form the basis for light-regulated expression [269-271].

4.8.2 Effect of light on AtSiR Expression. To examine if light regulated SIR abundance, the amount of AtSiR was assessed in light-grown and etiolated *Arabidopsis.* Soluble leaf protein extracts were prepared and analyzed by

Binding Site Name	Binding Site Start	Binding Site End	Binding Site Sequence	FUNCTION
AtMYC2 BS in RD22	1318858	1318863	cacatg	Abscisic acid responsive element
AtMYC2 BS in RD22	1318745	1318750	cacatg	Abscisic acid responsive element
ATB2/AtbZIP53/AtbZIP44/GBF5 BS	1318847	1318852	actcat	Responsive to hypo-osmolarity
W-box promoter motif	1319297	1319305	ttgacc	Responsive to plant defense
DPBF1&2 binding site motif	1319155	1319171	acacgcg	Abscisic acid responsive element
DPBF1&2 binding site motif	1319325	1319341	acacacg	Abscisic acid responsive element
DPBF1&2 binding site motif	1319266	1319282	acacgtg	Abscisic acid responsive element
DPBF1&2 binding site motif	1318745	1318761	acacatg	Abscisic acid responsive element
MYB4 binding site motif	1318489	1318504	aactaac	Controls cellular differentiation
RAV1-A binding site motif	1318867	1318871	caaca	Abscisic acid responsive element
RAV1-A binding site motif	1318872	1318876	caaca	Abscisic acid responsive element
RAV1-A binding site motif	1319163	1319167	caaca	Abscisic acid responsive element
RAV1-A binding site motif	1318443	1318447	caaca	Abscisic acid responsive element
LFY consensus binding site motif	1318319	1318329	ccaatg	Controls floral homeotic gene expression
LFY consensus binding site motif	1318974	1318984	ccaatg	Controls floral homeotic gene expression
LFY consensus binding site motif	1319299	1319309	ccattg	Controls floral homeotic gene expression
LFY consensus binding site motif	1319194	1319204	ccattg	Controls floral homeotic gene expression
LFY consensus binding site motif	1318464	1318474	ccactg	Controls floral homeotic gene expression
VOZ binding site	1319220	1319245	gcgttttacgc	Not well characterized
VOZ binding site	1319234	1319259	gcgtaaaacgc	Not well characterized
ABRE binding site motif	1318991	1319001	tacgtggc	Abscisic acid responsive element
ABRE-like binding site motif	1319257	1319274	cacgtgtc	Abscisic acid responsive element
ABRE-like binding site motif	1318991	1319008	tacgtggc	Abscisic acid responsive element
Box II promoter motif	1318392	1318397	ggttaa	Light-responsive element
GATA promoter motif	1318450	1318461	tgataa	Light-responsive element
GATA promoter motif	1319276	1319287	tgatag	Light-responsive element
GATA promoter motif	1319146	1319157	agataa	Light-responsive element
GATA promoter motif	1319086	1319097	tgataa	Light-responsive element
G-box promoter motif	1319267	1319272	cacgtg	Light-responsive element
G-box promoter motif	1319278	1319283	cacgtg	Light-responsive element
G-box promoter motif	1319277	1319282	cacgtg	Light-responsive element
G-box promoter motif	1319266	1319271	cacgtg	Light-responsive element
GCC-box promoter motif	1319260	1319265	gccgcc	Low-temperature and dehydration responsive
GCC-box promoter motif	1318398	1318403	gccgcc	Low-temperature and dehydration responsive
I-box promoter motif	1319156	1319161	gataag	Light-responsive element
T-box promoter motif	1319048	1319053	actttg	Light-responsive element
T-box promoter motif	1318815	1318820	actttg	Light-responsive element
T-box promoter motif	1318599	1318604	actttg	Light-responsive element
T-box promoter motif	1318520	1318525	actttg	Light-responsive element
T-box promoter motif	1318505	1318510	actttg	Light-responsive element
SORLIP2	1318469	1318473	gggcc	Light-responsive element
SORLIP2	1318889	1318893	gggcc	Light-responsive element

Figure 21. AtSiR Promoter Analysis.
Many of the promoter elements present in AtSiR can be categorized as light-responsive (light-gray) or abscisic acid responsive (dark-gray). The AGRIS database was used to search the putative SiR promoter region for transcription factor binding sites and motifs. These promoter elements were classified by the AGRIS database and refined by literature research.

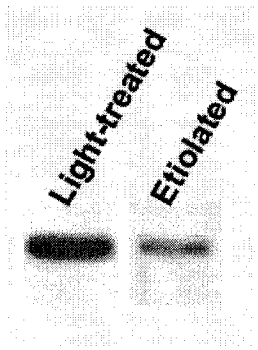

A

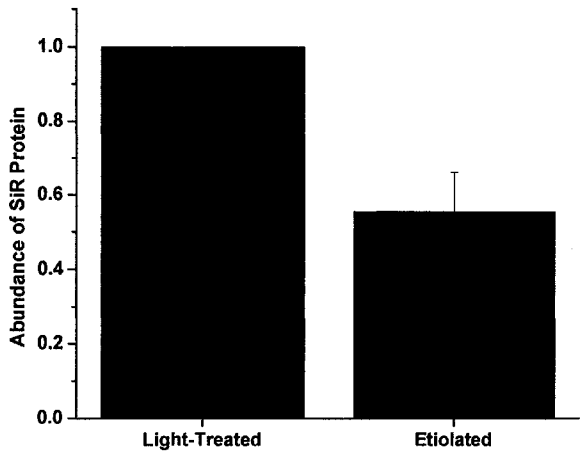

B

Figure 22. Light Enhances SiR Abundance in *Arabidopsis* Leaves.
Panel A. Representative immunoblots containing 20 □g of total protein isolated from light-treated and etiolated *Arabidopsis* plant leaves and probed with SiR antiserum.
Panel B. The densitometric signal of SiR in etiolated plants was normalized to that of light-treated *Arabidopsis*. The error bars represent the error in the abundance of SiR in light-treated and etiolated *Arabidopsis* leaves. At least three independently prepared soluble protein fractions were used for this analysis.

quantitative immunoblotting. The abundance of SiR in etiolated plants was approximately half of that in light-grown *Arabidopsis* (Figure 22), suggesting that the expression of AtSiR was stimulated by light. The fact that light may regulate the abundance of sulfite reductase is not altogether unexpected. Although SiR is active in maize roots, sulfur assimilation in leaves is thought to occur predominantly during the daylight hours during peak ATP synthesis [269, 272]. In fact, the first reaction of the sulfate pathway uses ATP to form a charged sulfo-compound, 5'-adenylsulfate [273].

4.9 Effect of Cysteine on Abundance and Distribution of SiR in SB-M Cells

The expression of several proteins in the sulfur assimilation pathway, such as sulfate permease, ATP sulfurylase, and serine acetyltransferase, is regulated by cysteine in maize [266]. It is possible that cysteine also influences the expression of SiR or the allocation of SiR to chloroplast nucleoids. Controlling the nutrient composition of *Arabidopsis* plants grown in soil would be problematic due to difficulties in obtaining a uniform concentration of cysteine the soil. Therefore, the effect of cysteine was determined in the SB-M cell line by supplementing the growth medium with cysteine.

4.9.1 Distribution of DCP68/SiR in the Presence of Cysteine. The distribution of SiR was assessed as outlined before (Figure 6). As a negative control, soluble and nucleoid-enriched fractions were obtained from SB-M cells two days post-transfer, prior to the addition of 400 μM cysteine. Samples were isolated 48

and 96 h later to determine the effect of cysteine on the allocation of SiR to chloroplast nucleoids. Approximately 90% of the total SiR was found to be present in plastid nucleoid-enriched fractions prepared from SB-M cells two-days post-transfer (Figure 23). The addition of 400 μM cysteine to the growth medium did not significantly affect the portion of SiR distributed to plastid nucleoid-enriched fractions (Figure 23).

4.9.2 Effect of Cysteine on the Abundance of SiR in SB-M Plastid Nucleoids. The abundance of SiR in SB-M chloroplast nucleoid was assessed by quantitative immunoblotting. By six days post-transfer, the amount of SiR found in a plastid nucleoid-enriched fraction increased 1.6-fold of the control in the presence of 400 μM cysteine (Figure 24). By contrast, the SiR abundance in nucleoid-enriched fractions decreased to less than half in SB-M cells two days post-transfer (Figure 17), suggesting that the expression of SiR was up-regulated. This would be distinct from the regulation of other genes of the sulfur assimilation pathway, whose expression appears to be down-regulated by cysteine [266, 274].

4.10 Post-translational Modification of SiR

The phosphorylation status of SiR has been of considerable interest, since it was demonstrated that the DNA-binding affinity of purified DCP68/SiR was altered when pre-treated with alkaline phosphatase [2]. An earlier study demonstrated that purified SB-M chloroplast nucleoids contained a 70 kDa phosphoprotein and the phosphorylation status of this protein changed during

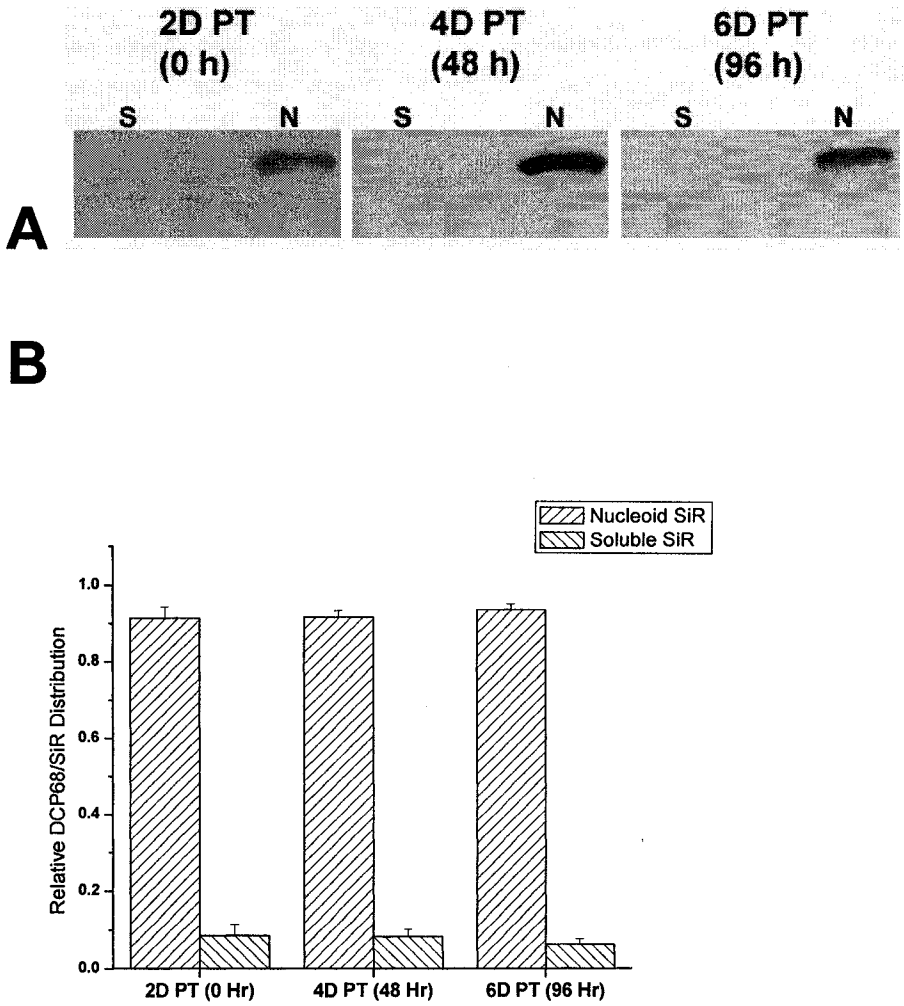

Figure 23. The Distribution of DCP68/SiR (from SB-M cells) in the Presence of Cysteine.

Panel A. Representative immunoblots of soluble and nucleoid-enriched fractions from SB-M cells. Samples were isolated from SB-M cells two, four, and six-days post-transfer (D PT) into fresh medium. Cysteine (400 μM) was added after sample preparation two-days post transfer. Panel B. The signal intensity was quantified by densitometry. Cysteine did not affect the distribution of DCP68/SiR between 48-96 h after the addition to the culture medium. The error bars represent the error in the proportion of SiR distributed to nucleoid-enriched and soluble fractions. At least three independently prepared soluble protein fractions, and the corresponding nucleoid-enriched fractions, were used for this analysis.

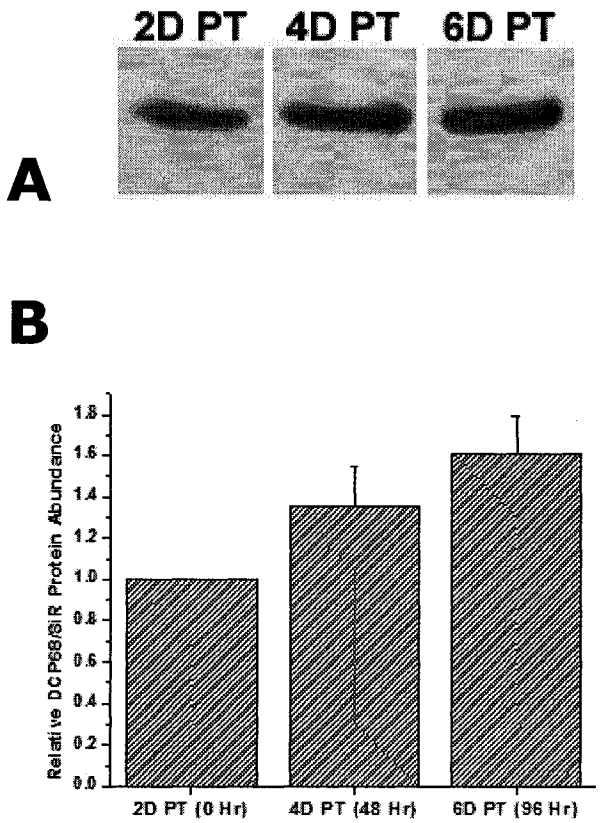

Figure 24. Abundance of DCP68/SiR (from SB-M cells) in the Presence of Cysteine.

Panel A. Representative nucleoid-enriched fractions from SB-M cells containing the 68 KDa band present on immunoblots of 1.0 μg of total protein.

Panel B. Densitometry was used to quantify the signal intensity in samples and 60 ng of rAtSiR that was used as a standard. The ratio of standard to sample signal was used to correct for small differences in immunoreactivity. These data indicate that there was a small increase in DCP68/SiR abundance after 48-96 h of exposure to 400 μM Cysteine. The abundance of SiR was normalized to the level present in 2D PT SB-M cells. The error bars represent the error in the abundance of SiR distributed to SB-M nucleoid-enriched fractions. At least three independently prepared nucleoid-enriched fractions, at each time point, were used for this analysis.

plastid development (G. Cannon and S. Heinhorst, unpublished observations). These data suggest the exciting possibility that the DNA-binding activity of SiR may be regulated by phosphorylation. As a first step towards examining this prospect, the isoelectric point (pI) profile of SiR isoforms was evaluated in extracts prepared from plants at different developmental stages.

4.10.1 Isoelectric Point Profile of AtSiR In Young and Mature Leaves. Phosphorylation and other post-translational modifications can affect the charge/mass ratio. These can be detected as differences in the pI profile using two-dimensional isoelectric focusing/SDS-PAGE (2D IEF/SDS-PAGE) [275-277]. Protein isoforms are separated based on their pI in the first dimension and then separated by molecular weight in the second. Soluble leaf extracts from *Arabidopsis* were prepared from young and mature plants. Numerous attempts were made to correlate the spots observed on 2D immunoblots with the proteins observed on silver stained gels. Evidently, the abundance of SiR in a soluble leaf extract was too low for visualization. In 2D immunoblots of mature *Arabidopsis* soluble leaf extracts, the observed pIs of SiR isoforms ranged from 6.4 to 7.4 (Figure 26). The most abundant isoforms had a calculated pI of 6.7, 6.8 and 7.1. In young *Arabidopsis* soluble leaf extracts, the observed pIs of SiR isoforms ranged from 6.2 to 7.3, with the most abundant isoforms at 6.7, 6.9 and 7.2.

The predicted pI of mature AtSiR is 7.6 [278]. Since the observed pI of SiR was significantly different from the predicted value, an isoelectric point

calculator was used to determine that the addition of a single phosphoryl residue to AtSiR was predicted to shift the pI to 7.1 [279]. Additional phosphoryl residues were predicted to shift the pI to the acidic range by approximately 0.2 pH units per modified residue. The observed pIs of SiR isoforms are consistent with phosphorylation, but there are other post-translational modifications, such as acetylation, that can result in an acidic shift to the pI.

4.10.2 pI Profile of AtSiR in Etiolated Leaves.

Soluble leaf extracts were prepared from etiolated and light-grown *Arabidopsis* plants. *Arabidopsis* was grown for two weeks under a normal 12 h light/dark cycle. To stimulate the formation of etioplasts, the plants were deprived of light for one week; control plants were not shifted to growth in the dark. In control plants, the observed pIs of SiR isoforms ranged from 6.3 to 7.4 with the most abundant isoforms occurring at a pI of 6.6, 6.9 and 7.2 (Figure 26). This was consistent with the previously determined pI profile of SiR isoforms in young *Arabidopsis* leaves (Figure 26). In etiolated plants of the same age, the observed pIs of SiR isoforms ranged from 6.8 to 7.3, with the most abundant isoforms occurring at pIs of 7.1 and 7.3.

The absence of the acidic isoforms on 2D immunoblots of etiolated *Arabidopsis* suggests that the post-translational modification of SiR was different in etioplasts. If the isoforms of SiR arose solely from phosphorylation, this may suggest that SiR carried fewer phosphoryl residues in etiolated plants. Alternatively, the pI profile may reflect the decrease in SiR abundance observed

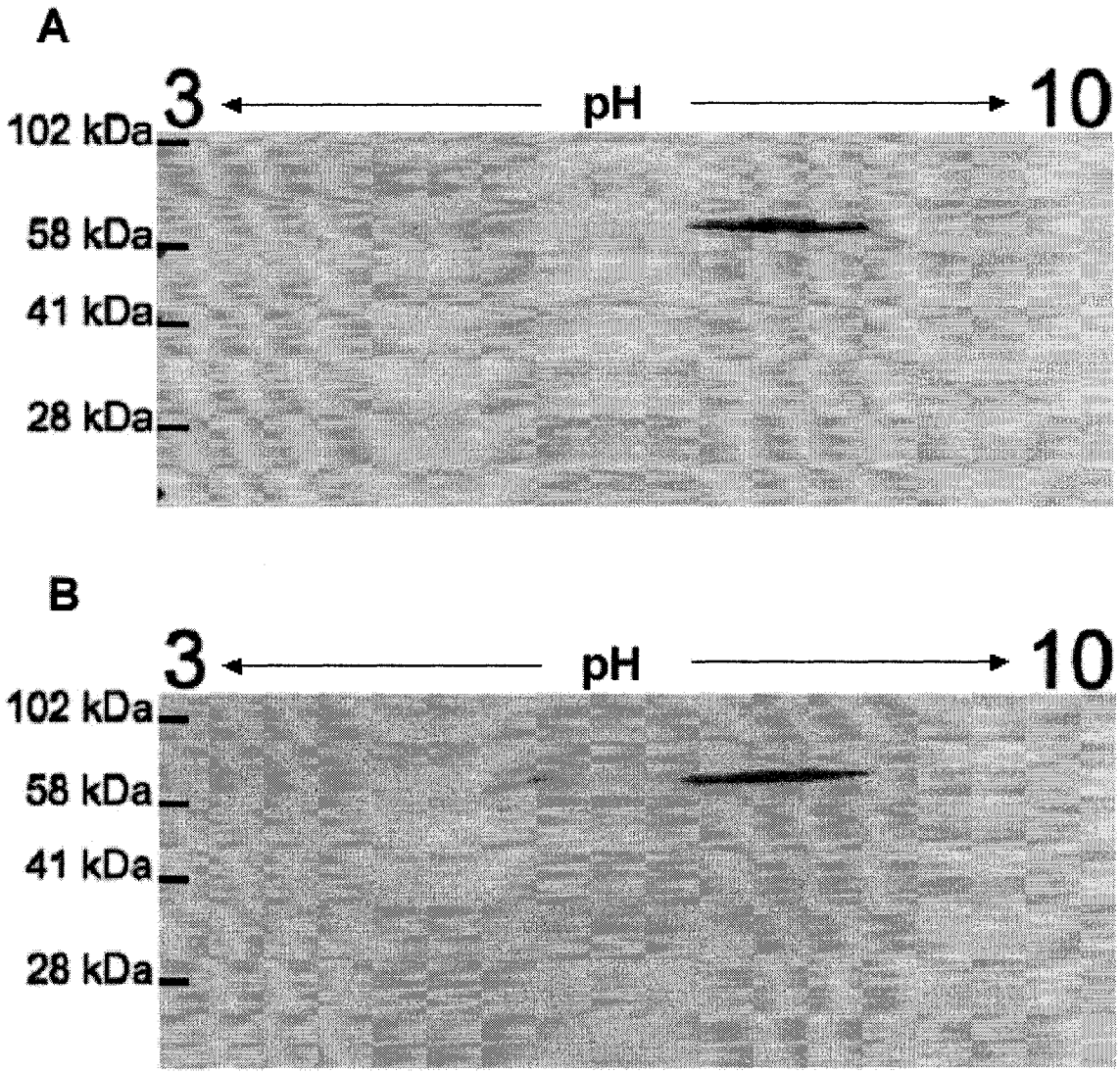

Figure 25. 2D IEF/SDS-PAGE of Soluble Leaf Protein Extracts from *Arabidopsis*.
Extracts (400 μg) prepared from (**A**) mature and (**B**) young *Arabidopsis* leaves were analyzed by two-dimensional isoelectric focusing/sodium dodecyl sulfate polyacrylamide gel electrophoresis (2D IEF/SDS-PAGE). The pI profile of SiR in mature leaves does not differ significantly from that of SiR in young leaves. The immunoblots were probed with αSiR antiserum (raised in chicken) and exposed for 20 min.

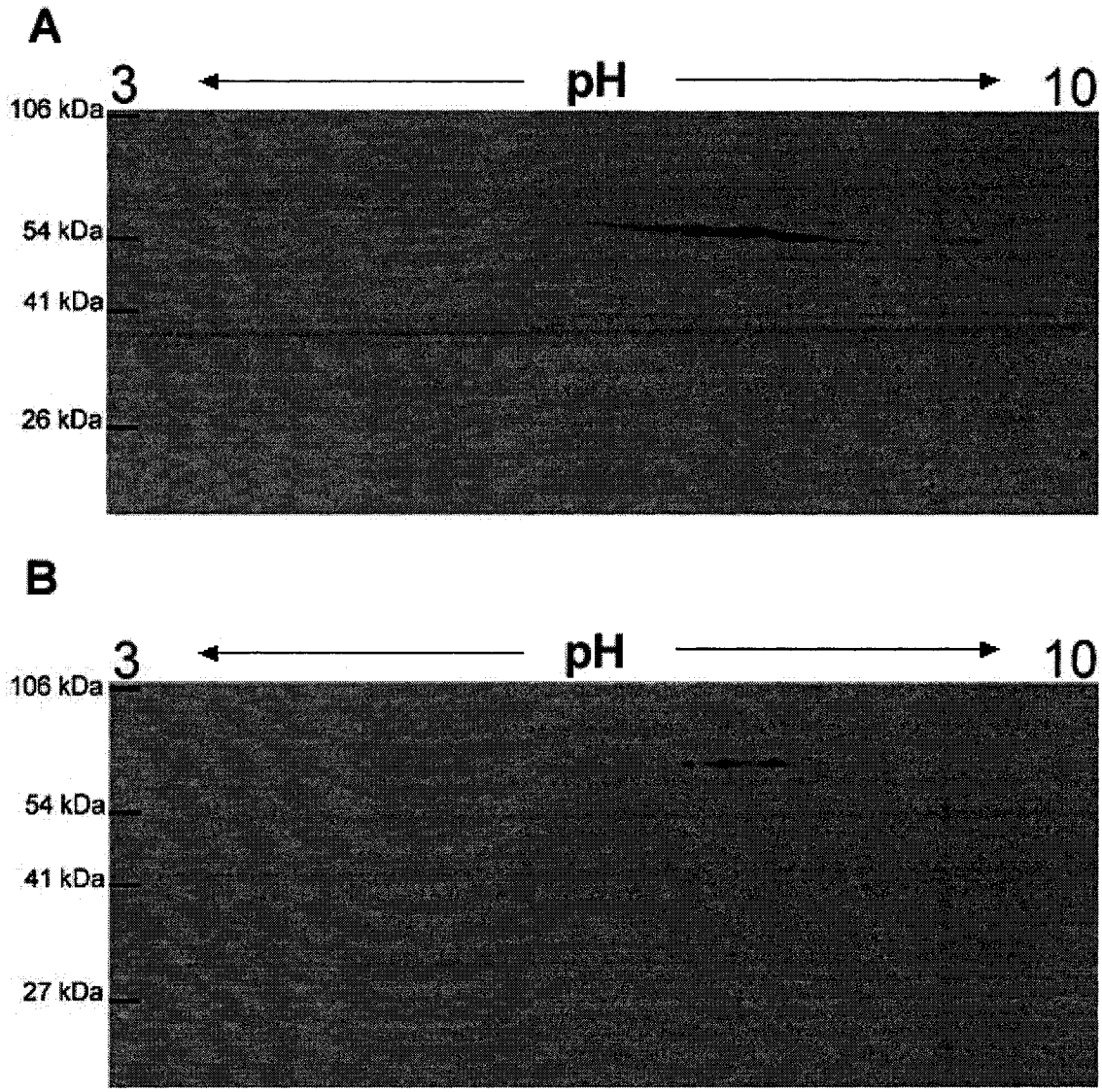

Figure 26. 2D IEF/SDS-PAGE of Light-Treated and Etiolated *Arabidopsis* Leaf Extracts.
Extracts (300 μg) prepared from (**A**) light-grown and (**B**) etiolated *Arabidopsis* were analyzed by 2D IEF/SDS-PAGE. The immunoblots were probed with αSiR antiserum (raised in rabbit) and exposed for 30 sec. The range of SiR isoforms in leaf extracts from etiolated plants was narrower than in leaf extracts from light-grown plants.

in etiolated plants (Figure 22), and the more acidic isoforms of SiR were below the limit of detection.

4.10.3 Isoelectric Point Profile of SiR in the Stromal and Nucleoid-Enriched Fraction. The experiments designed to detect potential differences in the pI profile of AtSiR were performed using soluble fractions of SiR, because more than 90% of the total SiR was found in the soluble fraction (Figure 7). Soluble and nucleoid-enriched fractions of AtSiR isolated from mature *Arabidopsis* leaves were analyzed by isoelectric focusing and SDS-PAGE, but no signal was present in the immunoblot of the nucleoid-enriched sample, even after a two hour exposure. By comparison, a 1 min exposure of a 2D immunoblot was capable of detecting SiR in a soluble protein extract prepared from young *Arabidopsis* leaves. This was likely a result of the relatively low abundance of SiR in *Arabidopsis* nucleoids.

Since a nucleoid-enriched fraction prepared from young soybean leaves contained higher abundance of SiR, the pI profiles of soluble and nucleoid-enriched fractions were analyzed in that tissue. The pI range of SiR isoforms from the nucleoid-enriched fraction was 5.2 to 5.5 (Figure 27). The pI range of SiR isoforms from soluble extracts of soybean leaves ranged from 4.9 to 7.2, with the most abundant isoforms possessing pIs of 5.2, 5.6, and 7.2.

The predicted pI of mature soybean SiR was 8.8, which was significantly different from the measured pI values in soybean leaves [278]. This could

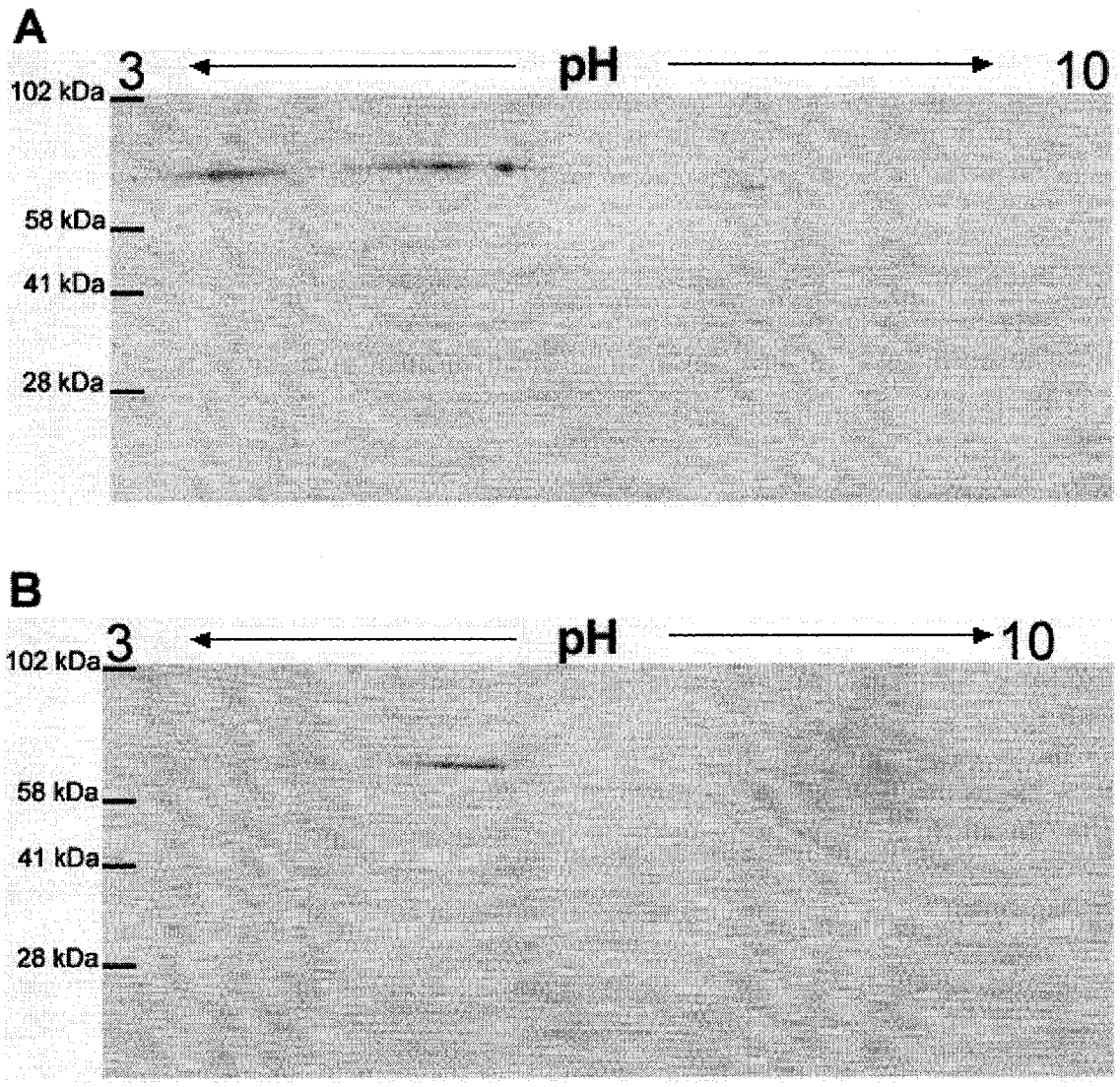

Figure 27. 2D IEF/SDS-PAGE of Nucleoid-Enriched and Soluble Fractions From Young Soybean Leaves.
Soluble extracts (200 μg) (**A**) and nucleoid-enriched extracts (7.5 μg) (**B**) displayed slightly different pI profiles of SiR. The pI profile of SiR in nucleoid-enriched fractions was narrower. The immunoblots were probed with αSiR antiserum (raised in rabbit) and exposed for 5 min.

be related to the clustering of charged residues in the soybean SiR sequence. Isoelectric points are predicted using fixed pKa values of side chain groups; however, this simplified approach fails when charged residues are clustered in the primary sequence [280]. In fact, the number and sequence of charged residues affect the isoelectric point of a protein. Since *Arabidopsis* and soybean SiR have a high amino acid sequence identity, it is reasonable to expect that the pIs of Arabidopsis and soybean SIR isoforms would deviate from the predicted pI to a similar degree. The reason for this deviation is not known. Perhaps phosphorylation results in a stronger than expected shift in pI that could explain the large deviation from the expected pI of soybean SiR. Therefore, the effect of phosphatases on the pI profile of SiR was examined.

4.10.4 Effects of Phosphatases on the pI of SiR. Bacteriophage λ protein phosphatase (λ-PPase) is an enzyme with broad substrate specificity [275, 281]. *Arabidopsis* soluble protein extracts were incubated with λ-PPase for several hours. An untreated soluble protein extract served as the negative control. Incubation with λ-PPase resulted in an unexpected acidic pI shift (Figure 28). Dephosphorylation should remove negatively charged phosphoryl groups, resulting in a greater abundance of basic isoforms. These results are confounding and could indicate that enzymes present in the *Arabidopsis* soluble protein extract may have post-translationally modified SiR during the incubation with λ-PPase.

It has previously been shown that treatment with calf intestinal alkaline phosphatase (CIAP) modulates the *in vitro* DNA-binding affinity of DCP68/SiR [2]. In *Arabidopsis* soluble protein extracts treated with CIAP, the pIs of SiR isoforms ranged from 6.2 to 7.3 (Figure 29). Similarly, the pI profile of SiR in untreated extracts ranged from 6.2 to 7.2, which may indicate that CIAP has low reactivity with AtSiR. DCP68/SiR purified from SB-M chloroplast nucleoids was treated with CIAP to determine if this had an effect on the pI profile of AtSiR.

Untreated DCP68/SiR displayed a pI range of 5.2 to 5.8, and the most abundant isoforms had a pI of 5.4, 5.5, and 5.7. DCP68/SiR treated with heat-inactivated alkaline phosphatase displayed a pI range of 4.9 to 6.2, and the most abundant isoform had a pI of 5.2. The observed pI profile of CIAP-treated DCP68/SiR was 4.9 to 5.3 and the most abundant isoform had a pI of 5.1 (Figure 30). These data are reminiscent of the observed effect of λ-PPase on soluble leaf extracts from *Arabidopsis* (Figure 28). In both cases, the effects of dephosphorylation resulted in an acidic shift in the pI profile.

Perhaps the presence of CIAP affected the isoelectric focusing resolution, due to its similar molecular weight (69 kDa) and predicted pI (5.7). The pI profile of untreated DCP68/SiR had several well-resolved isoforms (Figure 30A). More unresolved protein is present in 2D immunoblots of samples treated with CIAP (Figure 30B,C). This is evident as a 68 kDa smear on the acidic side of SiR. If the CIAP-treatment of DCP68/SiR actually resulted in more acidic isoforms, then

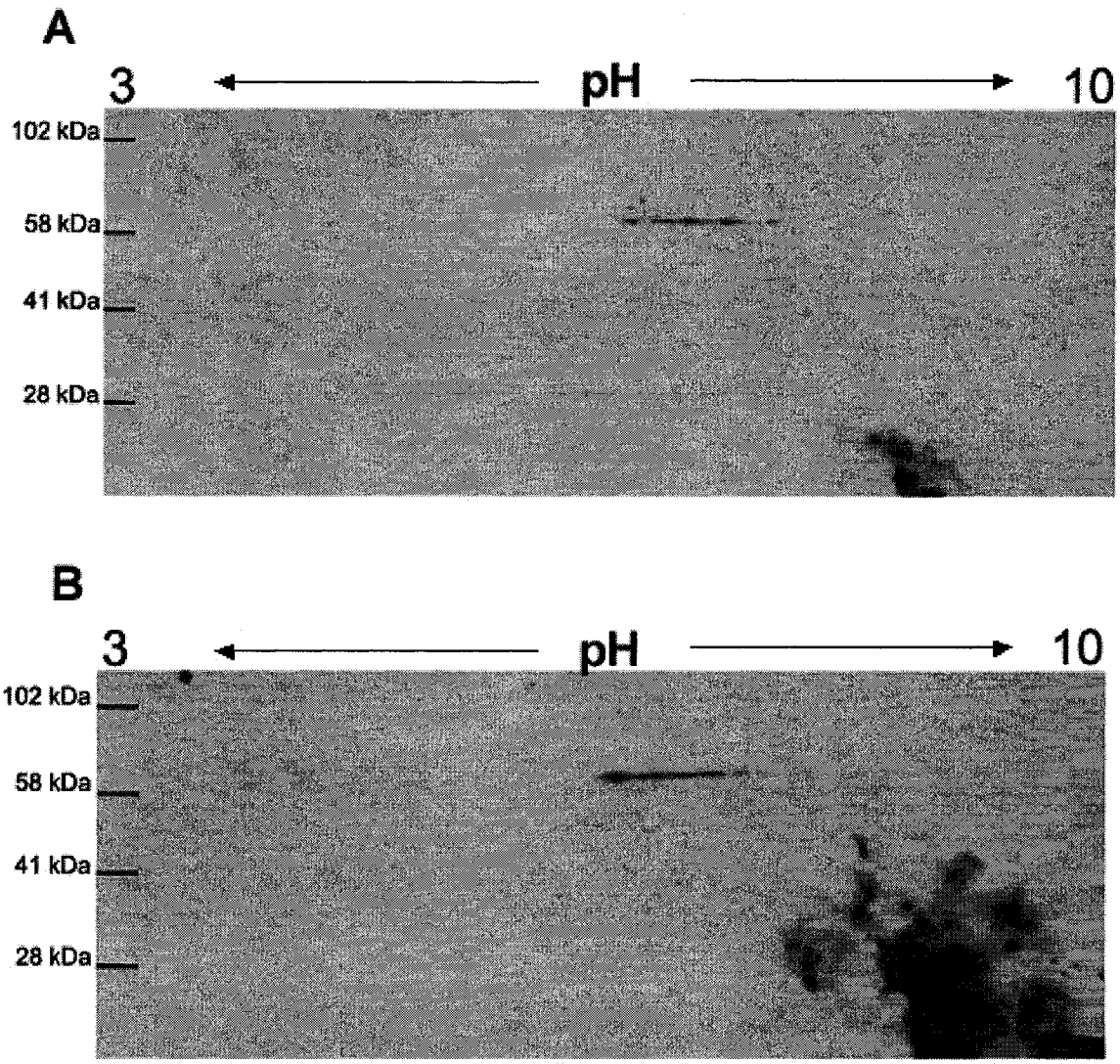

Figure 28. The Effect of λ-PPase on the pI Profile of AtSiR.
Arabidopsis soluble leaf extracts (400 μg) were incubated with (**A**) no enzyme or (**B**) λ-PPase. The immunoblots obtained following 2D IEF/SDS-PAGE were probed with SiR antiserum (raised in chicken) and a secondary antibody conjugated to horseradish peroxidase. After incubation with chemiluminescent substrate, the blot was exposed for 20 min.

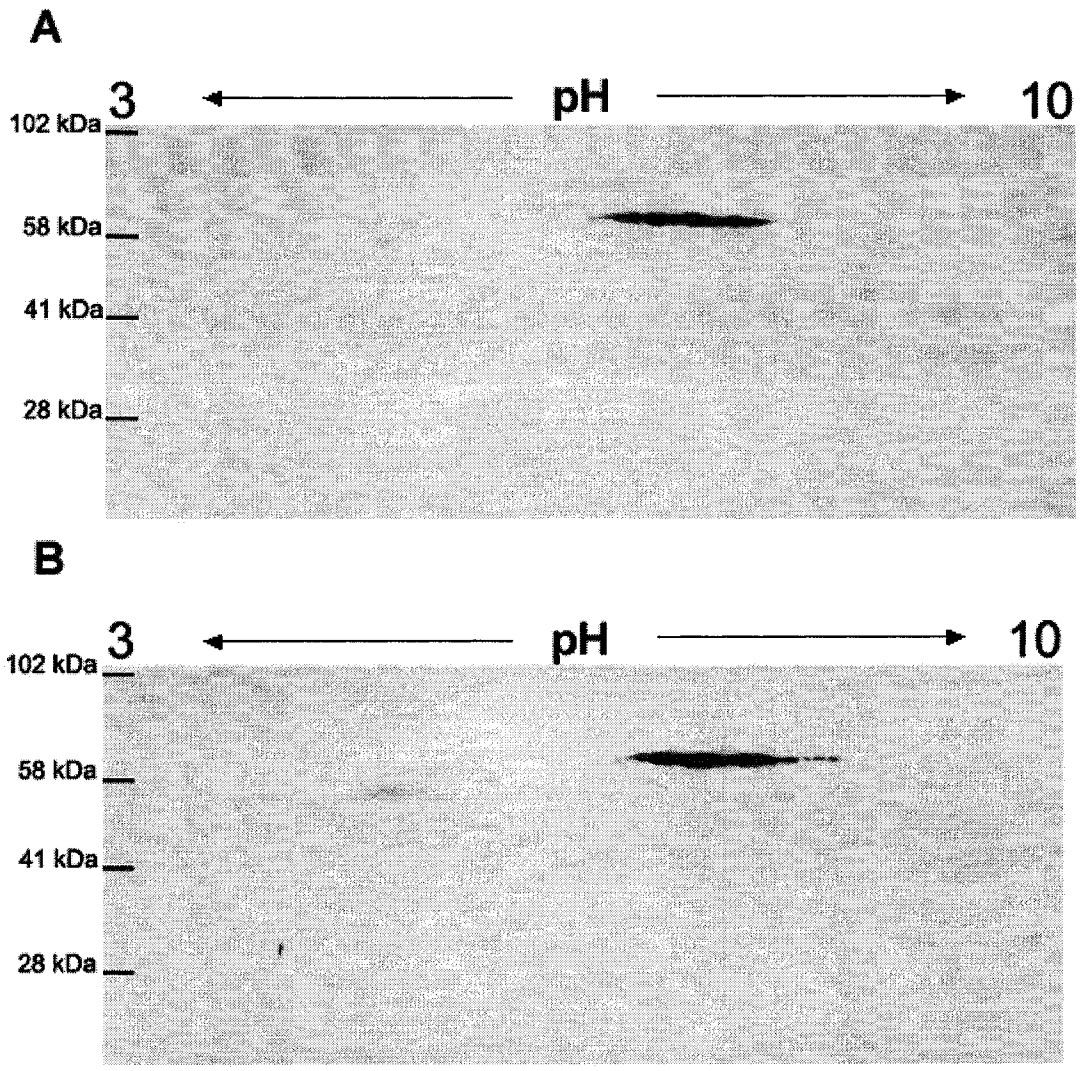

Figure 29. The Effect of Alkaline Phosphatase on the pI Profile of AtSiR.

Arabidopsis soluble leaf extracts (400 μg) were incubated with (**A**) no enzyme or (**B**) CIAP. The immunoblots obtained following 2D IEF/SDS-PAGE were probed with SiR antiserum (raised in chicken) and a secondary antibody conjugated to horseradish peroxidase. After incubation with chemiluminescent substrate, the blot was exposed for 20 min.

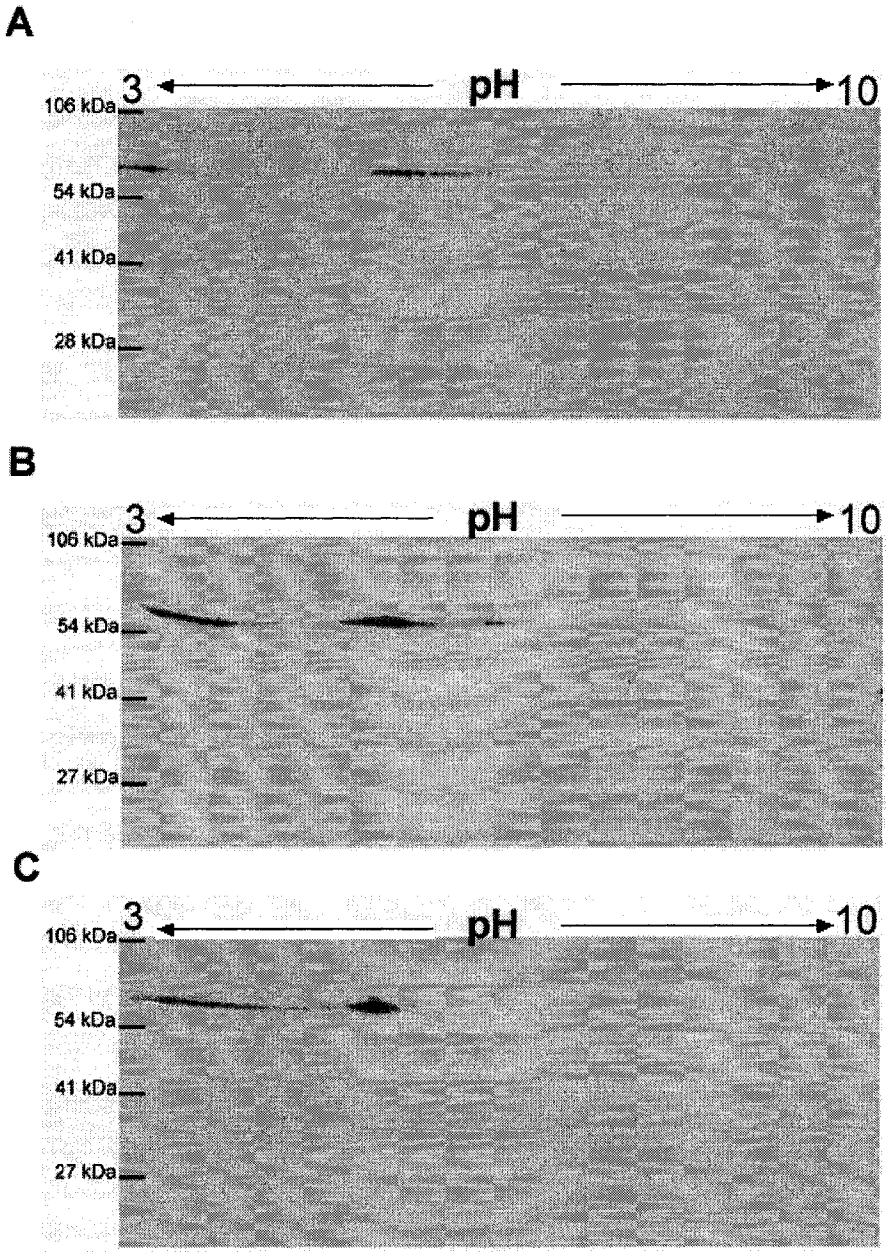

Figure 30. The Effect of Alkaline Phosphatase on the pI Profile of Purified DCP68/SiR.

DCP68/SiR (1.5 μg) was incubated with (**A**) no enzyme (**B**) active CIAP or (**C**) heat-killed CIAP. The immunoblots obtained following 2D IEF/SDS-PAGE were probed with SiR antiserum (raised in rabbit) and a secondary antibody conjugated to horseradish peroxidase. After incubation with chemiluminescent substrate, the blot was exposed for 30 sec.

untreated DCP68/SiR should show a similar isoform pattern to the sample treated with to the heat-inactivated CIAP. However, both samples that were treated CIAP had unresolved protein, which indicated that the presence of CIAP affected isoelectric focusing.

4.10.5 In Vitro Phosphorylation of SiR by CK2. An *in silico* approach was used in an attempt to identify potential kinases that may phosphorylate SiR *in vivo.* The reliability of phosphorylation prediction programs for plant proteins is uncertain, in part because these algorithms were trained on mammalian kinases that do not necessarily have homologs in plants. However, a putative role for a CK2-type enzyme in the phosphorylation of a chloroplast nucleoid protein (MFP1) suggested that this kinase warranted additional investigation [245]. CK2 phosphorylates serine or threonine residues that are followed by acidic residues in the consensus sequence (S/T-X-X-E/D) [237]. Most physiological targets have additional acidic residues in the +1, +2, +4, or +5 positions. The conservation of these sites supports the idea that they may be of regulatory importance. The amino acid sequence of SiR from soybean, *Arabidopsis,* pea, and tobacco each has a single conserved CK2 consensus sequence (Figure 31).

A kinase assay was performed to determine whether SiR could serve as an *in vitro* substrate for phosphorylation by CK2. The results of this assay demonstrate that rAtSiR was phosphorylated by CK2 (Figure 32, lanes 6-8). Two other polypeptides present in the rAtSiR sample were phosphorylated in addition to

AtSiR Amino Acid Sequence

```
1   MSSTFRAPAG AATVFTADQK IRLGRLDALR SSHSVFLGRY GRGGVPVPPS ASSSSSPIQ
61  AVSTPAKPET ATKRSKVEII KEKSNFIRYP LNEELLTEAP NVNESAVQLI KFHGSYQQYN
121 REERGGRSYS FMLRTKNPSG KVPNQLYLTM DDLADEFGIG TLRLTTRQTF QLHGVLKQNL
181 KTVMSSIIKN MGSTLGACGD LNRNVLAPAA PYVKKDYLFA QETADNIAAL LSPQSGFYYD
241 MWVDGEQFMT AEPPEVVKAR NDNSHGTNFV DSPEPIYGTQ FLPRKFKVAV TVPTDNSVDL
301 LTNDIGVVVV SDENGEPQGF NIYVGGGMGR THRMESTFAR LAEPIGYVPK EDILYAVKAI
361 VVTQREHGRR DDRKYSRMKY LISSWGIEKF RDVVEQYYGK KFEPSRELPE WEFKSYLGWH
421 EQGDGTWFCG LHVDSGRVGG IMKKTLREVI EKYKIDVRIT PNQNIVLCDI KTEWKRPITT
481 VLAQAGLLQP EFVDPLNQTA MACPAFPLCP LAITEAERGI PSILKRVRAM FEKVGLDYDE
541 SVVIRVTGCP NGCARPYMAE LGLVGDGPNS YQVWLGGTPN LTQIARSFMD KVKVHDLEKV
601 CEPLFYHWKL ERQTKESFGE YTTRMGFEKL KELIDTYKGV SQ
```

Figure 31. Putative CK2 Consensus Site in *Arabidopsis* SiR. ProSite, a phosphorylation prediction server was used to determine the presence of CK2 consensus phosphorylation sites in AtSiR [282, 283]. A single site (underlined) was predicted to occur that was conserved in the SiR sequences of *Arabidopsis thaliana* (CAA89154), *Glycine max* (AAG59996), *Pisum sativum* (BAD12837), and *Nicotiana tabacum* (BAA33796).

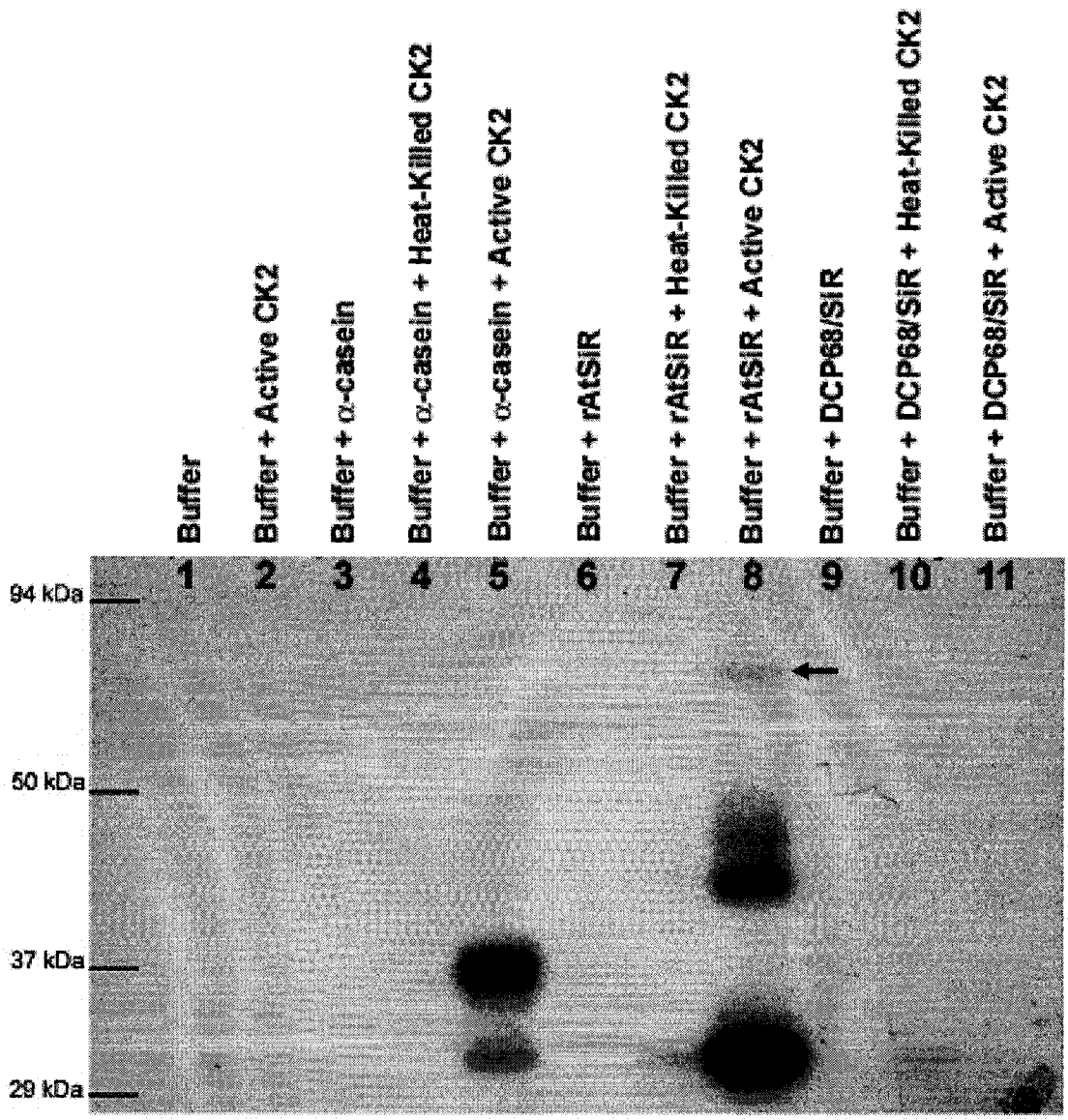

Figure 32. *In Vitro* CK2 Assay.
A kinase assay was performed to determine if CK2 could phosphorylate rAtSiR and purified DCP68/SiR in an *in vitro* assay. The kinase reaction was incubated for 12 h, processed on a 10% polyacrylamide gel, and exposed to a Phosphorimager screen for 2 h. The arrow indicates a phosphorylated reaction product that is the predicted molecular weight of rAtSiR.

rAtSiR. These proteins, migrating at approximately 35 kDa and 45 kDa may represent bacterial protein contaminants were present in the rAtSiR sample, or proteolytic degradation products of rAtSiR.

Equivalent amounts of SiR and α-casein were used as *in vitro* substrates but the SiR phosphorylation signal intensity was considerably weaker than that of α-casein. This may be related to the number of potential CK2 phosphorylation sites on the two proteins. There are 5 predicted CK2 phosphorylation sites in α-casein, as opposed to the single consensus site in rAtSiR. DCP68/SiR purified from SB-M chloroplast nucleoids was not phosphorylated by CK2 (Figure 32, lanes 9-11). The protein is a known phosphoprotein, and may have been phosphorylated at the CK2 phosphorylation site. Alternatively, these data could indicate that the predicted CK2 site is not phosphorylated *in vitro* by CK2.

CHAPTER V

DISCUSSION

Previous work in this laboratory identified DCP68 as an abundant chloroplast nucleoid protein in the SB-M cell line. *In vitro* tests showed that DCP68 has strong DNA-compacting activity and inhibits DNA synthesis in a concentration-dependent manner [1]. DCP68 was later identified as SiR by a series of biochemical assays [2]. These data imply that a well-characterized enzyme of sulfur assimilation is also involved in nucleoid compaction. It is possible that the sulfite reductase activity prevents sulfite ions from damaging chloroplast DNA [2]. Alternatively, DCP68/SiR may participate in a signal transduction pathway that regulates plastid gene expression. It is possible that the organellar redox status may influence nucleoid structure since ferredoxin is reduced in photosynthesis and is the electron donor for sulfite reduction. These scenarios posit that the interaction of DCP68/SiR with ctDNA is regulated. This study examined possible mechanisms of this regulation.

The Distribution of SiR to Chloroplast Nucleoids

The immunolocalization of SiR in young pea and SB-M chloroplasts suggested that most SiR is associated with the nucleoid, yet the amount of SiR detected in this study in nucleoid-enriched fractions from *Arabidopsis* was significantly lower than expected [2]. SiR was undetectable in nucleoid-enriched fractions from young leaves, and less than 5% of the total SiR was found in fractions prepared from mature leaves (Figure 7). *Arabidopsis* chloroplast

nucleoids may have a different structure, stability or even function from those described in soybean and pea. Alternatively, the small amount of SiR found to be present in nucleoid-enriched fractions from *Arabidopsis* may not be physiologically significant. Purified nucleoids have been noted to be 'sticky' complexes, with the potential for non-nucleoid proteins to interact with the complexes during purification [1]. However, recombinant AtSiR was shown to compact DNA *in* vitro, forming structures similar to plastid nucleoids (Figure 11). These data support a possible role of SiR in chloroplast nucleoids of *Arabidopsis* similar to its role in SB-M cells. It is significant, however, that the amount of SiR allocated to chloroplast nucleoids in *Arabidopsis* was significantly lower than in soybean plants or the SB-M cell line. More than 90% of the total SiR was present in chloroplast nucleoid-enriched fractions prepared from the SB-M cell line (Figure 17). In soybean plants, approximately one-third of the total SiR was allocated to chloroplast nucleoid-enriched fractions in young leaves, but this fell to less than 5% in mature leaves (Figure 19).

It was significant that SiR accumulated in chloroplast nucleoids from young soybean leaves but was undetectable in young *Arabidopsis* leaves. It is doubtful that the absence of SiR in chloroplast nucleoid-enriched fractions was due to fewer nucleoids present in young *Arabidopsis* leaves, since, the number of nucleoids is known to increase during the differentiation of proplastids to young chloroplasts [284]. It is unlikely that the absence of SiR in chloroplast nucleoid-enriched fractions was due to the lack of ctDNA replication in young *Arabidopsis*

leaves. It bears mentioning that ctDNA accounts for approximately 26% and 12% of the total DNA in SB-M cells and young soybean plants, respectively [57]. It seems reasonable that the amount of ctDNA may influence the amount of SiR associated with soybean chloroplast nucleoids, but does not explain the lack of detectable SiR in young *Arabidopsis* chloroplast-nucleoids.

The portion of SiR allocated to chloroplast nucleoids in young soybean leaves was much higher in cells active in ctDNA synthesis, since the observed distribution is the average of all leaf cells, of which most are no longer active in ctDNA replication. For example, SiR might be largely distributed to chloroplast nucleoids in cells that are active in ctDNA synthesis, but in cells that are inactive in ctDNA synthesis, most SiR might be soluble.

This study was important in demonstrating that the amount of SiR allocated to chloroplast nucleoids was different in young and mature leaves. This supports the notion that the interaction of SiR with ctDNA is regulated. It is tempting to speculate that a factor, possibly related to leaf development, may influence the amount of SiR allocated to chloroplast nucleoids.

It is possible that SiR might modulate plastome compaction as a mechanism to regulate organellar DNA replication or transcription. *In vitro* studies have shown that SiR inhibits ctDNA replication and transcription [1, 82]. Based on these studies, the highest abundance of nucleoid-associated SiR was expected to occur in leaf developmental stages that are least active in ctDNA replication and transcription. The data from this study contradict this notion and

raises the possibility that the presence of SiR in chloroplast nucleoids may not affect DNA replication or transcription in the manner *in vitro* studies have suggested.

In soybean plants, the proportion of SiR distributed to chloroplast nucleoids was much higher in young leaves than in mature leaves. This is significant since young chloroplasts have higher rates of ctDNA synthesis than mature chloroplasts. Furthermore, SiR was 2.5-fold more abundant in nucleoid-enriched fractions isolated from young soybean leaves than in mature leaves (Figure 19). This pattern was similar in SB-M cells. The abundance of SiR was approximately three-fold higher in nucleoid-enriched fractions prepared from two-day post-transfer cells than in 16-day post-transfer cells (Figure 18). Since the largest portion of SiR was distributed to chloroplast nucleoids of young soybean leaves and young SB-M cells, perhaps SiR functions as a nucleoid structural protein, during plastome amplification, which facilitates ctDNA-binding.

Azam *et al.* have shown that the abundance of prokaryotic nucleoid proteins is dependent upon the growth phase. During logarithmic growth, the most abundant nucleoid proteins are H-NS, HU, and Fis. However, the abundance of these proteins decreases upon entering stationary phase and the abundance of Dps increases. It was shown by Frienkel-Krispin *et al.* that the nucleoids of starved *E. coli*, which are predominated by Dps, form a toroidal structure that is extremely stable. Therefore, it is probable that the changes in prokaryotic nucleoid protein expression affect the structure/activity of the

nucleoid. Similarly, since the highest portion of Sir was present in young soybean leaves and young SB-M cells, perhaps DCP68/SiR functions as a scaffold protein during ctDNA amplification. Since there was no SiR detected in chloroplast nucleoid-enriched fractions from young *Arabidopsis* leaves, this could indicate that the structural composition of *Arabidopsis* chloroplast nucleoids is different from those observed in soybean or pea.

Possible Regulatory Mechanisms of DNA-Binding by SiR

If sulfur assimilation and DNA-binding are regulated by similar factors, this could suggest a novel regulatory strategy of modulating plastid gene expression. Although originally described as bifunctional protein, DCP68/SiR is more accurately described as a moonlighting protein. Moonlighting proteins contain a catalytic domain and an additional functional domain that mediates a distinct process [285]. Moonlighting proteins can switch between functions by several different mechanisms including differential localization, differential expression, oligomerization, concentration of ligand or substrate, presence of distinct binding sites, and phosphorylation [286]. None of these are mutually exclusive, and there are several cases that indicate multiple mechanisms aid in modulating the activity of the moonlighting function.

In several instances, the concentration of ligand or substrate affects the moonlighting function. For example, the intracellular concentration of iron affects whether aconitase functions as an enzyme or as an iron response element binding protein [287]. More interestingly, the *E. coli* PutA protein has proline

dehydrogenase and pyrroline-5-carboxylate dehydrogenase activity when substrate concentrations are high. However, when substrate concentrations decrease, PutA lacks enzymatic activity and binds to DNA as a transcriptional repressor. In both of these examples, the moonlighting function and the catalytic activity are mutually exclusive. Perhaps the DNA-binding activity of SiR is modulated by the concentration of substrate. SiR is probably maintained at a level that would prevent the accumulation of the toxic sulfite anion and, as such, it is difficult to imagine that there would be sufficient accumulation of sulfite to influence the allocation of SiR to chloroplast nucleoids [265].

It is possible that the binding of a ligand or cofactor could regulate the DNA-binding activity of SiR. For example, it is necessary for aconitase to lose its 4Fe-4S cluster in order to take on its role as an iron-responsive element binding protein [288]. SiR contains a bound siroheme complex as well as a 4Fe-4S complex. It is doubtful that the 4Fe-4S cluster modulates DNA binding, since it was previously shown that treatment with the iron-chelator dipyridyl, which modulates the function of aconitase, had no effect on the DNA-binding activity of SiR [260]. It is possible that the siroheme may regulate the DNA-binding activity of SiR. The incorporation of siroheme into recombinant maize SiR was essential for catalytic activity and DNA-binding. In this study, the incorporation of siroheme into recombinant *Arabidopsis* SiR was essential for DNA-binding activity. However, it is possible that the incorporation of siroheme was necessary for proper folding of SiR, rather than a requirement for DNA-binding. The relative

abundance of siroheme can be estimated by the 278/384 nm absorbance ratio, where a low ratio indicates that more siroheme is incorporated into the protein. The soluble SiR isolated from spinach chloroplasts had a 278/384 nm absorbance ratio of 2.2. SiR purified from SB-M chloroplast nucleoids had a ratio of 7.6, suggesting that less siroheme was present in the nucleoid-associated SiR. The 278/384 nm absorbance ratio for rAtSiR was 5.4. The recombinantly expressed AtSiR compacted DNA *in vitro* but required a long incubation time, as opposed to the almost instantaneous DNA-compaction that occurs for SiR purified from chloroplast nucleoids. It is possible that while siroheme may be required for proper folding in the expression cell line, it may not be necessary for DNA-binding.

It is possible that the two functions of SiR are regulated by oligomerization. Glyceraldehyde-3-phosphate dehydrogenase exists as a catalytically active tetramer, but as a monomer, functions as a nuclear uracil-DNA glycosylase [288]. Soluble SiR exists predominantly as a homodimer in plants; perhaps it is the monomeric form that has DNA-binding activity [289]. In a previous study, a Southwestern blot assay was used to demonstrate DNA-binding by the SiR monomer [260]. A weak DNA-binding band that might have corresponded to the SiR dimer was detected on the same Southwestern blot. Moreover, catalytic activity is preserved in the spinach SiR monomer [263]. These data could indicate that the SiR monomer is the predominant form that binds DNA.

It is doubtful that the DNA-binding and catalytic activities of SiR are mutually exclusive. SiR purified from tobacco chloroplast nucleoids was reported to have enzyme activity by Sato *et al.* [79], but no experimental evidence was provided to substantiate this claim. Likewise, recombinant maize SiR was reported to have both catalytic activity and DNA-binding activity, but no experimental evidence was presented [290]. Since approximately 90% of total SiR is distributed to chloroplast nucleoids in SB-M cells, it seems unlikely the cells would obtain sufficient reduced sulfur if the nucleoid-associated SiR were enzymatically inactive.

Post-translational Modification of SiR

SiR purified from SB-M chloroplast nucleoids is known to be a phosphoprotein [2]. It is possible that phosphorylation may regulate the functions of SiR. Phosphorylation has been shown to regulate the activity of several other moonlighting proteins as well as the DNA-binding activity of SiR *in vitro* [2]. Phosphorylation of phosphoglucose isomerase by CK2 results in the loss of enzymatic activity, but does not perturb is function as an autocrine motility factor [288]. Data from this study demonstrate that recombinantly expressed AtSiR, which is likely unphosphorylated, was capable of compacting DNA *in vitro.* This confirms previous observations by Chi-Ham *et al.* that SiR dephosphorylation may modulate the interaction of SiR with DNA but is not strictly required for DNA-compaction [2].

Perhaps the phosphorylation of SiR regulates the strength of DNA-compaction. For example, phosphorylation of Ets-1 functions as a 'molecular rheostat', where the number of phosphoryl residues that are tagged to an unstructured region modulates the DNA-binding activity of this transcription factor [291]. Although, Ets-1 is not a known moonlighting protein, perhaps the DNA-binding activity of SiR is regulated in a similar manner. One would expect, if phosphorylation regulated the DNA-binding activity of SiR, that the pI profile of nucleoid-associated SiR would be different than the pI profile of soluble SiR. However, the most abundant pIs of SiR in a chloroplast nucleoid-enriched fraction isolated from young soybean leaves were similar to those of a soluble fraction (Figure 27). This suggests that phosphorylation does not affect the portion of SiR allocated to chloroplast nucleoids. The range of SiR isoforms was broader in the soluble extract than in the nucleoid-enriched fraction, but this is most likely related to the higher abundance of soluble protein analyzed. These data could indicate that soluble and nucleoid-associated SiR were post-translationally modified to a similar degree, if at all, in young soybean leaves.

SiR purified from SB-M chloroplast nucleoids was shown to be a phosphoprotein, but no experimental data has indicated if this was true for AtSiR. Based on the amino acid sequence of AtSiR, phosphorylation was predicted to shift the pI of AtSiR from 7.6 to 7.2, with additional phosphoryl residues resulting in acidic shifts of 0.2 pH units. The pI profile of SiR in soluble leaf extracts was consistent with this prediction, which suggests that AtSiR may be phosphorylated

in vivo (Figure 25). *In silico* data mining also suggested that the GmSiR and AtSiR amino acid sequences contained several potential protein kinase consensus motifs for protein kinase C, CKII, and others. To further examine the possibility that AtSiR was phosphorylated, soluble leaf protein extracts were treated with λ-PPase and CIAP. λ-PPase-treated soluble leaf extracts resulted in an unexpected acidic shift in the pI profile of AtSiR (Figure 28). When soluble protein extracts were treated with CIAP, virtually no change was observed in the pI profile of AtSiR (Figure 29). Moreover, 2D IEF/SDS-PAGE of DCP68/SiR purified from SB-M plastid nucleoids did not display the predicted acidic shift after treatment with alkaline phosphatase. Since purified DCP68/SiR is a known phosphoprotein, the utility of this approach for further research into the post-translational modifications of SiR may be questionable for this system. Collectively, these data do not indicate that *Arabidopsis* SiR is phosphorylated. To further examine this possibility, purified *Arabidopsis* SiR could be analyzed by mass spectrometry.

A Working Model of Nucleoid Remodeling

A model for the packaging of ctDNA into the nucleoid was previously proposed by Chi-Ham [260]. Chloroplast DNA is attached to the inner envelope membrane of young chloroplasts by an anchoring protein such as PEND [65]. Chloroplast DNA replication may occur predominantly while the nucleoid is associated with the inner envelope membrane. As the chloroplast matures, the

nucleoids become associated with the thylakoid membrane, possibly via interaction with the MFP1 anchoring protein [72].

SiR and probably several other DNA-compacting nucleoid proteins condense the DNA in chloroplast nucleoids. Since the compaction of ctDNA may have a significant impact on organellar transcription and replication, SiR may need to be displaced prior to the onset of these processes. The high level of transcription and replication observed in young leaves indicates that plastome compaction by nucleoid proteins must be a regulated process [292-295]. In this study, it was found that the amount of SiR allocated to chloroplast nucleoids in young SB-M cells and soybean plants, decreased with age. These data suggests that SiR does not simply inhibit DNA replication or transcription *in planta.* Instead, SiR may function as a DNA scaffolding protein in young chloroplasts during ctDNA amplification since the youngest SB cells and soybean leaves contained the highest portion of nucleoid-associated SiR.

It is well documented that some bacterial nucleoid proteins compete for similar binding sites [106, 108, 167]. Perhaps the distribution of SiR to chloroplast nucleoids is affected by interactions with other nucleoid proteins that might bind to similar sites. Since SiR binds without apparent sequence specificity, virtually any other nucleoid protein with higher affinity for ctDNA could displace SiR. It is possible that future research that describes interactions between SiR and other plastid nucleoid proteins could bring a wealth of

information regarding the regulation of SiR and, ultimately, plastid nucleoid structure/function.

CHAPTER VI

CONCLUSION AND FUTURE WORK

The portion of SiR distributed to chloroplast nucleoids was examined in the model plants *Arabidopsis* and soybean. SiR was detected in a nucleoid-enriched fraction from *Arabidopsis*. In contrast to results from previous immunolocalization experiments in SB-M and young pea chloroplasts, the portion of SiR associated with *Arabidopsis* chloroplast nucleoids represented only a fraction of the total SiR. In addition, recombinantly expressed AtSiR compacted DNA into structures that resemble chloroplast nucleoids. The abundance of soluble SiR was examined in various *Arabidopsis* tissues and the evidence suggests that SiR is differentially regulated in leaf and root tissues. However, due to the low abundance of nucleoids in *Arabidopsis*, this may not be an appropriate model organism to study nucleoid dynamics.

A distribution study provided evidence that most SiR in the SB-M cell line was distributed to the nucleoid, confirming results from the previous immunolocalization study. In soybean and *Arabidopsis* plants, the portion of SiR distributed to chloroplast nucleoids varied with leaf developmental stage. The portion of SiR distributed to chloroplast nucleoids was significantly higher in young soybean leaves. Surprisingly, there was no detectable SiR in chloroplast nucleoid-enriched fractions from young *Arabidopsis* leaves. Since young leaves undergo significant plastome amplification, it is possible that the ctDNA amplification may influence the amount of SiR allocated to chloroplast nucleoids.

The absence of SiR in young *Arabidopsis* chloroplast nucleoids is noteworthy and could be related to inherent differences in *Arabidopsis* nucleoid structure, composition, or functions from those of pea, soybean, and tobacco in which chloroplast nucleoids have principally been studied. Moreover, these observations support the hypothesis that the interaction of SiR with ctDNA is regulated.

The pI profile of SiR was examined as a first step towards investigating the role of post-translational modifications that may affect the function of SiR. No evidence suggested that the post-translational modification of nucleoid-associated SiR was different from the soluble form.

In this study, several attempts were made to modify potential post-translational modification(s) of SiR by treatment with phosphatases. A more accurate determination of the post-translational modifications of SiR could be assessed by mass spectroscopy. Since these post-translational modifications may have different effects on DNA-binding and catalytic activity, this analysis could be performed with SiR purified from chloroplast nucleoids and soluble SiR. Mass spectroscopy can identify the specific residue(s) that may be post-translationally modified. Since kinases act on consensus sites, it may also be possible to identify the kinase(s) responsible for phosphorylation based on the sequence surrounding the phosphorylated residue(s).

Although this study focused on a single nucleoid protein, further research must be performed to determine the identity of other nucleoid proteins. Further

analysis of nucleoid proteins should be performed in soybean because chloroplast nucleoids are plentiful, there is an established protocol for purification, and the nucleoid polypeptide pattern has previously been examined [1]. In addition, there are efforts to sequence the soybean genome, which will provide a wealth of information to researchers. Initially, the identity of chloroplast nucleoid proteins could be determined by mass spectrometry of gel purified nucleoid proteins. Then, these proteins could be screened for their DNA-binding characteristics and their interaction with SiR using the yeast two-hybrid assay.

REFERENCES

1. Cannon, G.C., L.N. Ward, C.I. Case, and S. Heinhorst. (1999). *The 68 kDa DNA compacting nucleoid protein from soybean chloroplasts inhibits DNA synthesis in vitro.* Plant Mol Biol. **39**:835-845.
2. Chi-Ham, C.L., M.A. Keaton, G. Cannon, and S. Heinhorst. (2002). *The DNA-compacting protein DCP68 from soybean chloroplasts is ferredoxin:sulfite reductase and co-localizes with the organellar nucleoid.* Plant Mol Biol. **49**:621-31.
3. Dean, C. and R.J. Schmidt. (1995). *Plant genomes: a current description.* Annu Rev Plant Physiol Plant Mol Biol. **46**:395-418.
4. Buchanan, B., W. Gruissem, and R.L. Jones. (2000). *Biochemistry and molecular biology of plants.* Rockville, MD: American Society of Plant Physiologists.
5. Fosket, D.E. (1994). *Plant Growth and Development.* Plant growth and development. San Diego: Academic Press.
6. Margulis, L. (1993). *Symbiosis in cell evolution.* 2nd Edition ed. New York: Freeman.
7. Margulis, L. (1970). *Origin of eukaryotic cells.* New Haven, CT: Yale University Press.
8. Maliga, P. (2003). *Progress towards commercialization of plastid transformation technology.* Trends in Biotechnology. **21**:20-28.
9. Emes, M.J. and A.K. Tobin. (1993). *Control of metabolism and development in higher plant plastids.* International Review of Cytology. **145**:149-216.
10. Pyke, K.A. (1999). *Plastid division and development.* Plant Cell. **11**:549-556.
11. Pyke, K.A. and A.M. Page. (1998). *Plastid ontogeny during petal development in Arabidopsis.* Plant Physiol. **116**:797-803.
12. McCormac, D.J. and B.M. Greenberg. (1992). *Differential synthesis of photosystem cores and light-harvesting antenna during proplastid to chloroplast development in Spirodela oligorrhiza.* Plant Physiology. **98**:1011-9.
13. Thomson, W.W. and J.M. Whatley. (1980). *Development of nongreen plastids.* Ann. Rev. Plant Physiol. **31**:375-94.
14. Heinhorst, S. and G.C. Cannon. (1993). *DNA replication in chloroplasts.* J Cell Sci. **104**:1-9.
15. Odintsova, M.S. and N.P. Yurina. (2003). *Plastid genomes of higher plants and algae: Structure and functions.* Mol Biol. **37**:649-662.
16. Sugiura, M. (1989). *The chloroplast chromosomes in land plants.* Annual Reviews of Cell Biology. **5**:51-70.
17. Oldenburg, D.J. and A.J. Bendich. (2004). *Most chloroplast DNA of maize seedlings in linear molecules with defined ends and branched forms.* J Mol Biol. **335**:953-970.
18. Bendich, A.J. (2004). *Circular chloroplast chromosomes: the grand illusion.* Plant Cell. **16**:1661-6.

19. Tymms, M.J., N.S. Scott, and J.V. Possingham. (1982). *Chloroplast and nuclear DNA content of cultured spinach leaf discs.* J Exp Bot. **33**:831-837.
20. Scott, N.S. and J.V. Possingham. (1983). *Changes in chloroplast DNA levels during growth of spinach leaves.* J Exp Bot. **34**:1756-1767.
21. Fujie, M., H. Kuroiwa, S. Kawano, S. Mutoh, and T. Kuroiwa. (1994). *Behavior of organelles and their nucleoids in the shoot apical meristem during leaf development in Arabidopsis thaliana L.* Planta. **194**:395-405.
22. Miyamura, S., T. Nagata, and T. Kuroiwa. (1986). *Quantitative fluorescence microscopy on dynamic changes of plastid nucleoids during wheat development.* Protoplasma. **133**:66-72.
23. Boffey, S.A. and R.M. Leech. (1982). *Chloroplast DNA levels and the control of chloroplast division in light-grown wheat leaves.* Plant Physiol. **69**:1387-1391.
24. Lamppa, G. and A. Bendich. (1979). *Changes in chloroplast DNA levels during development of pea (Pisum sativum).* Plant Physiol. **64**:126-130.
25. Bennett, J. and C. Radcliffe. (1975). *Plastid DNA replication and plastid division in the garden pea.* FEBS Lett. **56**:222-225.
26. Tymms, M.J., N.S. Scott, and J.V. Possingham. (1983). *DNA content of Beta vulgaris chloroplasts during leaf cell expansion.* Plant Physiol. **71**:785-788.
27. Catley, M.A., C.M. Bowman, M.W. Bayliss, and M.D. Gale. (1987). *The pattern of amyloplast DNA accumulation during wheat endosperm development.* Planta. **171**:416-421.
28. Cannon, G., S. Heinhorst, J. Siedlecki, and A. Weissbach. (1985). *Chloroplast DNA synthesis in light and dark grown cultured Nicotiana tabacum cells as determined by molecular hybridization.* Plant Cell Rep. **4**:41-45.
29. Cannon, G., S. Heinhorst, and A. Weissbach. (1986). *Organellar DNA synthesis in permeabilized soybean cells.* Plant Mol Biol. **7**:331-341.
30. Bendich, A.J. (1987). *Why do chloroplasts and mitochondria contain so many copies of their genome?* Bioessays. **6**:279-282.
31. Scott, N.S. and J.V. Possingham. (1980). *Chloroplast DNA in expanding spinach leaves.* J Exp Bot. **31**:1081-1092.
32. Hansmann, P., H. Falk, K. Ronai, and P. Sitte. (1985). *Structure, composition, and distribution of plastid nucleoids in Narcissus pseudonarcissus.* Planta. **164**:459-472.
33. Yurina, N.P., G.G. Belkina, Y.P. Oleskina, N.V. Karapetyan, and M.S. Odintsova. (1995). *Composition and organization of chloroplast nucleoids.* Appl Biochem Microbiol. **31**:32-38.
34. Yurina, N.P., G.G. Belkina, N.V. Karapetyan, and M.S. Odintsova. (1995). *Nucleoids of pea chloroplasts: microscopic and chemical characterization, occurrence of histone-like proteins.* Biochem Mol Biol Int. **36**:145-154.

35. Nakano, T., F. Sato, and Y. Yamada. (1993). *Analysis of nucleoid-proteins in tobacco chloroplasts.* Plant Cell Physiol. **34**:873-880.
36. Rose, R. and J.V. Possingham. (1976). *Chloroplast growth and replication in germinating spinach cotyledons following massive γ-irradiation of the seed.* Plant Physiol. **57**:41-46.
37. Liu, J.W. and R.J. Rose. (1992). *The spinach chloroplast chromosome is bound to the thylakoid membrane in the region of the inverted repeat.* Biochem Biophys Res Commun. **184**:993-1000.
38. Lindbeck, A.G. and R.J. Rose. (1990). *Thylakoid-bound chloroplast DNA from spinach is enriched for replication forks.* Biochem Biophys Res Commun. **172**:204-210.
39. Sakai, A., T. Suzuki, N. Nagata, N. Sasaki, Y. Miyazawa, C. Saito, N. Inada, Y. Nishimura, and T. Kuroiwa. (1999). *Comparative analysis of DNA synthesis activity in plastid-nuclei and mitochondrial-nuclei simultaneously isolated from cultured tobacco cells.* Plant Sci. **140**:11-24.
40. Baumgartner, B.J. and J.E. Mullet. (1991). *Plastid DNA synthesis and nucleic acid binding proteins in developing barley chloroplasts.* J Photochem Phobiol B. **11**:203-218.
41. Nerozzi, A.M. and A.W. Coleman. (1997). *Localization of plastid DNA replication on a nucleoid structure.* Am J Bot. **84**:1028-1041.
42. Sakai, A., T. Suzuki, and T. Kuroiwa. (1998). *Comparative analysis of plastid gene expression in tobacco chloroplasts and proplastids: relationship between transcription and transcript accumulation.* Plant Cell Physiol. **39**:581.
43. Nemoto, Y., S. Kawano, S. Nakamura, T. Mita, T. Nagata, and T. Kuroiwa. (1988). *Studies on plastid-nuclei (nucleoids) in Nicotiana tabacum L. I. Isolation of proplastid-nuclei from cultured cells and identification of proplastid-nuclear proteins.* Plant Cell Physiol. **29**:167-177.
44. Nemoto, Y., S. Kawano, K. Kondoh, T. Nagata, and T. Kuroiwa. (1990). *Studies on plastid-nuclei (nucleoids) in Nicotiana tabacum L. III. Isolation of chloroplast-nuclei from mesophyll protoplasts and identification of chloroplast DNA-binding oroteins.* Plant Cell Physiol. **31**:767-776.
45. Baumgartner, B.J., J.C. Rapp, and J.E. Mullet. (1989). *Plastid transcription activity and DNA copy number increases early in barley chloroplast development.* Plant Physiol. **89**:1011-1018.
46. Kuroiwa, T., T. Suzuki, K. Ogawa, and S. Kawano. (1981). *The chloroplast nucleus: Distribution, number, size, and shape, and a model for the multiplication of the chloroplast genome during chloroplast development.* Plant Cell Physiol. **22**:381-396.
47. Hashimoto, H. (1985). *Changes in distribution of nucleoids in developing and dividing chloroplasts and etioplasts of Avena sativa.* Protoplasma. **127**:119-127.
48. Heinhorst, S., C.L. Chi-Ham, S.W. Adamson, and G.C. Cannon. *The somatic inheritance of plant organelles*, in *Molecular biology and*

biotechnology of plant organelles, H. Daniell and C.D. Chase, Editors. 2004, Springer-Verlag: New York, NY.

49. Miyamura, S., T. Kuroiwa, and T. Nagata. (1990). *Multiplication and differentiation of plastid nucleoids during development of chloroplasts and etioplasts from proplastids in Triticum aestivum.* Plant Cell Physiol. **31**:597-602.
50. Herrmann, R.G. and K.V. Kowallik. (1970). *Multiple amounts of DNA related to the size of chloroplasts. II. Comparison of electron-microscopic and autoradiographic data.* Protoplasma. **69**:365-72.
51. Dubell, A.N. and J.E. Mullet. (1995). *Differential transcription of pea chloroplast genes during light-induced leaf development.* Plant Physiol. **109**:105-12.
52. Dubell, A.N. and J.E. Mullet. (1995). *Continuous far-red light activates plastid DNA synthesis in pea leaves but not full cell enlargement or an increase in plastid number per cell.* Plant Physiol. **109**:95-103.
53. Sato, N., K. Ohshima, A. Watanabe, N. Ohta, Y. Nishiyama, J. Joyard, and R. Douce. (1998). *Molecular characterization of the PEND protein, a novel bZIP protein present in the envelope membrane that is the site of nucleoid replication in developing plastids.* Plant Cell. **10**:859-872.
54. Sodmergen, S. Kawano, S. Tano, and T. Kuroiwa. (1989). *Preferential digestion of chloroplast nuclei (nucleoids) during senescence of the coleoptile of Oryza sativa.* Protoplasma. **152**:65-68.
55. Lau, K.W., J. Ren, and M. Wu. (2000). *Redox modulation of chloroplast DNA replication in Chlamydomonas reinhardtii.* Antioxid Redox Signal. **2**:529-535.
56. Lawrence, M.E. and J.V. Possingham. (1986). *Microspectrofluorometric measurement of chloroplast DNA in dividing and expanding leaf cells of Spinacea oleracea.* Plant Physiol. **81**:708-710.
57. Cannon, G., S. Heinhorst, and A. Weissbach. (1986). *Plastid DNA content in a cultured soybean line capable of photoautotrophic growth.* Plant Physiol. **80**:601-603.
58. Boffey, S.A., J.R. Ellis, G. Sellden, and R.M. Leech. (1979). *Chloroplast division and DNA synthesis in light-grown wheat leaves.* Plant Physiol. **64**:502-505.
59. Boffey, S.A. (1985). *The chloroplast division cycle and its relationship to the cell division cycle.* Soc Exp Bot Sem Ser. **26**:233-246.
60. Picchulla, B., K.R.C. Imlay, and W. Gruissem. (1985). *Plastid gene expression during fruit ripening in tomato.* Plant Molecular Biology. **5**:373-84.
61. Picchulla, B., E. Plchersky, A.R. Cashmore, and W. Gruissem. (1986). *Expression of nuclear and plastid genes for photosynthesis-specific proteins during tomoato fruit development and ripening.* Plant Molecular Biology. **7**:367-76.

62. Ngernprasirtsiri, J., D. Macherel, H. Kobayashi, and T. Akazawa. (1988). *Expression of amyloplast and chloroplast DNA in suspension-cultured cells of sycamore (Acer pseudoplantanus L.).* Plant Physiology. **86**:137-42.
63. Sato, N., O. Misumi, Y. Shinada, M. Sasaki, and M. Yoine. (1997). *Dynamics of localization and protein composition of plastid nucleoids in light-grown pea seedlings.* Protoplasma. **200**:163-173.
64. Sakai, A., C. Saito, N. Inada, and T. Kuroiwa. (1998). *Transcriptional activities of the chloroplast-nuclei and proplastid-nuclei isolated from tobacco exhibit different sensitivities to taegtitoxin: implication of the presence of distinct RNA polymerases.* Plant Cell Physiol. **39**:928-934.
65. Sato, N., C. Albrieux, J. Joyard, R. Douce, and T. Kuroiwa. (1993). *Detection and characterization of a plastid envelope DNA-binding protein which may anchor plastid nucleoids.* Embo J. **12**:555-561.
66. Sato, N. and N. Ohta. (2001). *DNA-binding specificity and dimerization of the DNA-binding domain of the PEND protein in the chloroplast envelope membrane.* Nucl Acids Res. **29**:2244-2250.
67. Terasawa, K. and N. Sato. (2005). *Occurrence and characterization of PEND proteins in angiosperms.* Journal of Plant Research. **118**:111-9.
68. Wycliff, P., F. Sitbon, J. Wernersson, I. Ezcrra, M. Ellerstrom, and L. Rask. (2005). *Continuous expression in tobacco leaves of a Brassica napus PEND homologue blocks differentiation of plastids and development of palisade cells.* Plant Journal. **44**:1-15.
69. Harder, P., R.A. Silverstain, and I. Meier. (2000). *Conservation of matrix attachment region-binding filament-like protein 1 among higher plants.* plant physiol. **122**:225-234.
70. Meier, I., T. Phelan, W. Gruissem, S. Spiker, and D. Schneider. (1996). *MFP1, a novel plant filament-like protein with affinity for matrix attachment region DNA.* Plant Cell. **8**:2105-2115.
71. Gindullis, F. and I. Meier. (1999). *Matrix attachment region binding protein MFP1 is localized in discrete domains at the nuclear envelope.* Plant Cell. **11**:1117-1128.
72. Jeong, S.Y., A. Rose, and I. Meier. (2003). *MFP1 is a thylakoid-associated, nuceloid-binding protein with a coiled coil structure.* Nucl Acids Res. **31**:5175-5185.
73. Samaniego, R., S.Y. Jeong, C. de la Torre, I. Meier, and S.M.D. de la Espina. (2006). *CK2 phosphorylation weakens 90 kDa MFP1 association to the nuclear matrix in Allium cepa.* J Exp Bot. **57**:113-24.
74. Nakano, T., S. Murakami, T. Shoji, S. Yoshida, Y. Yamada, and F. Sato. (1997). *A novel protein with DNA binding activity from tobacco chloroplast nucleoids.* Plant Cell. **9**:1673-1682.
75. Kato, Y., S. Murakami, Y. Yamamoto, H. Chatani, Y. Kondo, T. Nakano, A. Yokota, and F. Sato. (2004). *The DNA-binding protease, CND41, and the*

degradation of ribulose-1,5-bisphosphate carboxylase/oxygenase in senescent leaves of tobacco. Planta. **220**:97-104.

76. Nakano, T., N. Nagata, T. Kimura, M. Sekimoto, H. Kawaide, S. Murakami, Y. Kaneko, H. Matsushima, Y. Kamiya, F. Sato, and S. Yoshida. (2003). *CND41, a chloroplast nucleoid protein that regulates plastid development, causes reduced gibberellin content and dwarfism in tobacco.* Physiol Plant. **117**:130-136.
77. Murakami, S., Y. Kondo, T. Nakano, and F. Sato. (2000). *Protease activity of CND41, a chloroplast nucleoid DNA-binding protein, isolated from cultured tobacco cells.* FEBS Lett. **468**:15-18.
78. Phillips, J.R., T. Hilbricht, F. Salamini, and D. Bartels. (2002). *A novel abscisic acid- and dehydration-responsive gene family from the resurrection plant Craterostigma plantagineum encodes a plastid-targeted protein with DNA-binding activity.* Planta. **215**:258-266.
79. Sato, N., M. Nakayama, and T. Hase. (2001). *The 70-kDa major DNA-compacting protein of the chloroplast nucleoid is sulfite reductase.* FEBS Lett. **487**:347-350.
80. Phinney, B.S. and J.J. Thelen. (2005). *Proteomic characterization of a triton-insoluble fraction from chloroplasts defines a novel group of proteins associated with macromolecular structures.* Journal of Proteome Research. **4**:497-506.
81. Chi-Ham, C.L. (2002). *Identification and characterization of DCP68 as a bifunctional DNA-binding nucleoid protein and sulfite reductase.* in *Department of Chemistry & Biochemistry.* University of Southern Mississippi: Hattiesburg. 134q.
82. Sekine, K., T. Hase, and N. Sato. (2002). *Reversible DNA compaction by sulfite reductase regulates transcriptional activity of chloroplast nucleoids.* J Biol Chem. **277**:24399-24404.
83. Bork, C., J.D. Schwenn, and R. Hell. (1998). *Isolation and characterization of a gene for assimilatory sulfite reductase from Arabidopsis thaliana.* Gene. **212**:147-153.
84. Jeffery, C.J. (2003). *Moonlighting proteins: old proteins learning new tricks.* Trends Genet. **19**:415-417.
85. Oleskina, Y.P., N.P. Yurina, T.I. Odintsova, T.A. Egorov, A. Otto, B. Wittmann-Liebold, and M.S. Odintsova. (1999). *Nucleoid proteins of pea chloroplasts: detection of a protein homologous to ribosomal protein.* Biochem Mol Biol Int. **47**:757-763.
86. Wang, S. and X.-Q. Liu. (1991). *The plastid genome of Cryptomonas Φ encodes an hsp70-like protein, a histone-like protein, and an acyl carrier protein.* Proc Natl Acad Sci U S A. **88**:10783-10787.
87. Wu, H. and X.Q. Liu. (1997). *DNA binding and bending by a chloroplast-encoded HU-like protein overexpressed in Escherichia coli.* Plant Mol Biol. **34**:339-343.

88. Kobayashi, T., M. Takhara, S.-Y. Miyagishima, H. Kuroiwa, N. Sasaki, N. Ohta, M. Matsuzaki, and T. Kuroiwa. (2002). *Detection and localization of a chloroplast-encoded HU-like protein that organizes chloroplast nucleoids.* Plant Cell. **14**:1579-1589.
89. Grasser, K.D., C. Ritt, M. Krieg, S. Fernandez, J.C. Alonso, and R. Grimm. (1997). *The recombinant product of the Chryptomonas phi plastid gene hlpA is an architectural HU-like protein that promotes the assembly of complex nucleoprotein structures.* Eur J Biochem. **249**:70-76.
90. Briat, J.-F., S. Letoffe, R. Mache, and J. Rouviere-Yaniv. (1984). *Similarity between the bacterial histone-like protein HU and a protein from spinach chloroplasts.* FEBS Lett. **172**:75-79.
91. Henschke, R.B. and E.J. Nuecken. (1989). *Proteins from organelles of higher plants with homology to the bacterial DNA-binding protein HU.* J Plant Physiol. **134**:110-112.
92. Sato, S., Y. Nakamura, T. Kaneko, E. Azamizu, and S. Tabata. (1999). *Complete structure of the chloroplast genome of Arabidopsis thaliana.* DNA Res. **6**:283-290.
93. Ishihama, A. (1999). *Modulation of the nucleoid, the transcription apparatus, and the translation machinery in bacteria for stationary phase survival.* Genes to Cells. **4**:135-43.
94. Sherratt, D.J. (2003). *Bacterial chromosome dynamics.* Science. **301**:780-97.
95. Hecht, R.M., R.T. Taggart, and D.E. Pettijohn. (1975). *Size and DNA content of purified E. coli nucleoids observed by fluorescence microscopy.* Nature. **253**:60-2.
96. Van Ness, J. and D.E. Pettijohn. (1979). *A simploe autoradiographic method for investigating long range chromosome substructure: size and number of DNA molecules in isolated nucleoids of Escherichia coli.* Journal of Molecular Biology. **129**:501-8.
97. Muela, A., I. Arana, J.I. Justo, C. Seco, and I. Barcina. (1999). *Changes in DNA content and cellular death during a starvation-survival process of Escherichia coli in river water.* Microbial Ecology. **37**:62-9.
98. Givskov, M., L. Eberl, and S. Molin. (1994). *Responses to nutrient starvation in Pseudomonas putida KT2442: two-dimensional electrophoretic analysis of starvation- and stress-induced proteins.* Journal of Bacteriology. **176**:4816-24.
99. Zimmerman, S.B. and L.D. Murphy. (2001). *Release of compact nucleoids with characteristic shapes from Escherichia coli.* Journal of Bacteriology. **183**:5041-9.
100. Hinnebusch, B.J. and A.J. Bendich. (1997). *The bacterial nucleoid visualized by fluorescence microscopy of cells lysed within agarose: comparison of Escherichia coli and spirochetes of the gene Borrelia.* Journal of Bacteriology. **179**:2228-37.

101. McLeod, S.M. and R.C. Johnson. (2001). *Control of transcription by nucleoid proteins.* Current Opinion in Microbiology. **4**:152-9.
102. Thanbichler, M., P.H. Viollier, and L. Shapiro. (2005). *The structure and function of the bacterial chromosome.* Current Opinion in Genetics & Development. **15**:153-62.
103. Thanbichler, M., S.C. Wang, and L. Shapiro. (2005). *The bacterial nucleoid: a highly organized and dynamic structure.* Journal of Cellular Biochemistry. **96**:506-21.
104. Kepes, F. (2004). *Periodic transcriptional organization of the E. coli genome.* Journal of Molecular Biology. **340**:957-64.
105. Ninnemann, O., C. Koch, and R. Kahmann. (1992). *The E. coli fis promoter is subject to stringent control and autoregulation.* EMBO Journal. **11**:1075-83.
106. Dorman, C.J. and P. Deighan. (2003). *Regulation of gene expression by histone-like proteins in bacteria.* Current Opinion in Genetics & Development. **13**:179-84.
107. Finkel, S.E. and R.C. Johnson. (1992). *The Fis protein: it's not just for DNA inversion anymore.* Mol Microbiol. **6**:3257-65.
108. Dame, R.T. (2005). *The role of nucleoid-associated proteins in the organization and compaction of bacterial chromatin.* Molecular Microbiology. **56**:858-70.
109. Schneider, R., R. Lurz, G. Luder, C. Tolksdorf, A. Travers, and G. Muskhelishvili. (2001). *An architectural role of the Escherichia coli chromatin protein Fis in organizing DNA.* Nucl Acids Res. **29**:5107-14.
110. Ussery, D.W., J.C. Hinton, B.J. Jordi, P.E. Granum, A. Seirafi, R.J. Stephen, and A.E. Tupper. (1994). *The chromatin-associated protein H-NS.* Biochimie. **76**:968-80.
111. Williams, R.M. and S. Rimsky. (1997). *Molecular aspects of the E. coli nucleoid protein, H-NS: a central controller of gene regulatory networks.* FEMS Microbiol Lett. **156**:175-185.
112. Schroeder, O. and R. Wagner. (2002). *The bacterial regulatory protein H-NS- a versatile modulator of nucleic acid structures.* Biol Chem. **383**:945-60.
113. Hommais, F., E. Krin, C. Laurent-Winter, O. Soutourina, A. Malpertuy, J.P. Le Caer, A. Danchin, and P. Bertin. (2001). *Large-scale monitoring of pleiotropic regulation of gene expression by the prokaryotic nucleoid-associated protein, H-NS.* Molecular Microbiology. **40**:20-36.
114. McGovern, V., N.P. Higgins, R.S. Chiz, and A. Jaworski. (1994). *H-NS over-expression induces an artificial stationary phase by silencing global transcription.* Biochimie. **76**:1019-29.
115. Atlung, T. and H. Ingmer. (1997). *H-NS: a modulator of environmentally regulated gene expression.* Molecular Microbiology. **24**:7-17.
116. Dame, R.T., C. Wyman, and N. Goosen. (2001). *Structural basis for preferential binding of H-NS to curved DNA.* Biochimie. **83**:231-4.

117. Dame, R.T., C. Wyman, R. Wurm, R. Wagner, and N. Goosen. (2002). *Structural basis for H-NS-mediated trapping of RNA polymerase in the open initiation complex at the rrnB P1.* J Biol Chem. **277**:2146-50.
118. Dame, R.T., M.S. Luijsterburg, E. Krin, P.N. Bertin, R. Wagner, and G.J. Wuite. (2005). *DNA bridging: a property shared among H-NS-like proteins.* J Bacteriol. **187**:1845-8.
119. Schroeder, O. and R. Wagner. (2000). *The bacterial DNA-binding protein H-NS represses ribosomal RNA transcription by trapping RNA polymerase in the initiation complex.* J Biol Chem. **298**:737-48.
120. Dai, X. and L.B. Rothman-Denes. (1999). *DNA structure and transcription.* Current Opinion in Microbiology. **2**:126-30.
121. Kamashev, D. and J. Rouviere-Yaniv. (2000). *The histone-like protein HU binds specificially to DNA recombination and repair intermediates.* EMBO J. **19**:6527-35.
122. Baladina, A., D. Kamashev, and J. Rouviere-Yaniv. (2002). *The bacterial histone-like protein HU specifically recognized similar structures in all nucleic acids.* J Biol Chem. **277**:27622-8.
123. Pettijohn, D.E. (1988). *Histone-like proteins and bacterial chromosome structure.* J Biol Chem. **263**:12793-12796.
124. Rouviere-Yaniv, J., J. Germond, and M. Yaniv. (1979). Cell. **17**:265-74.
125. Drlica, K. and J. Rouviere-Yaniv. (1987). *Histonelike proteins of bacteria.* Microbiol Rev. **51**:301-319.
126. Goodman, S.D., N.J. Velten, Q. Gao, S. Robinson, and A.M. Segall. (1999). *In vitro selection of integration host factor binding sites.* J Bacteriol. **181**:3246-55.
127. Ali, B.M., R. Amit, I. Braslavsky, A.B. Oppenheim, O. Gileadi, and J. Stavans. (2001). *Compaction of single DNA molecules induced by binding of integration host factor (IHF).* Proc Natl Acad Sci U S A. **98**:10658-63.
128. Arfin, S.M., A.D. Long, E.T. Ito, L. Tolleri, M.M. Riehle, and E.S. Paegle. (2000). *Global gene expression profiling in Escherichia coli K12. The effects of integration host factor.* Journal of Biological Chemistry. **275**:29672-84.
129. Azam, T.A. and A. Ishihama. (1999). *Twelve species of the nucleoid-associated protein from Escherichia coli. Sequence recognition specificity and DNA binding affinity.* J Biol Chem. **274**:33105-33113.
130. Azam, T.A. (1999). *Growth phase-dependent variation in protein composition of the Escherichia coli nucleoid.* Journal of Bacteriology. **181**:6361-70.
131. Martinez, A. and R. Kolter. (1997). *Protection of DNA during oxidative stress by the nonspecific DNA- binding protein Dps.* J Bacteriol. **179**:5188-5194.
132. Choi, S.H., D.J. Baumler, and C.W. Kaspar. (2000). *Contribution of dps to acid stress tolerance and oxidative stress tolerance in Escherichia coli O157:H7.* Applied and Environmental Microbiology. **66**:3911-6.

133. Grant, R.A., D.J. Filman, S.E. Finkel, R. Kolter, and J.M. Hogle. (1998). *The crystal structure of Dps, a ferritin homolog that binds and protects DNA.* Nature Structural Biology. **5**:294-303.
134. Frenkiel-Krispin, D., I. Ben-Avraham, J. Englander, E. Shimoni, S.G. Wolf, and A. Minsky. (2004). *Nucleoid restructuring in stationary-state bacteria.* Molecular Microbiology. **51**:395-405.
135. Frenkiel-Krispin, D., S. Levin-Zaidman, E. Shimoni, S.G. Wolf, E.J. Wachtel, T. Arad, S.E. Finkel, R. Kolter, and A. Minsky. (2001). *Regulated phase transitions of bacterial chromatin: a non-enzymatic pathway for generic DNA protection.* EMBO J. **20**:1184-81.
136. Ueguchi, C., M. Kakeda, H. Yamada, and T. Mizuno. (1994). *An analogue of the DnaJ molecular chaperone in Escherichia coli.* Proc Natl Acad Sci U S A. **91**:1054-8.
137. Yamashino, T., M. Kakeda, C. Ueguchi, and T. Mizuno. (1994). *An analogue of the DnaJ molecular chaperone whose expression is controlled by sigma S during the stationary phase and phosphate starvation in Escherichia coli.* Molecular Microbiology. **13**:475-83.
138. Jair, K.-W., X. Yu, K. Skarstad, B. Thony, N. Fujita, A. Ishihama, and R.E. Wolf. (1996). *Transcriptional activation of promoters of the superoxide and multiple antibiotic resistance regulons by Rob, a binding protein of the Escherichia coli origin of chromosomal replication.* Journal of Bacteriology. **178**:2507-13.
139. Ariza, R.R., Z. Li, N. Ringstad, and B. Demple. (1995). *Activation of multiple antibiotic resistance and binding of stress-inducible promoters of Escherichia coli Rob protein.* Journal of Bacteriology. **177**:1655-61.
140. Fuller, R.S., B.E. Funnell, and A. Kornberg. (1984). *The dnaA protein complex with the E. coli chromosomal replication origin (oriC) and other DNA sites.* Cell. **38**:889-900.
141. Boeneman, K. and E. Crooke. (2005). *Chromosomal replication and the cell membrane.* Current Opinion in Microbiology. **8**:143-8.
142. Fujimitsu, K. and T. Katayama. (2004). *Reactivation of DnaA by DNA sequence-specific nucleotide exchange in vitro.* Biochem Biophys Res Commun. **322**:411-9.
143. Messer, W. and C. Weigel. (1997). *DnaA initiator-also a transcription factor.* Molecular Microbiology. **24**:1-6.
144. Hwang, D.S. and A. Kornberg. (1990). *A novel protein binds a key origin sequence to block replication of an E. coli minichromosome.* Cell. **63**:325-31.
145. Hwang, D.S., B. Thony, and A. Kornberg. (1992). *IciA protein, a specific inhibitor of initiation of Escherichia coli chromosomal replication.* Journal of Biological Chemistry. **267**:2209-13.
146. Wei, T. and R. Bernander. (1996). *Interaction of the IciA protein with AT-rich regions in plasmid replication origins.* Nucl Acids Res. **24**:1865-72.

147. Shi, X. and G.N. Bennett. (1994). *Plasmids bearing hfq and hns-like gene stpA complement hns mutants in modulating arginine decarboxylase gene expression in Escherichia coli.* Journal of Bacteriology. **176**:6769-75.
148. Zhang, A. and M. Belfort. (1992). *Nucleotide sequence of a newly-identified Escherichia coli gene, stpA, encoding an H-NS-like protein.* Nucl Acids Res. **20**:6735.
149. Zhang, A., S. Rimsky, M.E. Reaban, H. Buc, and M. Belfort. (1996). *Escherichia coli protein analogs StpA and H-NS: regulatory loops, similar and disparate effects on nucleic acid dynamics.* EMBO J. **15**:1340-9.
150. Cusick, M.E. and M. Belfort. (1998). *Domain structure and RNA annealing activity of the Escherichia coli, regulatory protein StpA.* Molecular Microbiology. **28**:847-57.
151. Grossberger, R., O. Mayer, C. Waldsich, K. Semrad, S. Urschitz, and R. Schroeder. (2005). *Influence of RNA structural stability on the RNA chaperone activity of the Escherichia coli protein StpA.* Nucl Acids Res. **33**:2280-9.
152. Tani, T.H., A. Khodursky, R.M. Blumenthal, P.O. Brown, and R.G. Matthews. (2002). *Adaptation to famine: a family of stationary-phase genes revealed by microarray analysis.* Proc Natl Acad Sci U S A. **99**.
153. Hung, S.P., P. Baldi, and G.W. Hatfield. (2002). *Global gene expression profiling in Escherichia coli K12. The effects of leucine-responsive regulatory protein.* Journal of Biological Chemistry. **277**:40309-23.
154. Calvo, J.M. and R.G. Matthews. (1994). *The leucine-responsive regulatory protein, a global regulator of metabolism in Escherichia coli.* Microbiology and Molecular Biology Reviews. **58**.
155. D'Ari, R., R.T. Lin, and E.B. Newman. (1993). *The leucine-responsive regulatory protein: more than a regulator?* Trends Biochem Sci. **18**:260-3.
156. Wang, Q. and J.M. Calvo. (1993). *Lrp, a major regulatory protein in Escherichia coli, bends DNA and can organize the assembly of a higher-order nucleoprotein structure.* EMBO J. **12**:2495-501.
157. Chen, S., M. Iannolo, and J.M. Calvo. (2005). *Cooperative binding of the leucine-responsive regulatory protein (Lrp) to DNA.* Journal of Molecular Biology. **345**:251-64.
158. Cui, Y., Q. Wang, G.D. Stormo, and J.M. Calvo. (1995). *A consensus sequence for binding of Lrp to DNA.* Journal of Bacteriology. **177**:4872080.
159. Chen, X.J., X. Wang, B.A. Kaufman, and R.A. Butow. (2005). *Aconitase couples metabolic regulation to mitochondrial DNA maintenance.* Science. **307**:714-7.
160. Chen, S. and J.M. Calvo. (2002). *Leucine-induced dissociation of Escherichia coli Lrp hexadecamers to octamers.* Journal of Molecular Biology. **318**:1031-42.

161. Wolringh, C.L., P.R. Jensen, and H.V. Westerhoff. (1995). *Structure and partitioning of bacterial DNA: determined by a abalance of compaction and expansion forces.* FEMS Microbiol Lett. **131**:235-42.
162. Kim, J., S.H. Yoshimura, K. Hizume, R.L. Ohniwa, A. Ishihama, and K. Takeyasu. (2004). *Fundamental structural units of Escherichia coli nucleoid revealed by atomic force microscopy.* Nucleic Acids Res. **32**:1982-92.
163. Murphy, L.D. and S.B. Zimmerman. (1994). *Macromolecular crowding effects on the interaction of DNA with Escherichia coli DNA-binding proteins: a model for bacterial nucleoid stabilization.* Biochimica et Biophysica Acta. **1219**:277-84.
164. Murphy, L.D. and S.B. Zimmerman. (1997). *Isolation and characterization of spermidine nucleoids from Escherichia coli.* J Struct Biol. **119**:321-335.
165. Murphy, L.D. and S.B. Zimmerman. (1997). *Stabilization of compact spermidine nucleoids from Escherichia coli under crowded conditions: implications for in vivo nucleoid structure.* J Struct Biol. **119**:336-346.
166. Brunetti, R., G. Prosseda, E. Beghetto, B. Colonna, and G. Micheli. (2001). *The looped domain organization of the nucleoid in histone-like protein defective Escherichia coli strains.* Biochimie. **83**.
167. Dame, R.T. and H. Goosen. (2002). *HU: promoting or counteracting DNA compaction?* FEBS Letters. **529**:151-6.
168. Lemon, K.P. and A.D. Grossman. (1998). *Localization of bacterial DNA polymerase: evidence for a factory model of replication.* Science. **282**:1516-9.
169. Wu, L.J. (2004). *Structure and segregation of the bacterial nucleoid.* Current Opinion in Genetics & Development. **14**:126-32.
170. Maleszka, R., P.J. Skelly, and G.D. Clark-Walker. (1991). *Rolling circle replication of DNA in yeast mitochondria.* EMBO J. **10**:3923-9.
171. Shadel, G.S. and D.A. Clayton. (1997). *Mitochondrial DNA maintenance in vertabrates.* Annual Reviews of Biochemistry. **66**:409-35.
172. Sakai, A., H. Takano, and T. Kuroiwa. (2004). *Organelle nuclei in higher plants: structure, composition, function and evolution.* International Review of Cytology. **238**:59-118.
173. Kuroiwa, T. (1982). *Mitochondrial Nuclei.* International Review of Cytology. **75**:1-59.
174. Friddle, R.W., J.E. Klare, S.S. Martin, M. Corzett, R. Balhorn, E.P. Baldwin, R.J. Baskin, and A. Noy. (2004). *Mechanism of DNA compaction by yeast mitochondrial protein Abf2p.* Biophysical Journal. **86**:1632-9.
175. Landsman, D. and M. Bustin. (1993). Bioessays. **15**:1-8.
176. MacAlpine, D.M., P.S. Perlman, and R.A. Butow. (1998). *The high mobility group protein Abf2p influences the level of yeast mitochondrial DNA recombination intermediates in vivo.* Proc Natl Acad Sci U S A. **95**:6739-6743.

177. Diffley, J.F. and B. Stillman. (1991). *A close relative of the nuclear, chromosomal high-mobility group protein HMG1 in yeast mitochondria.* Proc Natl Acad Sci U S A. **88**:7864-7868.
178. Zelenaya-Troitskaya, O., S.M. Newman, K. Okamoto, P.S. Perlman, and R.A. Butow. (1998). *Functions of the high mobility group protein, Abf2p, in mitochondrial DNA segregation, recombination and copy number in Saccharomyces cerevisiae.* Genetics. **148**:1763-1776.
179. Newman, S.M., O. Zelenaya-Troitskaya, P.S. Perlman, and R.A. Butow. (1996). *Analysis of mitochondrial DNA nucleoids in wild-type and a mutant strain of Saccharomyces cerevisiae that lacks the mitochondrial HMG box protein Abf2p.* Nucl Acids Res. **24**:386-393.
180. Chen, X.J., M.X. Guan, and G.D. Clark-Walker. (1993). *MGM101, a nuclear gene involved in maintenance of the mitochondrial genome in Saccharomyces cerevisiae.* Nucl Acids Res. **21**:3473-7.
181. Meeusen, S., Q. Tieu, E. Wong, E. Weiss, D. Schieltz, J.R. Yates, and J. Nunnari. (1999). *Mgm101p is a novel component of the mitochondrial nucleoid that binds DNA and is required for the repair of oxidatively damaged mitochondrial DNA.* J Cell Biol. **145**:291-304.
182. Kaufman, B.A., J.E. Kolesar, P.S. Perlman, and R.A. Butow. (2003). *A function for the mitochondrial chaperonin Hsp60 in the structure and transmission of mitochondrial DNA nucleoids in Saccharomyces cerevisiae.* J Cell Biol. **163**:in press.
183. Kaufman, B.A., S.M. Newman, R.L. Hallberg, C.A. Slaughter, P.S. Perlman, and R.A. Butow. (2000). *In organello formaldehyde crosslinking of proteins to mtDNA: Identification of bifunctional proteins.* Proc Natl Acad Sci USA. **97**:7772-7777.
184. Bulteau, A.-L., M. Ikeda-Saito, and L.I. Szweda. (2003). *Redox-dependent modulation of aconitase activity in intact mitochondria.* Biochemistry. **42**:14846-55.
185. Shadel, G.S. (2005). *Mitochondrial DNA, aconitase 'wraps' it up.* Trends in Biochemical Sciences. **30**:294-6.
186. Haile, D.J., T.A. Rouault, J.B. Harford, M.C. Kennedy, G.A. Blondin, H. Beinert, and R.D. Klausner. (1992). *Cellular regulation of the iron-responsive element binding protein: disassembly of the cubane iron-sulfur cluster results in high-affinity RNA binding.* Proc Natl Acad Sci U S A. **89**:11735-9.
187. Kennedy, M.C., L. Mende-Mueller, G.A. Blondin, and H. Beinert. (1992). *Purification and characterization of cytosolic aconitase from beef liver and its relationship to the iron-responsive element binding protein.* Proc Natl Acad Sci U S A. **89**:11730-4.
188. Gray, N.K., S. Quick, B. Goossen, A. Constable, H. Hirling, L.C. Kuhn, and M. Hentze. (1993). *Recombinant iron-regulatory factor functions as an iron-responsive-element-binding protein, a translational repressor and an aconitase.* Eur J Biochem. **218**:657-67.

189. Sedman, T., P. Joers, S. Kuusk, and J. Sedman. (2005). *Helicase Hmi1 stimulates the synthesis of concatameric mitochondrial DNA molecules in yeast Saccharomyces cerevisiae.* Current Genetics. **47**:213-22.
190. Zelenaya-Troitskaya, O., P.S. Perlman, and R.A. Butow. (1995). *An enzyme in yeast mitochondria that catalyzes a step in branched-chain amino acid biosynthesis also functions in mitochondrial DNA stability.* Embo J. **14**:3268-3276.
191. MacAlpine, D.M., P.S. Perlman, and R.A. Butow. (2000). *The numbers of individual mitochondrial DNA molecules and mitochondrial DNA nucleoids in yeast are co-regulated by the general amino acid control pathway.* Embo J. **19**:767-775.
192. Hinnebusch, A.G. (1988). *Mechanisms of gene regulation in the general control of amino acid biosynthesis in Saccharomyces cerevisiae.* Microbiology Reviews. **52**:248-73.
193. Bateman, J.M., M. Iacovino, P.S. Perlman, and R.A. Butow. (2002). *Mitochondrial DNA instability mutants of the bifunctional protein Ilv5p have altered organization in mitochondria and are targeted for degradation by Hsp78 and the Pim1p protease.* J Biol Chem. **277**:47946-47953.
194. Bateman, J.M., P.S. Perlman, and R.A. Butow. (2002). *Mutational dissection of the mitochondrial DNA stability and amino acid biosynthetic functions.* Genetics. **161**:1043-1052.
195. Sia, R.A.L., B.L. Urbonas, and E.A. Sia. (2003). *Effects of ploidy, growth conditions and the mitochondial nucleoid-associated protein Ilv5p on the rate of mutation of mitochondrial DNA in Saccharomyces cerevisiae.* Current Genetics. **44**:26-37.
196. Cabiscol, E., G. Belli, J. Tamarit, P. Echave, E. Herrero, and J. Ros. (2002). *Mitochondrial Hsp60, resistance to oxidative stress, and the labile iron pool are closely connected in Saccharomyces cerevisiae.* Journal of Biological Chemistry. **277**:44531-8.
197. McCammon, M.T., C.B. Epstein, B. Przybyla-Zawislak, L. McAlister-Henn, and R.A. Butow. (2003). *Global transcription analysis of Krebs tricarboxylic acid cycle mutants reveals an alternating pattern of gene expression and effects on hypoxic and oxidative genes.* Molecular Biology of the Cell. **14**:958-72.
198. Contamine, V. and M. Picard. (2000). *Maintenance and integrety of the mitochondrial genome: a plethora of nuclear genes in the budding yeast.* Microbiol Mol Biol Rev. **64**:281-315.
199. Cupp, J.R. and L. McAlister-Henn. (1992). *Cloning and characterization of the gene encoding the IDH1 subunit of NAD+-dependent isocitrate dehydrogenase from Saccharomyces cerevisiae.* Journal of Biological Chemistry. **267**:16417-23.
200. de Jong, L., S.D.J. Elzinga, M.T. McCammon, L.A. Grivell, and H. van der Spek. (2000). *Increased synthesis and decreased stability of mitochondrial*

translation products in yeast as a result of loss of mitochondrial (NAD+)-dependent isocitrate dehydrogenase. FEBS Letters. **483**:62-66.

201. Bogenhagen, D.F., Y. Wang, E.L. Shen, and R. Kobayashi. (2003). *Protein components of mitochondrial DNA nucleoids in higher eukaryotes.* Mol Cell Proteomics. **in press**.
202. Wenzel, T.J., M.A. van den Berg, W. Visser, J.A. van den Berg, and H.Y. de Steensma. (1992). *Characterization of Saccharomyces cerevisiae mutants lacking the E1alpha subunit of the pryvuate dehydrogenase complex.* Eur J Biochem. **209**:697-705.
203. Duchniewicz, M., A. Germaniuk, B. Westermann, W. Neupert, E. Schwarz, and J. Marszalek. (1999). *Dual role of the mitochondrial chaperone Mdj1p in inheritance of mitochondrial DNA in yeast.* Molecular and Cellular Biology. **19**:8201-10.
204. *Delta Mass: a database of protein post translational modifications.* http://www.abrf.org/index.cfm/dm.home
205. Champion, A., M. Kreis, K. Mockaitis, A. Picaud, and Y. Henry. (2004). *Arabidopsis kinome: after the casting.* Func Integr Genomics. **4**:163-87.
206. Luan, S. (2003). *Protein phosphatases in plants.* Annual Reviews of Plant Biology. **54**:63-92.
207. Allfrey, V.G., R. Faulkner, and A.E. Mirsky. (1964). *Acetylation and methylation of histones and their possible role in the regulation of RNA synthesis.* Proc Natl Acad Sci U S A. **51**:786-94.
208. Wade, P.A., D. Pruss, and A.P. Wolffe. (1997). *Histone acetylation: chromatin in action.* Trends Biochem Sci. **22**:128-32.
209. Lo, W.-S., R.C. Trievel, J.R. Rojas, L. Duggan, J.-Y. Hsu, C.D. Allis, R. Marmorstein, and S.L. Berger. (2000). *Phosphorylation of serine 10 in histone H3 is functionally linked in vitro and in vivo to Gcn5-mediated acetylation at lysine 14.* Mol Cell. **5**:917-26.
210. Turner, B.M. (1993). *Decoding the nucleosome.* Cell. **75**:5-8.
211. Inagaki, M., N. Inagaki, T. Takahashi, and Y. Takai. (1997). Journal of Biochemistry. **12**:407-14.
212. Goto, H., Y. Tomono, K. Ajiro, H. Kosako, M. Fujita, M. Sakurai, K. Okawa, A. Iwamatsu, T. Okigaki, T. Takahashi, and M. Inagaki. (1999). *Identification of a novel phosphorylation site on histone H3 coupled with mitotic chromosome condensation.* Journal of Biological Chemistry. **274**:25543-9.
213. Houben, A., T. Wako, R. Furushima-Shimogawara, G. Presting, G. Kunzel, I.I. Schubert, and K. Fukui. (1999). *The cell cycle dependent phosphorylation of histone H3 is correlated with the condensation of plant mitotic chromosomes.* Plant J. **18**:675-679.
214. Downs, J.A., N.F. Lowndes, and S.P. Jackson. (2000). *A role for Saccharomyces cerevisiae histone H2A in DNA repair.* Nature. **408**:1001-4.

215. Rogakou, E.P., E.R. Pilch, A.H. Orr, V.S. Ivanova, and W.M. Bonner. (1998). *DNA double-stranded breaks induce histone H2AX phosphorylation on serine 139.* Journal of Biological Chemistry. **273**:5858-68.
216. Redon, C., D. Pilch, E. Rogakou, O. Sedelnikova, K. Newrock, and W. Bonner. (2002). *Histone H2A variants H2AX and H2AZ.* Curr. Opin. Genet. Dev. **12**.
217. Ichijima, Y., R. Sakasai, N. Okita, K. Asahina, S. Mizutani, and H. Teraoka. (2005). *Phosphorylation of histone H2AX at M phase in human cels without DNA damage response.* Biochem Biophys Res Commun. **336**:807-12.
218. Talasz, H., W. Helliger, B. Sarg, P.L. Debbage, B. Puschendorf, and H. Lindner. (2002). *Hyperphosphorylation of histone H2A.X and dephosphorylation of histone H1 subtypes in the course of apoptosis.* Cell Death Differ. **9**:27-39.
219. Kleinschmidt, J.A., A. Seiter, and H. Zentgraf. (1990). *Nucleosome assembly in vitro: separate histone transfer and synergistic interaction of native histone complexes purified from nuclei of Xenopus laevis oocytes.* Embo J. **9**:1309-1318.
220. Kleinschmidt, J.A. and H. Steinbeisser. (1991). *DNA-dependent phosphorylation of histone H2A.X during nucleosome assembly in Xenopus laevis oocytes: involvement of protein phosphorylation in nucleosome spacing.* Embo J. **10**:3043-3050.
221. Singh, K.B., R.C. Foley, and L. Onate-Sanchez. (2002). *Transcription factors in plant defense and stress responses.* Current Opinion in Plant Biology. **5**:430-6.
222. Jackson, S.P. (1992). *Regulating transcription factor activity by phosphorylation.* Trends in Cell Biology. **2**:104-8.
223. Treier, M. and D. Bohmann. *Phosphorylation of transcription factors*, in *Protein phosphorylation*, F. Marks, Editor. 1996, VCH: Weinheim, Germany.
224. Gu, Y.Q., C. YUang, V.K. Thara, J. Zhou, and G.B. Martin. (2000). *Pti4 is induced by ethylene and salicylic acid, and its product is phosphorylated by the Pto kinase.* Plant Cell. **12**:771-86.
225. Cheong, Y.H., B.C. Moon, J.K. Kim, C.Y. Kim, M.C. Kim, I.H. Kim, C.Y. Park, J.C. Kim, B.O. Park, S.C. Koo, H.W. Yoon, W.S. Chung, C.O. Lim, S.Y. Lee, and M.J. Cho. (2003). *BWMK1, a rice mitogen-activated protein kinase, locates in the nucleus and mediates pathogenesis-related gene expression by activation of a transcription factor.* Plant Physiol. **132**:1961-72.
226. Ciceri, P., E. Gianazza, B. Lazzari, G. Lippoli, A. Genga, G. Hoschek, R.J. Schmidt, and A. Viotti. (1997). *Phosphorylation of Opaque2 changes diurnally and impacts its DNA binding activity.* Plant Cell. **9**:97-108.

227. Danon, A. (1997). *Translational regulation in the chloroplasts.* Plant Physiol. **115**.
228. Danon, A. and S.P. Mayfield. (1994). *Light-regulated translation of chloroplast messenger RNAs through redox potential.* Science. **266**:1717-1719.
229. Trebitsh, T., A. Levitan, A. Sofer, and A. Danon. (2000). *Translation of chloroplast psbA mRNA is modulated in the light by counteracting oxidizing and reducing activities.* Molecular and Cellular Biology. **20**:1116-23.
230. Homann, A. and G. Link. (2003). *DNA-binding and transcription characteristics of three cloned sigma factors from mustard (Sinapis alba L.) suggest overlapping and distinct roles in plastid gene expression.* Eur J Biochem. **270**:1288-1300.
231. Tiller, K. and G. Link. (1993). *Phosphorylation and dephosphorylation affect functional characteristics of chloroplast and etioplast transcription systems from mustard (Sinapis alba L.).* Embo J. **12**:1745-1753.
232. Ogrzewalla, K., M. Piotrowski, S. Reinbothe, and G. Link. (2002). *The plastid transcription kinase from mustard (Sinapis alba L.) : A nuclear-encoded CK2-type chloroplast enzyme with redox-sensitive function.* European Journal of Biochemsitry. **269**:3329-37.
233. Loschelder, H., A. Homann, K. Ogrzewalla, and G. Link. (2004). *Proteomics-based sequence analysis of plant gene expression-- the chloroplast transcription apparatus.* Phytochemistry. **65**:1785-93.
234. Baginsky, S., K. Tiller, and G. Link. (1997). *Transcription factor phosphorylation by a protein kinase associated with chloroplast RNA polymerase from mustard (Sinapis alba).* Plant Mol Biol. **34**:181-189.
235. Baginsky, S., K. Tiller, T. Pfannschmidt, and G. Link. (1999). *PTK, the chloroplast RNA polymerase-associated protein kinase from mustard (Sinapis alba), mediates redox control of plastid in vitro transcription.* Plant Mol Biol. **39**:1013-1023.
236. Link, G. (2005). *Plastid protein kinase.* S. Heinhorst, Editor: Bochum, Germay.
237. Riera, M., G. Peracchia, and M. Pages. (2001). *Distinctive features of plant protein kinase CK2.* Molecular and Cellular Biochemistry. **227**:119-27.
238. Sugano, S., C. Andronis, M.S. Ong, R.M. Green, and E.M. Tobin. (1999). *The protein kinase CK2 is involved in regulation of circadian rhythms in Arabidopsis.* Proc Natl Acad Sci U S A. **96**:12362-6.
239. Sugano, S., C. Andronis, R.M. Green, Z.-Y. Wang, and E.M. Tobin. (1998). *Protein kinase CK2 interacts with and phosphorylates the Arabidopsis circadian clock-associated 1 protein.* Proc Natl Acad Sci U S A. **95**:11020-5.

240. Lee, Y., A.M. Lloyd, and S.J. Roux. (1999). *Antisense expression of the CK2 alpha-subunit gene in Arabidopsis. Effects on light-regulated gene expression and plant growth.* Plant Physiol. **119**:989-1000.
241. Ralet, M.-C., D. Fouques, J. Leonil, D. Molle, and J.-C. Meunier. (1999). *Soybean beta-conglycinin alpha subunit is phosphorylated on two distinct serines by protein kinase CK2 in vitro.* Journal of Protein Science. **18**:315-23.
242. Testi, M.G., R. Croce, P. Polverino-De Laureto, and R. Bassi. (1996). *A CK2 site is reversibly phosphorylated in the photosystem II subunit CP29.* FEBS Lett. **399**:245-50.
243. Kanekatsu, M., H. Saito, K. Motohashi, and T. Hisabori. (1998). *The beta subunit of chloroplast ATP synthase (CF0CF1-ATPase) is phosphorylated by casein kinase II.* Biochem Mol Biol Int. **46**:99-105.
244. Pagano, M.A., S. Sarno, G. Poletto, G. Cozza, L.A. Pinna, and F. Meggio. (2005). *Autophosphorylation at the regulatory beta subunit reflects the supramolecular organization of protein kinase CK2.* Molecular and Cellular Biochemistry. **274**:23-29.
245. Jeong, S.Y., N. Peffer, and I. Meier. (2004). *Phosphorylation by protein kinase CKII modulates the DNA-binding activity of a chloroplast nucleoid-associated protein.* Planta. **219**:298-302.
246. Murashige, T. and D. Skoog. (1962). *A revised medium for rapid growth and bioassays with tobacco tissue cultures.* Physiologica Plantarum. **15**:473-97.
247. Heinhorst, S., G.C. Cannon, and A. Weissbach. (1990). *Chloroplast and mitochondrial DNA polymerases from cultured soybean cells.* Plant Physiol. **92**:939-945.
248. Horn, M.E., J.H. Sherrard, and J.M. Widholm. (1983). *Photoautotrophic growth of soybean cells in suspension culture.* Plant Physiol. **72**:426-429.
249. Bradford, M.M. (1976). *A rapid and sensitive method for the quantitation of microgram quantities of protein utilizing the principle of protein-dye binding.* Anal Biochem. **72**:248-254.
250. Laemmli, U.K. (1970). *Cleavage of structural proteins during the assembly of the head of bacteriophage T4.* Nature. **227**:680-5.
251. Chi-Ham, C.L., M.A. Keaton, G.C. Cannon, and S. Heinhorst. *Soybean chloroplast nucleoid proteins and their interactions with DNA.* in *6th International Congress of Plant Molecular Biology*. 2000. Quebec, Canada.
252. Davuluri, R.V., H. Sun, S.K. Palaniswamy, N. Matthews, C. Molina, M. Kurtz, and E. Grotewold. (2003). *AGRIS: Arabidopsis Gene Regulatory Information Server, an information resource of Arabidopsis cis-regulatory elements and transcription factors.* BMC Bioinformatics. **4**:25.
253. . *The Arabidopsis Gene Regulatory Information Server.*

254. Blom, N., S. Gammeltoft, and S. Brunak. (1999). *Sequence- and structure-based prediction of eukaryotic protein phosphorylation sites.* Journal of Molecular Biology. **294**:1351-1362.
255. . *NetPhos 2.0 Server.*
256. Sato, N., N. Rolland, M.A. Block, and J. Joyard. (1999). *Do plastid envelope membranes play a role in the expression of the plastid genome?* Biochimie. **81**:619-629.
257. Hell, R., J.D. Schwenn, and C. Bork. *Light and sulphur sources modulate mRNA levels of several genes of sulphate assimilation.*, in *Sulphur metabolism in higher plants*, W.J. Cram, L.J. De Kok, I. Stulen, C. Brunold, and H. Rennenberg, Editors. 1997, Backhuys: Leiden. 181-5.
258. Volkov, R.A., I.I. Panchuk, and F. Schoffl. (2003). *Heat-stres-dependency and developmental modulation of gene expression: the potential of house-keeping genes as internal standards in mRNA expression profiling using real-time RT-PCR.* J Exp Bot. **54**:2343-9.
259. Mullet, J.E. (1988). *Chloroplast development and gene expression.* Annu Rev Plant Physiol. **39**:475-502.
260. Chi-Ham, C.L. (2002). *Identification and characterization of DCP68 as a bifunctional DNA-binding nucleoid protein and sulfite reductase.* in *Department of Chemistry & Biochemistry.* University of Southern Mississippi: Hattiesburg. 134.
261. Nakayama, M., T. Akashi, and T. Hase. (2000). *Plant sulfite reductase: molecular structure, catalytic function and interaction with ferredoxin.* J Inorg Biochem. **82**:27-32.
262. Bellissimo, D.B. and L.S. Privalle. (1995). *Expression of spinach nitrite reductase in excherichia coli: Site-directed mutagenesis of predicted active site amino acids.* Arch Biochem Biophys. **323**:155-163.
263. Krueger, R.J. and L.M. Siegel. (1982). *Spinach siroheme enzymes: Isolation and characterization of ferredoxin-sulfite reductase and comparison of properties with ferredoxin-nitrite reductase.* Biochemistry. **21**:2892-2904.
264. Yonekura-Sakakibara, K., T. Ashikari, Y. Tanaka, T. Kusumi, and T. Hase. (1998). *Molecular characterization of tobacco sulfite reductase: enzyme purification, gene cloning, and gene expression analysis.* J Biochem. **124**:615-621.
265. Leustek, T., M. Martin, J. Bick, and J.P. Davies. (2000). *Pathways and regulation of sulfur metabolism revealed through molecular and genetics studies.* Annu Rev Plant Physiol Plant Mol Biol. **51**:141-165.
266. Bolchi, A., S. Petrucco, P.L. Tenca, C. Foroni, and S. Ottonello. (1999). *Coordinate modulation of maize sulfate permease and ATP sulfurylase mRNAs in response to variations in sulfur nutritional status: stereospecific down-regulation by L-cysteine.* Plant Mol Biol. **39**:527-537.

267. Lamppa, G.K., L.V. Elliot, and A.J. Bendich. (1980). *Changes in chloroplast number during pea leaf development: an analysis of a protoplast population.* Planta. **148**:437-43.
268. *The Arabidopsis Gene Regulatory Information Server.* http://arabidopsis.med.ohio-state.edu/
269. Harmer, S.L., J.B. Hogenesch, M. Straume, C. Hur-Song, B. Han, T. Zhu, X. Wang, J.A. Kreps, and S.A. Kay. (2000). *Orchestrated transcription of key pathways in Arabidopsis by the circadian clock.* Science. **290**:2110-3.
270. Teakle, G.R., I.W. Manfield, J.F. Graham, and P.M. Gilmartin. (2002). *Arabidopsis thaliana GATA factors: organization, expression and DNA-binding characteristics.* Plant Mol Biol. **50**:43-57.
271. Gilmartin, P.M., L. Sarokin, J. Memelink, and C. Nam-Hai. (1990). *Molecular light switches for plant genes.* Plant Cell. **2**:369-78.
272. Yonekura-Sakakibara, K., Y. Onda, T. Ashikari, Y. Tanaka, T. Kusumi, and T. Hase. (2000). *Analysis of reductant supply systems for ferredoxin-dependent sulfite reductase in photosynthetic and nonphotosynthetic organs of maize.* Plant Physiol. **122**:887-894.
273. Leustek, T. and K. Saito. (1999). *Sulfate transport and assimilation in plants.* Plant Physiol. **120**:637-644.
274. Saito, K. (2000). *Regulation of sulfate transport and synthesis of sulfur-containing amino acids.* Curr Op Plant Biol. **3**:188-195.
275. Yamagata, A., D.B. Kristensen, Y. Takeda, Y. Miyamoto, K. Okada, M. Inamatsu, and K. Yoshizato. (2002). *Mapping of phosphorylated proteins on two-dimensional polyacrylamide gels using protein phosphatase.* Proteomics. **2**:1267-76.
276. *Delta Mass: a database of protein post translational modifications*, (2006). http://www.abrf.org/index.cfm/dm.home
277. Zhu, K., J. Zhao, and D.M. Lubman. (2005). *Protein pI shifts due to posttranslational modifications in the separation and characterization of proteins.* Analytical Chemistry. **77**:2745-55.
278. Gasteiger, E., C. Hoogland, A. Gattiker, S. Duvaud, M.R. Wilkens, R.D. Appel, and A. Bairoch. *Protein identification and analysis tools on the ExPASy server*, in *The proteomics protocols handbook*, J.M. Walker, Editor. 2005, Humana Press. 571-607.
279. Bjellqvist, B., G.J. Hughes, C. Pasquali, N. Paquet, F. Ravier, J.-C. Sanchez, S. Frutiger, and D.F. Hochstrasser. (1993). *The focusing positions of polypeptides in immobilized pH gradients can be predicted from their amino acid sequences.* Electrophoresis. **14**:1023-31.
280. Rodionov, I. (2006). S.W. Adamson, Editor.
281. Leno, G.H., A.D. Mills, A. Philpott, and R.A. Laskey. (1996). *Hyperphosphorylation of nucleopolasmin facilitates Xenopus sperm decondensation at fertilization.* The Journal of Biological Chemsitry. **271**:7253-56.

282. Sigrist, C.J.A., L. Cerutti, N. Hulo, A. Gattiker, L. Falquet, M. Pagni, A. Bairoch, and P. Bucher. (2002). *PROSITE: a documented database using patterns and profiles as motif descriptors.* Bioinformatics. **3**:265-74.
283. Hulo, N., C.J.A. Sigrist, V. Le Saux, P.S. Langendijk-Genevaux, L. Bordoli, A. Gattiker, E. De Castro, P. Bucher, and A. Bairoch. (2004). *Recent improvements to the PROSITE database.* Nucl Acids Res. **32**:132-7.
284. Kuroiwa, T. (1991). *The replication, differentiation, and inheritance of plastids with emphasis on the concept of organelle nuclei.* Int Rev Cytol. **128**:1-62.
285. Moore, B.D. (2004). *Bifunctional and moonlighting enzymes: lighting the way to regulatory control.* Trends Plant Sci. **9**:221-8.
286. Sriram, G., J.A. Martinez, E.R.B. McCabe, J.C. Liao, and K.M. Dipple. (2005). *Single-gene disorders: what role could moonlighting enzymes play?* Am J Hum Genet. **76**:911-24.
287. Klausner, R.D. and T.A. Rouault. (1993). *A double life: cytosolic aconitase as a regulatory RNA binding protein.* Molecular Biology of the Cell. **4**:1-5.
288. Jeffery, C.J. (1999). *Moonlighting proteins.* Trends Biochem Sci. **24**:8-11.
289. Hell, R. (1997). *Molecular physiology of plant sulfur metabolism.* Planta. **202**:138-48.
290. Ideguchi, T., A. Tetsuyuki, Y. Onda, and T. Hase. *cDNA cloning and functional expression of ferredoxin-dependent sulfite reductase from maize in E. coli cells*, in *Photosynthesis: from Light to Biosphere, Vol. 2*, P. Mathis, Editor. 1995, Kluwer. 713-716.
291. Pufall, M.A., G.M. Lee, M.L. Nelson, H. Kang, A. Velyvis, L.E. Kay, L.P. McIntosh, and B.J. Graves. (2005). *Variable control of Ets-1 DNA binding by multiple phosphates in an unstructured region.* Science. **309**:142-5.
292. Briat, J.F., C. Gigot, J.P. Laulhere, and R. Mache. (1982). *Visualization of a spinach plastid transcriptionally active DNA-protein complex in a highly condensed structure.* Plant Physiol. **69**:1205-1211.
293. Reiss, T. and G. Link. (1985). *Characterization of transcriptionally active DNA-protein complexes from chloroplasts and etioplasts of mustard (Sinapis alba L.).* Eur J Biochem. **148**:207-212.
294. Rose, R.J. and J.V. Possingham. (1976). *The localization of [^{3}H]thymidine incorporation in the DNA of replicating spinach chloroplasts by electron-microscope autoradiography.* J Cell Sci. **20**:341-355.
295. Rose, R.J., D.G. Cran, and J.V. Possingham. (1975). *Changes in DNA synthesis during cell growth and chloroplast replication in greening spinach leaf disks.* J Cell Sci. **17**:27-41.